BILLINGS & GUSSMAN, INC.

OC 108

HANDBOOK OF AEROSOL BEHAVIOR IN SATURATION DIVING ENVIRONMENTS

by: Robert A. Gussman

with: Anthony M. Sacco
John Beeckmans
Charles E. Billings
Robert Abilock

1 October 1971

Contract No.: N00014-71-M-0006

Office of Naval Research
Arlington, Virginia

BILLINGS & GUSSMAN INC.
1254 Main Street
Waltham, Massachusetts 02154

TABLE OF CONTENTS

TABLE OF CONTENTS - con't.

UNCLASSIFIED

Security Classification

DOCUMENT CONTROL DATA - R & D

(Security classification of title, body of abstract and indexing annotation must be entered when the overall report is classified)

1. ORIGINATING ACTIVITY (Corporate author)

Billings & Gussman, Inc.
1254 Main Street
Waltham, Massachusetts 02154

2a. REPORT SECURITY CLASSIFICATION

2b. GROUP

3. REPORT TITLE

Handbook on Aerosol Behavior in Saturation Living Environments

4. DESCRIPTIVE NOTES *(Type of report and inclusive dates)*

Final Report

5. AUTHOR(S) *(First name, middle initial, last name)*

Robert A. Gussman

6. REPORT DATE	7a. TOTAL NO. OF PAGES	7b. NO. OF REFS
1 October 1971	213	42

8a. CONTRACT OR GRANT NO.	9a. ORIGINATOR'S REPORT NUMBER(S)
N00014-71-M-0006	OC 108
b. PROJECT NO. RR 041-06-01	
c. NR 108-948	9b. OTHER REPORT NO(S) *(Any other numbers that may be assigned this report)*
d.	

10. DISTRIBUTION STATEMENT

This document has been approved for public release and sale.
Distribution is unlimited.

11. SUPPLEMENTARY NOTES	12. SPONSORING MILITARY ACTIVITY
Written and published by contract with Office of Naval Research	Navy Toxicology Unit Naval Medical Research Institute Bethesda, Maryland

13. ABSTRACT

A compilation of the known and unknown quantities as described in the literature required to accomplish the following goals:

1. Investigate and extrapolate the possibly altered behavior of aerosols in the helium-oxygen environment.

2. Determine methods for removing potentially harmful aerosols from the environment.

3. Determine possible altered toxicological behavior of aerosols.

DD FORM 1 NOV 65 1473 (PAGE 1)

S/N 0101-807-6801

UNCLASSIFIED

Security Classification

TABLE OF CONTENTS - con't.

LIST OF FIGURES

LIST OF FIGURES - con't.

LIST OF FIGURES - con't.

LIST OF TABLES

LIST OF TABLES - con't.

SECTION 1.0: PREFACE

Although it is probably impossible to accurately define the age of the science of aerosols, the major works in this area began to appear about 50 years ago. The only excuse for a curiosity about the age of a field of interest is if one wants to assess the possibility of doing something "new." In examining aerosol behavior in the realm of the saturation diver nothing new has been done. Rather, the opportunity has been afforded to retrace old ground under a new set of physical constraints. Given the extreme pressure conditions of the saturation diving environment and a gaseous composition whose properties differ significantly from those of air, it is necessary to go back to the beginning. The origins of the accepted relationships for the motions and properties of aerosols must be viewed with respect to what was meant and intended by their originators. Therefore, while the material presented herein is not "new" the opportunity to gain the keenest insight in ones chosen field has never been greater.

For having provided the opportunity to perform these studies and for his guidance and insight, we are indebted to Captain Jacob Siegel, U. S. N., M. S. C., Director of the U. S. Navy Toxicology Laboratory and also to Dr. Robert Jennings for his continued and unfailing support.

Several individuals have made direct material contributions to this effort and deserve to be identified. The bulk of the laboratory investigations were performed

by Anthony M. Sacco. Charles E. Billings has materially edited several sections on aerosol generation and contributed to the solution of the problem of combined aerosol behavior in a spherical vessel. John Beeckmans performed the computer analysis of his own pulmonary deposition model under the high pressure environmental conditions. Robert Abilock achieved a solution to the difficult mathematical problem of combined aerosol behavior in a spherical vessel for which we are particularly in his debt. Thanks are due also to Raymond Wanta who provided the encouragement for undertaking this task and both edited and commented upon the early phases of the work.

SECTION 2.0: INTRODUCTION

The project which forms the basis for this handbook was an investigation of aerosol behavior in high pressure environments. Conventional fleet-type or nuclear submarines and deep submergence research vehicles maintain internal environmental air pressures and compositions nearly equivalent to sea-level, regardless of depth of submergence, without decompression penalty. Deep submergence saturation diving habitats utilize synthetic respirable atmospheres at hydrostatic pressures equivalent to the depth, and allow free diver excursions to the surrounding sea for tasks such as marine research, salvage and mining. During extended submerged operations, recycled respiration gas atmospheres may become contaminated by emissions from construction materials, protective coatings, instruments, control system components, and from occupants and their operations and activities associated with prolonged habitation in a closed environment. The specific environment considered was the helium-oxygen atmosphere used in saturation diving environments for depths to 1,000 feet. In order to proceed in as logical a fashion as possible and yet deal with the several interrelated aspects of the problem simultaneously, a clear statement of goals was necessary.

1. Investigate and extrapolate the possibly altered behavior of aerosols in the helium-oxygen environment.
2. Determine methods for removing potentially harmful aerosols from the environment.

3. Determine possible altered toxicological behavior of aerosols.

The atmosphere is unique, the stress levels are high, the environment is amenable to almost total control and monitoring. Given the goals stated above and the potentially high level of environmental control and monitoring attainable, the solution to the problems may proceed by a logical progression. The succeeding sections detail the known and unknown quantities as described in the literature, the physical details of the breathing mixture and with this as a background, developed information for the achievement of each of the stated goals.

SECTION 3.0: LITERATURE SURVEY

The first task in this study was to determine, through a search of the literature, the extent of available knowledge relevant to aerosol behavior under high pressures. As the search progressed, it became apparent that virtually no information was available on aerosols in environments, or even on process systems at elevated pressures. Numerous professional contacts were made in the United States and abroad in an effort to uncover pertinent unpublished information, but all responses were negative. While the internal hull pressures of nuclear submarines seldom exceed normal ambient conditions, they do represent a closed environment. Therefore, a large body of literature pertaining to contaminant studies within these vessels was felt to be of direct value to this study. The literature on nuclear submarines was heavily reviewed and it, along with related information, is presented in Appendix V as an annotated bibliography.

Some technological information dealing with aerosol behavior at reduced pressures, concerning electrification, agglomeration, and filtration, was uncovered. For the most part, this material proved to be of value and will be discussed in the following sections.

Without reference to any specific paper reviewed, it is possible to evolve a general picture of submarine atmosphere, contaminants, and control methods.

Chief among the gases to be removed from submarine atmospheres is carbon monoxide, which is burned catalytically with some benefits being accrued in destroying hydrocarbons; although the bulk of the hydrocarbon removal is accomplished with a charcoal adsorption system.

Carbon dioxide is currently controlled with a monoethanolamine (MEA) scrubbing system that is apparently completely satisfactory save that some aerosol problems arise from the generation of irritating MEA mists. Use of this system is based on an economic comparison between it and lithium hydroxide absorbants. For nuclear submarines, the economic balance develops in favor of the MEA system.

A long list of trace substances in submarine atmospheres has been compiled only because the environment is closed for a long period of time and concentrations of the contaminants can build up to detectable, if not troublesome, levels. Construction and finishing materials are chief sources of these substances. These toxic substances have chiefly been controlled by substitution.

According to several authors, the chief source of aerosol in closed environments is cigarette smoking, followed closely by cooking. For these activities, aerosol concentrations as high as 400 γ/M^3 can be observed. Removal of particulates is accomplished by electrostatic precipitation and recommended final levels are about 100 γ/M^3. While there is no clear statement regarding the size distribution of aerosols found in submarine atmospheres, condensation

nuclei that range in concentration from 3,000 to 11,000 particles/cm^3 are frequently mentioned. Generally, aerosol particles may be as large as 100 microns; but, while virtually all aerosol particles can serve as centers of condensation, nuclei counters are seldom useful on particles of diameters greater than 1 micron. Smoking generally gives rise to submicron particles (approximately 0.3 μ); but cooking may yield a very wide spectrum, including some rather large sizes.

Both positive and negative ions are found in the submarine atmosphere; average concentrations range from 1,500 to 2,000 ions/cm^3 and excursions up to 15,000 ions/cm^3 can be recorded. Positive ions predominate, probably because of the higher mobility of negative ions that are more readily attached to aerosol particles. With an increase in aerosol concentration there appears to be a gain in the number of medium (0.003-0.03 μ) and large (0.03-0.1 μ) ions.

There are a large number of papers dealing with the physiological effects of air ions. The authors agree, in a general way, that negative ions seem to be beneficial while positive ions seem to provoke feelings of distress and unhappiness. Additionally, some physiological responses are noted, chiefly in the rate of ciliary action in the lung. Negative ions tend to increase the ciliary beat rate and thereby promote more rapid clearance of deposited materials from the lung. A criticism of much of the work carried out on the effects of air ions is that investigators paid little or no attention to aerosol concentration with relation to the quantity of ions generated. Therefore, be-

cause of wall losses or other unaccounted effects, the actual number of free ions reaching a subject could have been remarkably different than that which was generated.

Much consideration has been given to determining modified threshold limit values (TLV) for the closed environment. As usually defined, the threshold limit value indicates the highest exposure to which an individual may be safely exposed during a 7 or 8 hour work day, five days per week. In nuclear submarines, the exposure is continuous for periods of approximately 60 days and nights. Studies by the Navy conclude that lower limit values are necessary.

The contaminants found in the closed environments of submarines appear to be well identified and the methods of controlling their impact upon the living organism have been successfully approached and utilized.

SECTION 4.0: PROPERTIES OF THE GASEOUS MIXTURE

Before examining the behavior of aerosols in high pressure environments, one must first define the gaseous composition of that environment. Aerosols are composed of particulates, of greater than molecular dimensions, that have describable motions dependent upon the characteristics of the medium in which they are suspended. The ultimate goal of this study's parent project is to determine the toxicological impact of aerosols in high-pressure environments inhabited by man. Certain definite statements can be made at this time about the gas mixture in which the aerosol particles will be suspended. A given factor in this consideration is that the maximum pressure to be considered is 500 psia, or 34 atmospheres.

Bond[1] states that, for long term exposures under high pressures, the nitrogen component of the atmosphere is not suitable and helium must be substituted. He also noted that, as the pressure is increased, the percentage of oxygen must be decreased and what is required for life-support is a partial oxygen pressure (PO_2) of approximately 160 mm Hg. While small percentages of nitrogen and other trace gases are used, we have chosen to make a minor simplifying assumption in that we will only consider a binary mixture of oxygen and helium.

The general aerosol properties that are to be considered and extrapolated for the high pressure artificial environment include sedimentation, diffusion,

agglomeration, electrification, nucleation, and the effect of inter-molecular slip. The equations for many of these motions require a numerical value for the density, viscosity, and mean free path of the gas mixture. Therefore, these items have been considered and determined.

Figure 1 shows a working graph of the atmosphere composition for pressures ranging from 10 to 500 psia. Since the partial pressure of the oxygen is to be maintained at 160 mm Hg (3.095 psi), the percentage of oxygen content of the atmosphere decreases from 21% at 1 atmosphere to 0.62% at 34 atmospheres. The balance of the mixture consists of the helium. Figure 2 indicates that the density of the varying mixture increases with increasing pressure. The calculations assumed the mixture to be an ideal gas. Errors arising from this assumption have been checked and are found to be less than 1% at 500 psia.

The viscosity of the two gases are quite similar at atmospheric pressure and 20°C (He = 194 μpoise; O_2 = 202 μpoise). Because of this close similarity and the difficulty in applying the equations that determine viscosity of mixtures to a gas as light as helium, Table 1 represents a comparison of viscosity with increasing pressure (changing composition) based on a simple averaging of the viscosities according to percentage composition.

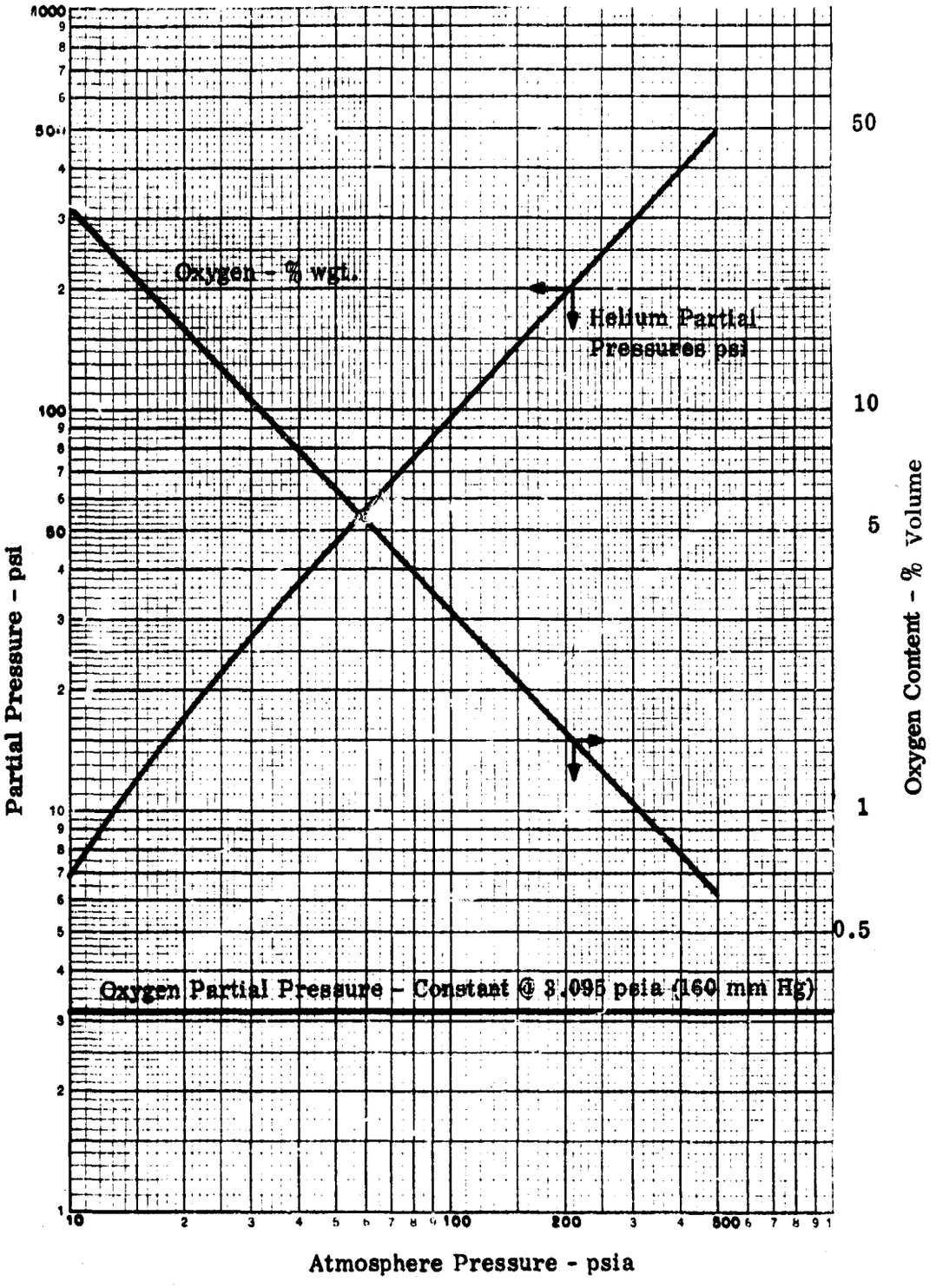

Figure 1. Oxygen-Helium Atmosphere Pressure vs Composition. (PO_2 = 160 mm Hg; T = 20°C).

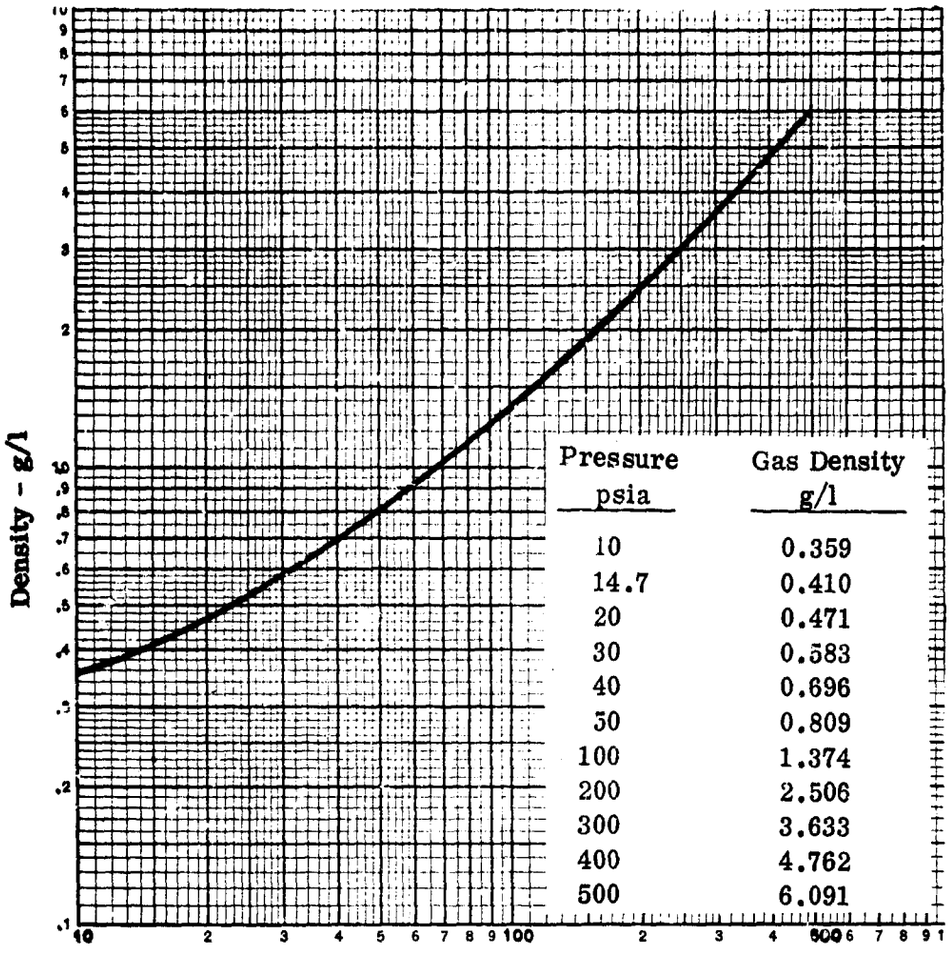

Figure 2. Oxygen-Helium Atmosphere Pressure vs Density. (PO_2 = 160 mm Hg; T = 20°C).

TABLE I

He - O_2 VISCOSITY vs PRESSURE

Pressure - psia	Viscosity - micro poise
10	196.47
14.7	195.68
20	195.24
30	194.82
40	194.68
50	194.46
100	194.23
200	194.22
300	194.08
400	194.06
500	194.05

Increasing pressure does not effect viscosity for a perfect gas. The degree of deviation for an imperfect gas is similar to the pressure (density) deviation that, for our mixture, has already been noted as less than 1%.[2]

The values of the mean free path (λ) of the mixture have been calculated according to equations given by Loeb[3] for λ of one gas in the presence of a quantity of another. The values expressed in Figure 3 are, therefore, average path lengths based on the mole fractions present and include corrections for pressure, temperature, and composition.

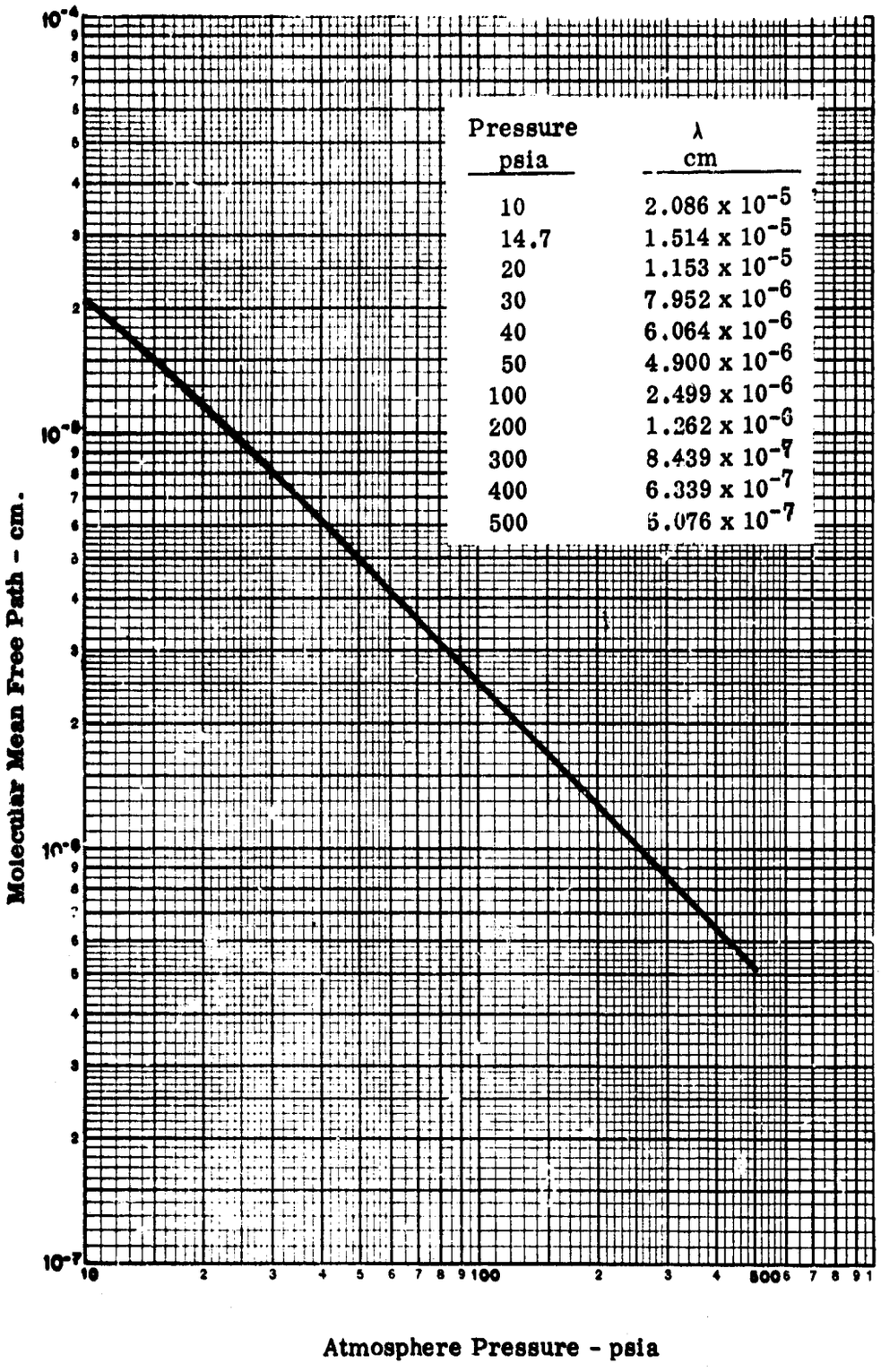

Figure 3. Oxygen-Helium Atmosphere vs Mean Free Path. (PO_2 = 160 mm Hg; T = 20°C).

SECTION 5.0: AEROSOL MECHANICS

5.1 SLIP CORRECTION

Common practice in aerosol physics calculations is initially to discuss the basic relationships for particulate motion, such as sedimentation, agglomeration, diffusion, etc., and then to introduce the concept of the "slip factor", which accounts for the increased mobility of particulates as their dimensions become comparable with the mean free path of the gas molecules. For air at ambient conditions, the slip factor becomes negligible for particles of diameter greater than 1 micron. However, helium has a much longer mean free path than air (He = 27.45×10^{-6} cm; Air = 6.53×10^{-6} cm); therefore, it is necessary first to consider the magnitude and importance of this factor before proceeding to other calculations.

The evolution of the slip factor and the basis for currently accepted values of its constants have been thoroughly discussed by Davies[4] and Green and Lane.[5]

Davies' studies, reported in 1945, are of particular interest. He reviews in detail the work of several earlier investigators, evaluates their findings, and evolves numerical values for the constants contained in the slip correction equation. The work of these investigators, as described in Davies' paper, present a concise history of the factor. According to Davies, the factor was first expressed in its present form by Knudsen and Webber:

$$1 + \frac{2A\lambda}{d} \quad , \qquad (1)$$

where λ is the mean free path of the gas molecules, d is the particle diameter, and A is a numerical factor having a value of approximately unity.

According to Davies,[4] Knudsen and Webber, working with glass spheres in air, observed the damping of torsional oscillations of a suspended beam to which a sphere was fixed. Millikan derived values for the factor from his work with the famous oil drop apparatus and from other experiments with a rotating drum viscometer. Mattauch's studies on oil drops in nitrogen were similar to Millikan's technique. Davies does not specifically detail what procedures were used by Monch for his work with tobacco smoke.

The factor A was actually found to vary with particulate diameter according to the equation

$$A = A_o + B \exp(-Cd/2\lambda) \quad , \qquad (2)$$

where $A_o = 1.257$, $B = 0.400$, and $C = 1.10$.

Davies determined values for the factor on the basis of work by each of these men. He disregarded Knudsen and Webber's values because of their methods and gave double weight to Millikan's and Mattauch's values over Monch's numbers for tobacco smoke. The reason stated for giving less weight to the work of Monch is that "there exists no confirmation that the slip coefficient for tobacco smoke particles in air is the same as for oil in nitrogen."

Subsequent to Davies' considerations, Flanagan and Tayler,[6] Metnieks and Pollak[7] and Billings and Gussman (see Appendix I) constructed tabulations of the slip factor, using only the data of Millikan for oil droplets in air. The use of these data is certainly not open to dispute for the aerosols and gases investigated. Because the experimental values of A_o, B, and C are available only for air at conditions closely approximating ambient, there is no direct method of theoretically extrapolating the slip factor to other gases and pressures with any assurance of exact results.

Fortunately, Fuchs and Stechkina[8] have developed a theoretical relationship as a correction for the mobility of small particles.

Mobility, B is defined as ratio of the velocity of a particle U_o to the drag F:

$$B = \frac{U_o}{F} = \frac{1}{3\pi \eta d} \quad , \tag{3}$$

where η is the coefficient of viscosity of the gas.

As the particulate diameter becomes small, a correction is required for slip. The correction for mobility is expressed as:[8]

$$B = \left[\frac{1}{1+\beta\chi} + \frac{2.25\chi}{\delta}\right] (3\pi \eta d)^{-1} \quad , \tag{4}$$

where $\beta = \frac{2.25}{1+\pi s/8} - 2\gamma \left(\frac{2}{s} - 1\right)$;

δ = 1, for specular reflection of the molecules from a particle;

δ = 1 + (π/8), for completely diffuse reflection (however, for the general case, δ = (1+π s/8), where s is the fraction of the molecules reflected diffusely);

γ = 0.499, as extracted from the current expression for λ;[6] and

$\chi = \frac{2\lambda}{d}$, the Knudsen number

Extracting the slip factor from Equation (4) and substituting the above terms, yields

$$\frac{1}{1+\left[\frac{2.25}{1+\frac{\pi s}{8}} - 2(0.499)\left(\frac{2}{s}-1\right)\right]\frac{2\lambda}{d}} + \frac{2.25(2\lambda)}{(1+\frac{\pi s}{8})d} \quad . \tag{5}$$

Reducing this expression,

$$\left\{1+\left[\frac{4.5}{1+0.392s} - 1.996\left(\frac{2}{s}-1\right)\right]\frac{\lambda}{d}\right\}^{-1} + \frac{4.5}{1+0.392s}\frac{\lambda}{d} \quad . \tag{6}$$

Equation (6) should be useful as a slip factor for aerosols in most gases under a wide variety of conditions. The remaining problem is to determine a value of s, i.e., the percentage of molecules reflected diffusely from the surface of the particles.

According to Loeb,[3] Blankenstein found that for many gases, s values approached unity. Loeb questions these values on the basis of Millikan's results and concludes that the factor is quite high, stating: "thus s for gases should increase with increasing density of the gases but is in any case near unity."

Setting s = 1 for the helium oxygen mixture considered over the pressure range of 10 to 500 psia (Eq. 6) reduces to the form:

$$(1 + 1.23\frac{\lambda}{d})^{-1} + 3.23\frac{\lambda}{d} \qquad (7)$$

Calculated curves for several particulate diameters are given in Figure 4; Table 2 gives working values.

A method for determining the percentage of particles reflected diffusely (s) is described in great detail by Millikan.[9] His apparatus consisted of two concentric cylinders, the outer one rotating at a constant angular velocity. The cylinders contain the gas under investigation; the cylinder walls are coated with the material of which the aerosol is composed. Therefore, a measurement of the torsional moment due to the viscous drag on the inner cylinder can be obtained and the value of s is then determined through certain calculations. Millikan discusses in some detail the simplicity with which the measurement of s may be obtained with this apparatus and speaks of the high correlation of his results with the results of other experimenters using the same technique. Millikan concludes that this technique for determining s values is far superior to that using the oil drop apparatus.

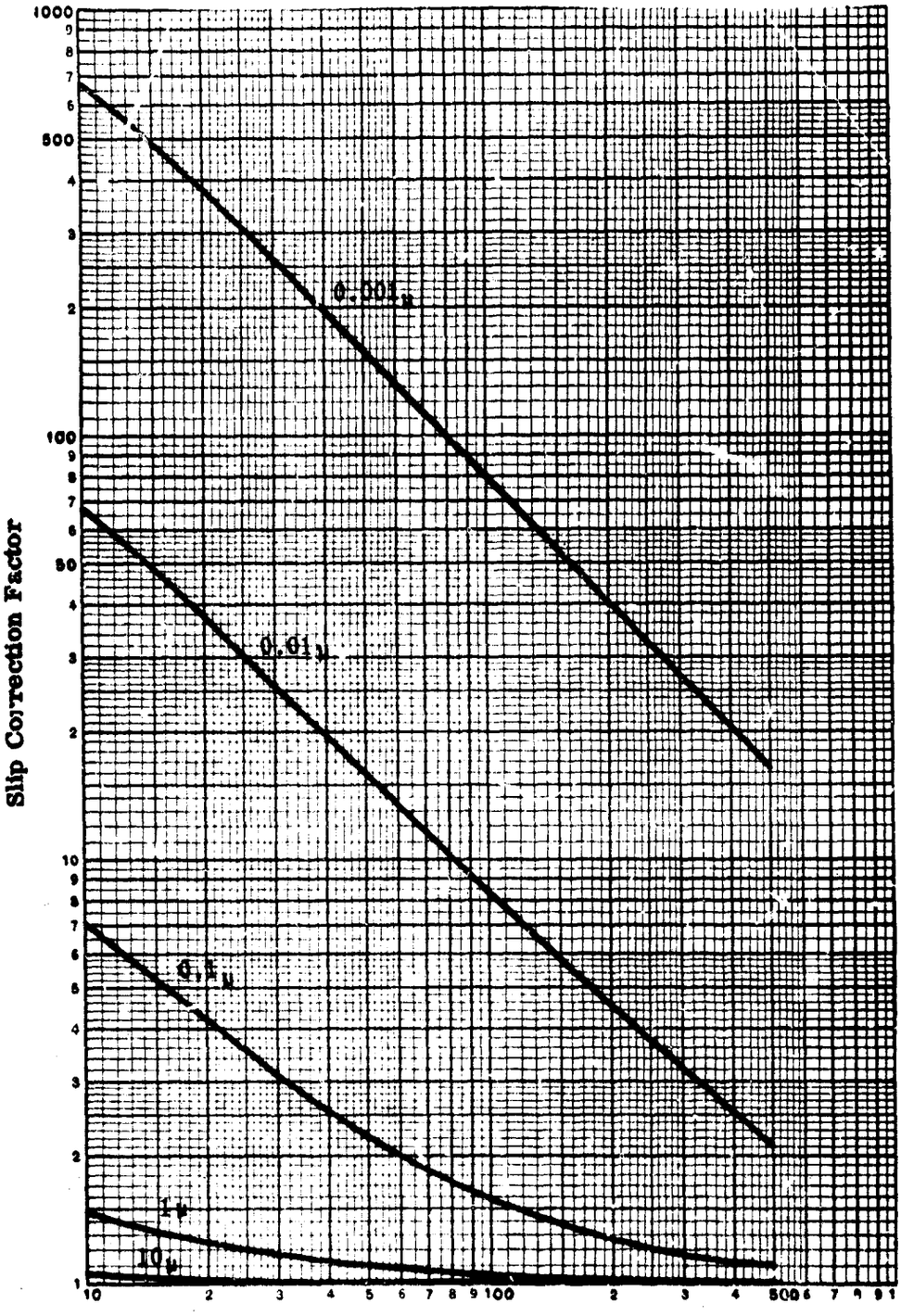

Figure 4. Oxygen - Helium Atmosphere Pressure vs Molecular Slip Correction Factor for Various Particulate Diameters. (PO_2 = 160 mm Hg; T = 20°C).

Atmosphere Pressure psia	Slip Correction Factor				
	Particle Diameter - μ				
	0.001	0.01	0.1	1	10
10.0	673.7819	67.4153	7.0182	1.4696	1.0424
14.7	489.0273	48.9532	5.2396	1.3320	1.0306
20.0	372.4260	37.3078	4.1377	1.2482	1.0233
30.0	256.8597	25.7777	3.0740	1.1678	1.0160
40.0	195.8804	19.7049	2.5315	1.1265	1.0122
50.0	158.2863	15.9693	2.2066	1.1014	1.0098
100.0	80.7492	8.3172	1.5721	1.0509	1.0050
200.0	40.8231	4.4681	1.2733	1.0255	1.0025
300.0	27.3458	3.2165	1.1785	1.0170	1.0017
400.0	20.5886	2.6094	1.1324	1.0127	1.0013
500.0	16.5335	2.2552	1.1052	1.0102	1.0010
Air (14.7 psia)	216.97	22.218	2.8667	1.1642	1.0164

Table 2. Molecular Slip Correction Factor for Various Pressures and Particle Diameters in a Helium-Oxygen Gas Mixture. (PO_2 = 160 mm Hg; T = 20°C).

No operating versions of Millikan's concentric drum apparatus are known to exist in the U. S. at the present time. If measurements were to be conducted at high pressures, an entire new device would probably have to be constructed. An alternate procedure for measuring slip at high pressures might be evolved from the apparatus described by Megaw and Wells.[10] These investigators have constructed a parallel plate aerosol spectrometer wherein particles are deposited upon a foil at locations which vary according to their mobility. The variation in the deposition sites of well characterized aerosol, streams with increasing pressure, could provide an accurate measure of the slip correction. This device has the additional advantage of no moving parts and is therefore well adapted to high pressure studies.

The new relationships of Fuchs and Stechkina, when used in conjunction with Millikan's or possibly Megaw and Wells apparatus, represent a positive method for determining slip corrections for virtually any gas and aerosol combination.

At this time no actual efforts have been made to experimentally determine slip factors for the atmosphere in question. It may be observed in Table 2, that at pressures higher than 40 psia, the correction for air is greater than for $He-O_2$. Therefore, the importance of obtaining actual measurements does not seem great.

5.2 SEDIMENTATION

The primary equation for describing the sedimentation velocity of aerosol particles is Stokes' law:[5]

$$v = \frac{(\rho - \rho')g\,d^2}{18\,\eta} \quad \text{(slip correction)} \quad , \tag{8}$$

where

v = sedimentation velocity,

ρ = density of the particle,

ρ' = density of the fluid medium,

g = gravitational acceleration,

d = diameter of the particle, and

η = viscosity of the fluid medium.

All the values necessary for calculating a sedimentation velocity at any of the high-pressure helium-oxygen conditions are presented in the preceeding section. Usually in calculations of sedimentation velocities in air, the term ρ is substituted for the expression $\rho - \rho'$ because the density of the gas is insignificant compared to the density of the particle. Maximum density being considered in the high pressure environment is 6×10^{-3} grams per cc (which

is still insignificant in comparison to particulate densities that could be encountered). The slip correction factor is applied to Stokes' law whenever the diameter of the particles approaches the mean free path of the gas molecules. For particle diameters greater than 10 microns, the correction is unnecessary.

Davies[4] upon reviewing considerable sedimentation data and performing much experimentation, found that the error incurred by using Stokes' law for particles falling in various fluids would not exceed 1% for Reynolds numbers (R_e) up to 0.05. At higher Reynolds numbers, the deviation becomes greater and Stokes' law over-estimates the settling velocity. Davies evolved an equation that is valid for Reynolds numbers up to 4; but its use first requires the introduction of other parameters. The drag coefficient (C_D) is defined as the ratio of the resistance of a particle to the product of its cross-section and the dynamic pressure:

$$C_D = \frac{\pi}{6} d^3 \rho g \cdot \frac{8}{\rho' v^2 \pi d^2} \quad , \tag{9}$$

reducing:

$$C_D = \frac{4}{3} \frac{\rho g d}{\rho' v^2} \tag{10}$$

Stokes law may be expressed in terms of the drag coefficient and Reynolds number as:

$$C_D = 24/R_e \quad . \tag{11}$$

C_D and R_e both contain velocity, therefore the equation is usually expressed as:

$$R_e = C_D R_e^2/24 \quad . \tag{12}$$

Davies expression for sedimentation velocity up to $R_e = 4$ is given as:

$$R_e = C_D R_e^2/24 - 2.3363 \times 10^{-4} (C_D R_e^2)^2 + 2.0154 \times 10^{-6} (C_D R_e^2)^3$$

$$- 6.9105 \times 10^{-9} (C_D R_e^2)^4 \quad . \tag{13}$$

Equation (12) (for Reynolds numbers up to 0.05) and Equation (13)(for settling velocities up to $R_e = 4$) makes it possible to calculate a table of diameters vs the expression $C_D R_e^2/24$ and to perform the appropriate substitution in either Equation (12) or (13).

For Reynolds numbers in the range 3 to 400, Fuchs[11] quotes the equation derived by Klyachko:

$$C_D = 24/R_e + 4/(R_e)^{\frac{1}{3}} \quad . \tag{14}$$

To construct a working table of settling velocities for the pressure range being considered, we first calculated Table 3, which consists of Reynolds number values for particles ranging in size from 0.001 to 100 microns and

Table 3. Reynolds Number vs Particle Diameter (He-O_2; PO_2 = 160 mm Hg; T = 20°C)

$$R_e = \frac{C_D R_e^2}{24} \quad \text{(Slip Correction)}$$

Particle Diameter-μ	psia → 1.0	14.7	14.7 (Air)	20.0	30.0	40.0	50.0	100.0	200.0	300.0	400.0	500.0
.001	5.42-12	2.65-13		2.51-13	2.15-13	1.96-13	1.85-13	1.60-13	1.48-13	1.44-13	1.42-13	1.46-13
.010	5.42-11	2.66-11	4.52-11	2.51-11	2.16-11	1.97-11	1.86-11	1.65-11	1.62-11	1.69-11	1.80-11	1.99-11
.100	5.26-09	3.06-09	5.78-09	2.79-09	2.57-09	2.53-09	2.57-09	3.12-09	4.61-09	6.19-09	7.80-09	9.74-09
1.000	7.45-07	7.77-07	2.53-06	3.41-07	9.78-07	1.13-06	1.28-06	2.09-06	3.71-06	5.35-06	6.98-06	8.91-06
10.000	5.21-04	8.31-04	2.05-03	6.89-04	8.51-04	1.01-03	1.18-03	1.99-03	3.63-03	5.27-03	6.90-03	8.83-03
20.000	4.97-03	1.61-02	5.39-03	6.70-03	8.01-03	9.33-03	1.59-02	2.90-02	4.21-02	5.51-02	7.20-02	
30.000	1.47-02	1.34-02	5.42-02	1.82-02	2.26-02	2.70-02	3.15-02	5.36-02	9.78-02	1.42-01	1.86-01	2.38-01
40.000	2.74-02	3.73-02	1.29-01	4.31-02	5.36-02	6.41-02	7.46-02	1.27-01	2.32-01	3.36-01	4.41-01	5.64-01
50.000	5.29-02	7.29-02	2.51-01	8.42-02	1.05-01	1.25-01	1.46-01	2.48-01	4.53-01	6.57-01	8.61-01	1.10+00
100.000	2.11-01	2.94-01	9.91+00	6.73-01	8.37-01	1.00+00	1.17+00	1.98+00	3.62+00	5.26+00	6.90+00	8.83+00

	1.0	14.7	14.7	20.0	30.0	40.0	50.0	100.0	200.0	300.0	400.0	500.0
.001	5.63-13	5.71-13		5.02-13	4.30-13	3.92-13	3.69-13	3.21-13	2.96-13	2.87-13	2.84-13	2.92-13
.010	5.63-11	5.71-11	9.04-11	5.02-11	4.32-11	3.94-11	3.72-11	3.30-11	3.24-11	3.38-11	3.60-11	3.95-11
.100	7.11-09	6.12-09	1.16-08	5.57-09	5.15-09	5.07-09	5.15-09	6.24-09	9.22-09	1.24-08	1.56-08	1.95-08
1.000	1.49-06	1.55-06	4.66-06	1.68-06	1.96-06	2.25-06	2.57-06	4.17-06	7.43-06	1.07-05	1.40-05	1.78-05
10.000	1.36-03	1.20-03	4.10-03	1.38-03	1.70-03	2.03-03	2.35-03	3.99-03	7.26-03	1.05-02	1.38-02	1.76-02
20.000	5.11-03	9.34-03	3.21-02	1.08-02	1.34-02	1.60-02	1.87-02	3.18-02	5.79-02	8.41-02	1.10-01	1.41-01
30.000	2.74-02	3.15-02	1.08-01	3.64-02	4.52-02	5.40-02	6.30-02	1.07-01	1.96-01	2.84-01	3.72-01	4.76-01
40.000	6.49-02	7.47-02	2.57-01	8.62-02	1.07-01	1.28-01	1.49-01	2.54-01	4.63-01	6.73-01	8.82-01	1.13+00
50.000	1.27-01	1.46-01	5.02-01	1.68-01	2.09-01	2.50-01	2.91-01	4.96-01	9.05-01	1.31+00	1.72+00	2.20+00
100.000	1.01+00	1.17+00	4.02+00	1.35+00	1.67+00	2.00+00	2.33+00	3.97+00	7.24+00	1.05+01	1.38+01	1.76+01

	1.0	14.7	14.7	20.0	30.0	40.0	50.0	100.0	200.0	300.0	400.0	500.0
.001	1.02-12	8.56-13		7.52-13	6.45-13	5.88-13	5.54-13	4.81-13	4.43-13	4.31-13	4.26-13	4.37-13
.010	1.03-11	8.57-11	1.36-10	7.54-11	6.47-11	5.92-11	5.59-11	4.95-11	4.85-11	5.07-11	5.39-11	5.96-11
.100	1.07-08	9.17-09	1.74-08	8.36-09	7.72-09	7.60-09	7.72-09	9.36-09	1.38-08	1.86-08	2.34-08	2.92-08
1.000	2.23-06	2.33-06	6.99-06	2.52-06	2.93-06	3.38-06	3.85-06	6.26-06	1.11-05	1.60-05	2.09-05	2.67-05
10.000	1.59-03	1.80-03	6.15-03	2.07-03	2.55-03	3.04-03	3.53-03	5.98-03	1.09-02	1.58-02	2.07-02	2.65-02
20.000	1.22-02	1.40-02	4.82-02	1.62-02	2.01-02	2.40-02	2.80-02	4.76-02	8.69-02	1.26-01	1.65-01	2.12-01
30.000	4.11-02	4.73-02	1.63-01	5.45-02	6.78-02	8.11-02	9.44-02	1.61-01	2.93-01	4.26-01	5.58-01	7.14-01
40.000	9.73-02	1.12-01	3.86-01	1.29-01	1.61-01	1.92-01	2.24-01	3.81-01	6.95-01	1.01+00	1.32+00	1.69+00
50.000	1.90-01	2.19-01	7.53-01	2.53-01	3.14-01	3.75-01	4.37-01	7.44-01	1.36+00	1.97+00	2.58+00	3.31+00
100.000	1.52+00	1.75+00	6.03+00	2.02+00	2.51+00	3.00+00	3.50+00	5.95+00	1.09+01	1.58+01	2.07+01	2.64+01

pressures ranging from 10 to 500 psia. This table is presented graphically (for $\rho = 1$) in Figure 5. In the construction of the table, the gas mixture of helium and oxygen has been varied with increasing pressure while keeping the partial pressure of the oxygen constant at 160 mm. Appropriate values for density and viscosity have been used as previously determined. The slip correction has been applied in all cases where the values are significant and, for comparative purposes, a column has been added for air at ambient pressure. The heavy line running horizontally in Table 3 represents the cutoff point for values up to $R_e = 0.05$ for which Stokes' law may be used for calculating the settling velocity. Below the solid line but above the dashed line, Davies' relationship may be utilized and, below the dashed line ($R_e > 4$), the equation of Klyachko may be used. Table 4 represents corresponding values of $\eta / \rho' d$ by which Reynolds number is multiplied to obtain the sedimentation velocity. The final table, (5) represents a working chart of sedimentation velocities for particles of three densities vs particle diameter for all the ranges of gas pressure. This table and Figure 6 fully consider all the variables of composition, pressure, viscosity, etc., and the applicable equation for the actual Reynolds number range. It may be considered correct and usable within the constraints of the theories and extrapolations utilized.

Having established the approximate sedimentation velocities for particulates in the submarine environment, it is then possible to determine the rate of particulate loss from the environment. The basic differential equation for the rate of deposition of particles in an enclosed vessel is given by:[5]

Figure 5. Particle Reynolds Number vs Diameter.
(He - O_2; PO_2 160 mm Hg; T 20°C; ρ 1)

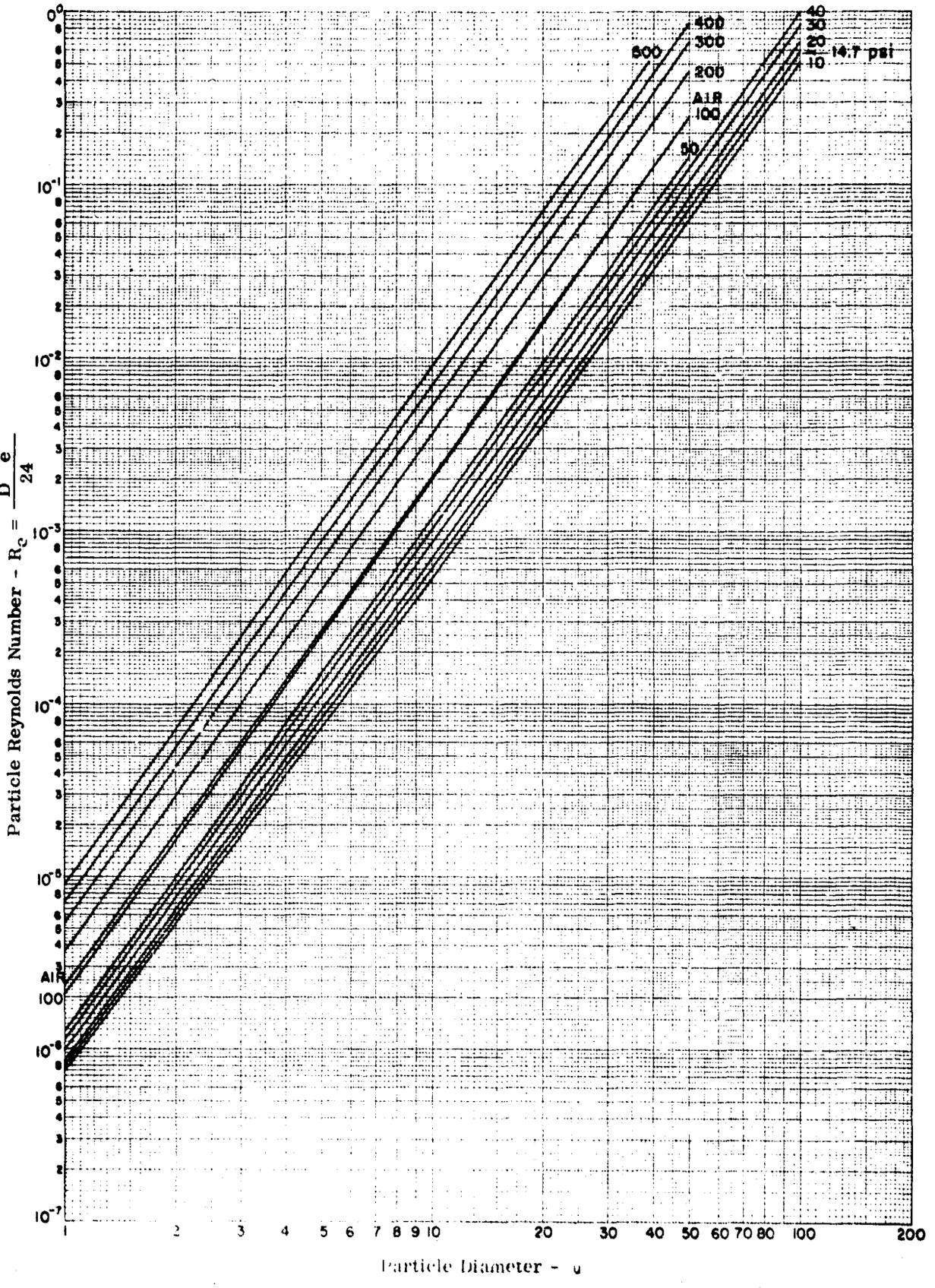

Table 4 Factor for Multiplying Particulate R_e to Determine Sedimentation Velocity

(He - O_2; PO_2 = 160 mm Hg; T = 20°C)

Particle Diameter-μ	10	14.7	14.7 (Air)	20	30	40 ←Pressure - psia
.001	5.47+06	4.77+06	1.50+06	4.15+06	3.34+06	2.80+06
.010	5.47+05	4.77+05	1.50+05	4.15+05	3.34+05	2.80+05
.100	5.47+04	4.77+04	1.50+04	4.15+04	3.34+04	2.80+04
1.000	5.47+03	4.77+03	1.50+03	4.15+03	3.34+03	2.80+03
10.000	5.47+02	4.77+02	1.50+02	4.15+02	3.34+02	2.80+02
20.000	2.74+02	2.39+02	7.50+01	2.07+02	1.67+02	1.40+02
30.000	1.82+02	1.59+02	5.00+01	1.38+02	1.11+02	9.32+01
40.000	1.37+02	1.19+02	3.75+01	1.04+02	8.35+01	6.99+01
50.000	1.09+02	9.55+01	3.00+01	8.29+01	6.68+01	5.59+01
100.000	5.47+01	4.77+01	1.50+01	4.15+01	3.34+01	2.80+01

	50	100	200	300	400	500
.001	2.40+06	1.41+06	7.75+05	5.34+05	4.08+05	3.19+05
.010	2.40+05	1.41+05	7.75+04	5.34+04	4.08+04	3.19+04
.100	2.40+04	1.41+04	7.75+03	5.34+03	4.08+03	3.19+03
1.000	2.40+03	1.41+03	7.75+02	5.34+02	4.08+02	3.19+02
10.000	2.40+02	1.41+02	7.75+01	5.34+01	4.08+01	3.19+01
20.000	1.20+02	7.07+01	3.88+01	2.67+01	2.04+01	1.59+01
30.000	8.01+01	4.71+01	2.58+01	1.78+01	1.36+01	1.06+01
40.000	6.01+01	3.53+01	1.94+01	1.34+01	1.02+01	7.96+00
50.000	4.81+01	2.83+01	1.55+01	1.07+01	8.15+00	6.37+00
100.000	2.40+01	1.41+01	7.75+00	5.34+00	4.08+00	3.19+00

Table 5. Sedimentation Velocity of Spherical Particles vs Diameter. (He - O_2; PO_2 = 160 mm Hg; T = 20°C)

Particle Diameter- μ	psia →	10.0	14.7	14.7 (Air)	20.0	30.0	40.0	50.0	100.0	200.0	300.0	400.0	500.0
		Sedimentation Velocity - cm/sec											
ρ = 1	.001	1.87-06	1.36-06		1.04-06	7.19-07	5.48-07	4.44-07	2.27-07	1.15-07	7.68-08	5.78-08	4.64-08
	.010	1.87-05	1.36-05	6.78-06	1.04-05	7.21-06	5.52-06	4.48-06	2.33-06	1.25-06	9.03-07	7.33-07	6.33-07
	.100	1.95-04	1.46-04	8.68-05	1.16-04	8.60-05	7.09-05	6.18-05	4.41-05	3.57-05	3.31-05	3.18-05	3.10-05
	1.000	4.08-03	3.71-03	3.50-03	3.48-03	3.27-03	3.15-03	3.09-03	2.95-03	2.88-03	2.86-03	2.84-03	2.84-03
	10.000	2.89-01	2.87-01	3.07-01	2.86-01	2.84-01	2.83-01	2.83-01	2.82-01	2.81-01	2.81-01	2.81-01	2.81-01
	20.000	1.11+00	1.11+00	1.21+00	1.12+00	1.12+00	1.12+00	1.12+00	1.12+00	1.12+00	1.12+00	1.12+00	1.11+00
	30.000	2.50+00	2.51+00	2.69+00	2.51+00	2.52+00	2.52+00	2.52+00	2.51+00	2.49+00	2.48+00	2.47+00	2.45+00
	40.000	4.44+00	4.46+00	4.74+00	4.47+00	4.44+00	4.44+00	4.44+00	4.41+00	4.36+00	4.30+00	4.25+00	4.19+00
	50.000	6.88+00	6.90+00	7.29+00	6.90+00	6.90+00	6.88+00	6.87+00	6.79+00	6.63+00	6.48+00	6.34+00	6.20+00
	100.000	2.60+01	2.59+01	2.48+01	2.57+01	2.53+01	2.49+01	2.46+01	2.31+01	2.16+01	1.87+01	1.75+01	1.64+01
		10.0	14.7	14.7	20.0	30.0	40.0	50.0	100.0	200.0	300.0	400.0	500.0
ρ =2	.001	3.74-06	2.72-06		2.08-06	1.44-06	1.10-06	8.87-07	4.53-07	2.29-07	1.54-07	1.16-07	9.29-08
	.010	3.74-05	2.73-05	1.36-05	2.08-05	1.44-05	1.10-05	8.95-06	4.67-06	2.51-06	1.81-06	1.47-06	1.27-06
	.100	3.89-04	2.92-04	1.74-04	2.31-04	1.72-04	1.42-04	1.24-04	8.82-05	7.15-05	6.62-05	6.36-05	6.21-05
	1.000	8.15-03	7.42-03	6.99-03	6.97-03	6.53-03	6.31-03	6.17-03	5.90-03	5.76-03	5.71-03	5.69-03	5.67-03
	10.000	5.78-01	5.74-01	6.15-01	5.71-01	5.68-01	5.67-01	5.66-01	5.64-01	5.63-01	5.63-01	5.62-01	5.62-01
	20.000	2.22+00	2.23+00	2.41+00	2.23+00	2.24+00	2.24+00	2.24+00	2.24+00	2.23+00	2.22+00	2.21+00	2.21+00
	30.000	4.99+00	5.01+00	5.35+00	5.02+00	5.04+00	5.00+00	5.00+00	4.98+00	4.92+00	4.87+00	4.82+00	4.76+00
	40.000	8.80+00	8.82+00	9.33+00	8.83+00	8.83+00	8.81+00	8.79+00	8.69+00	8.47+00	8.28+00	8.10+00	7.9?+00
	50.000	1.36+01	1.37+01	1.42+01	1.37+01	1.36+01	1.35+01	1.35+01	1.32+01	1.26+01	1.22+01	1.18+01	1.14+01
	100.000	4.94+01	4.89+01	4.24+01	4.82+01	4.71+01	4.61+01	4.53+01	4.27+01	3.46+01	3.12+01	2.87+01	2.64+01
		10.0	14.7	14.7	20.0	30.0	40.0	50.0	100.0	200.0	300.0	400.0	500.0
ρ=3	.001	5.61-06	4.09-06		3.12-06	2.16-06	1.65-06	1.33-06	6.80-07	3.44-07	2.30-07	1.73-07	1.39-07
	.010	5.61-05	4.09-05	2.03-05	3.12-05	2.16-05	1.65-05	1.34-05	7.00-06	3.76-06	2.71-06	2.20-06	1.90-06
	.100	5.84-04	4.38-04	2.60-04	3.47-04	2.58-04	2.13-04	1.86-04	1.32-04	1.07-04	9.93-05	9.54-05	9.31-05
	1.000	1.22-02	1.11-02	1.05-02	1.05-02	9.80-03	9.46-03	9.26-03	8.85-03	8.63-03	8.57-03	8.53-03	8.51-03
	10.000	8.67-01	8.61-01	9.22-01	8.57-01	8.53-01	8.50-01	8.49-01	8.46-01	8.44-01	8.44-01	8.44-01	8.43-01
	20.000	3.33+00	3.34+00	3.62+00	3.35+00	3.36+00	3.36+00	3.36+00	3.37+00	3.33+00	3.31+00	3.30+00	3.28+00
	30.000	7.49+00	7.52+00	7.97+00	7.49+00	7.49+00	7.48+00	7.47+00	7.42+00	7.30+00	7.18+00	7.08+00	6.96+00
	40.000	1.31+01	1.32+01	1.38+01	1.32+01	1.31+01	1.31+01	1.31+01	1.28+01	1.24+01	1.20+01	1.17+01	1.13+01
	50.000	2.03+01	2.03+01	2.07+01	2.03+01	2.02+01	2.00+01	1.99+01	1.92+01	1.82+01	1.74+01	1.68+01	1.64+01
	100.000	7.09+01	7.00+01	5.83+01	6.89+01	6.73+01	6.59+01	6.49+01	5.44+01	4.63+01	4.11+01	3.74+01	3.40+01

Figure 6-a. Sedimentation Velocity of Spherical Particles vs Pressure
($He - O_2$; PO_2 = 160 mm Hg; T = 20°C; ρ = 1)

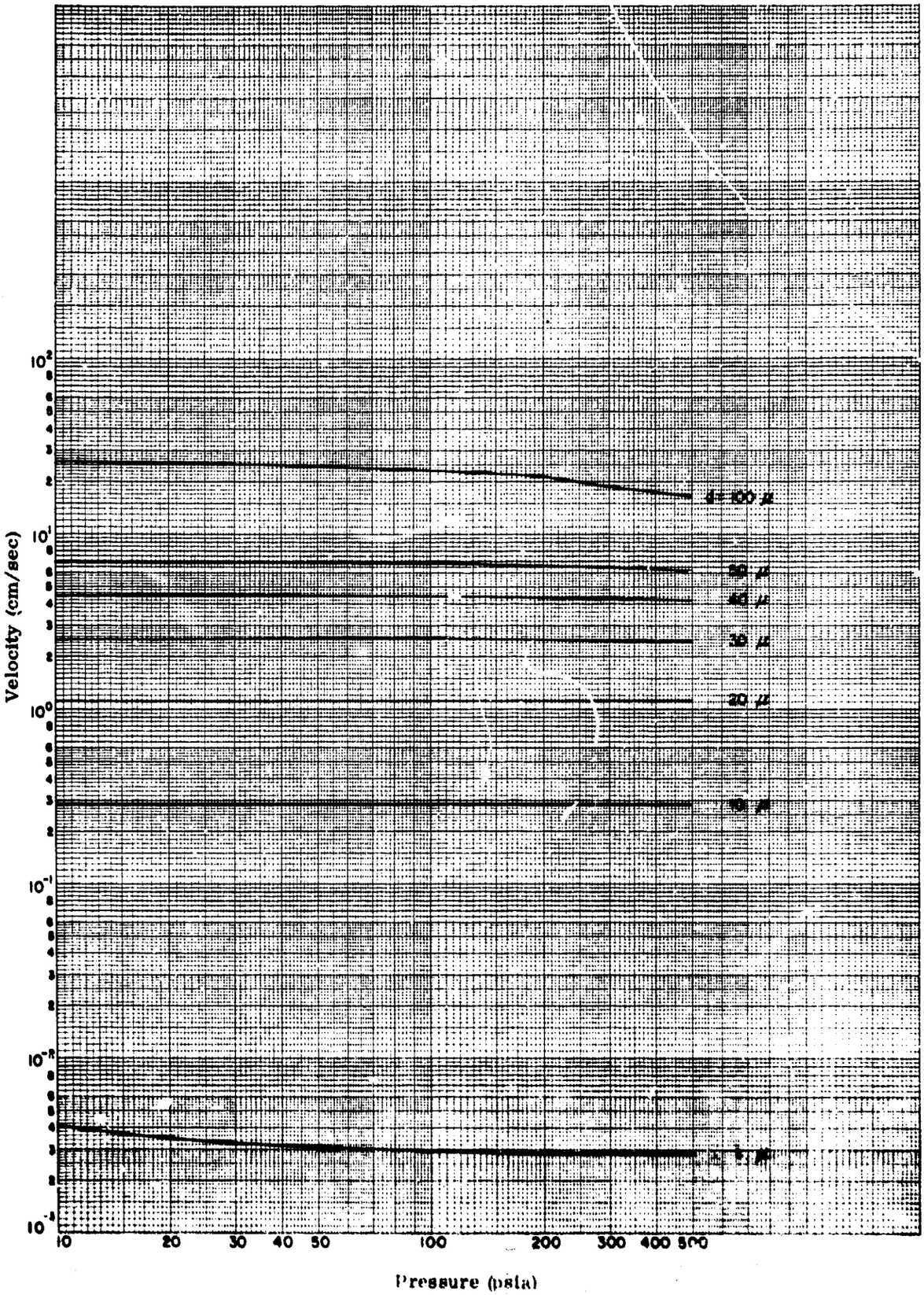

Figure 6-b. Sedimentation Velocity of Spherical Particles vs Pressure
(He - O_2; PO_2 = 160 mm Hg; T = 20°C; ρ = 1)

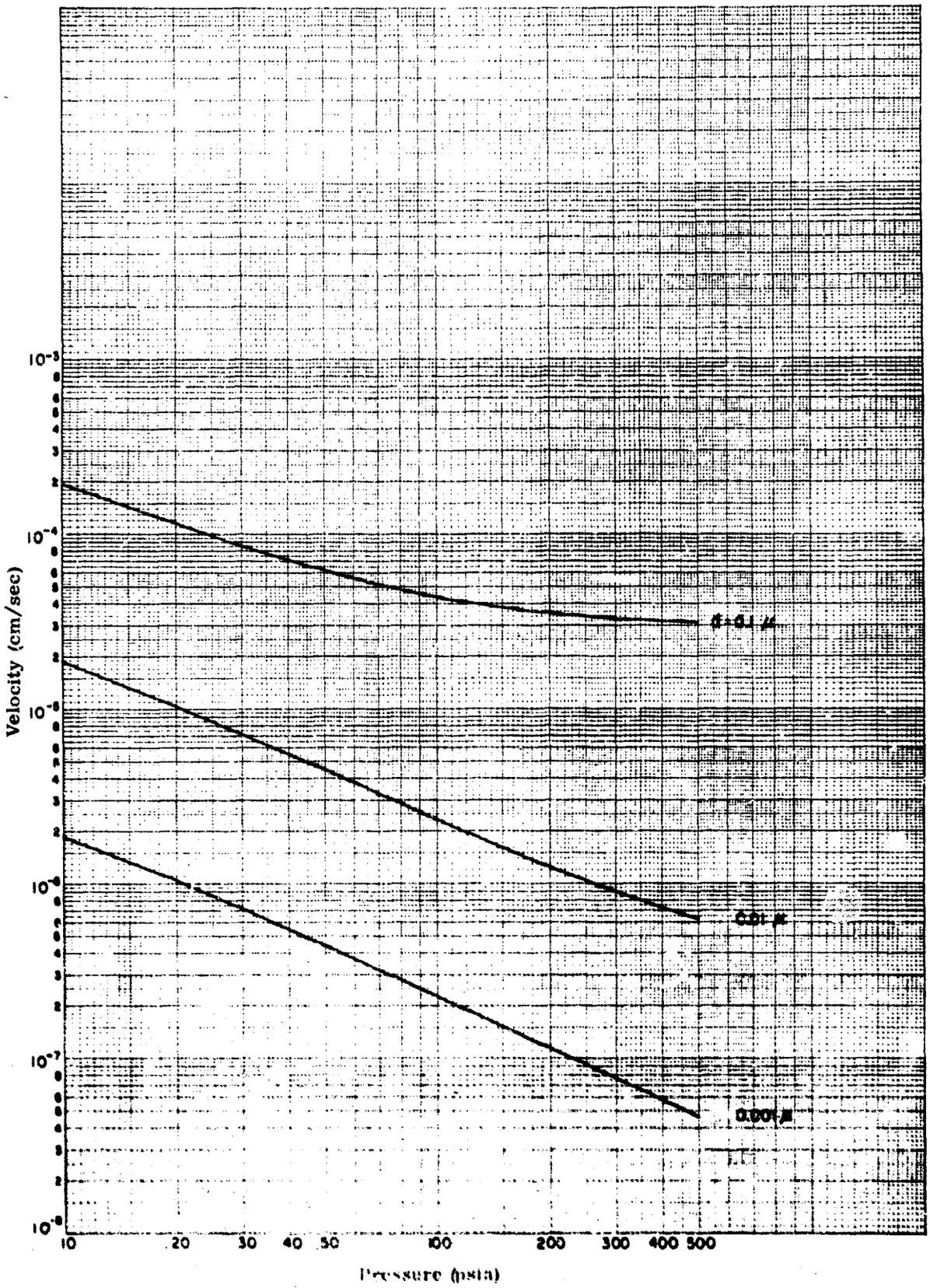

$$-\frac{dn}{dt} = \frac{nv}{h} \quad , \tag{15}$$

where

n = number concentration of particles,

v = sedimentation velocity, and

h = height of the vessel.

Integrating the above equation gives:

$$n = n_o \exp(-vt/h) \quad , \tag{16}$$

where

n_o = the initial concentration of particles, and

n = concentration at any time t.

5.3 DIFFUSION

The diffusion of aerosol particles in a gas is the result of their bombardment by molecules of the gas, i.e., Brownian motion. Generally, the diffusional movement of particles is not considered for sizes above 10 microns and usually the calculations are applied only to particles below 1 micron. In considering the effects of the high pressure helium-oxygen atmosphere on diffusivity of aerosols, the factor to be evaluated is the diffusion coefficient, expressed as:[5]

$$D = kBT \text{ (slip correction)} \quad , \tag{17}$$

where

k = Boltzmann's constant,

B = mobility, and

T = absolute temperature.

Boltzmann's constant is the universal gas constant divided by Avogadro's number and has an accepted value of 1.3708×10^{-16} erg/^{o}C. Neither of these constants is affected by pressure or composition for an ideal gas.

The mobility (B) of the particle is defined as:

$$B = \frac{1}{3 \pi \eta d} \quad , \tag{18}$$

where

d = diameter of the particle and

η = viscosity of the fluid medium.

This is principally a definition of convenience since this quantity appears in several calculations of use in aerosol physics and tables of mobility versus diameter have been computed by various authors.[6,7] The only terms in the mobility expression that are affected by gas composition and pressure are the viscosity of the gas (which has been shown to be almost invariant over the range considered) and the slip correction (which has been discussed previously). The chart and graph shown here (Figure 7) for diffusion coefficient vs diameter are for all pressures of the mixture up to 500 psi.

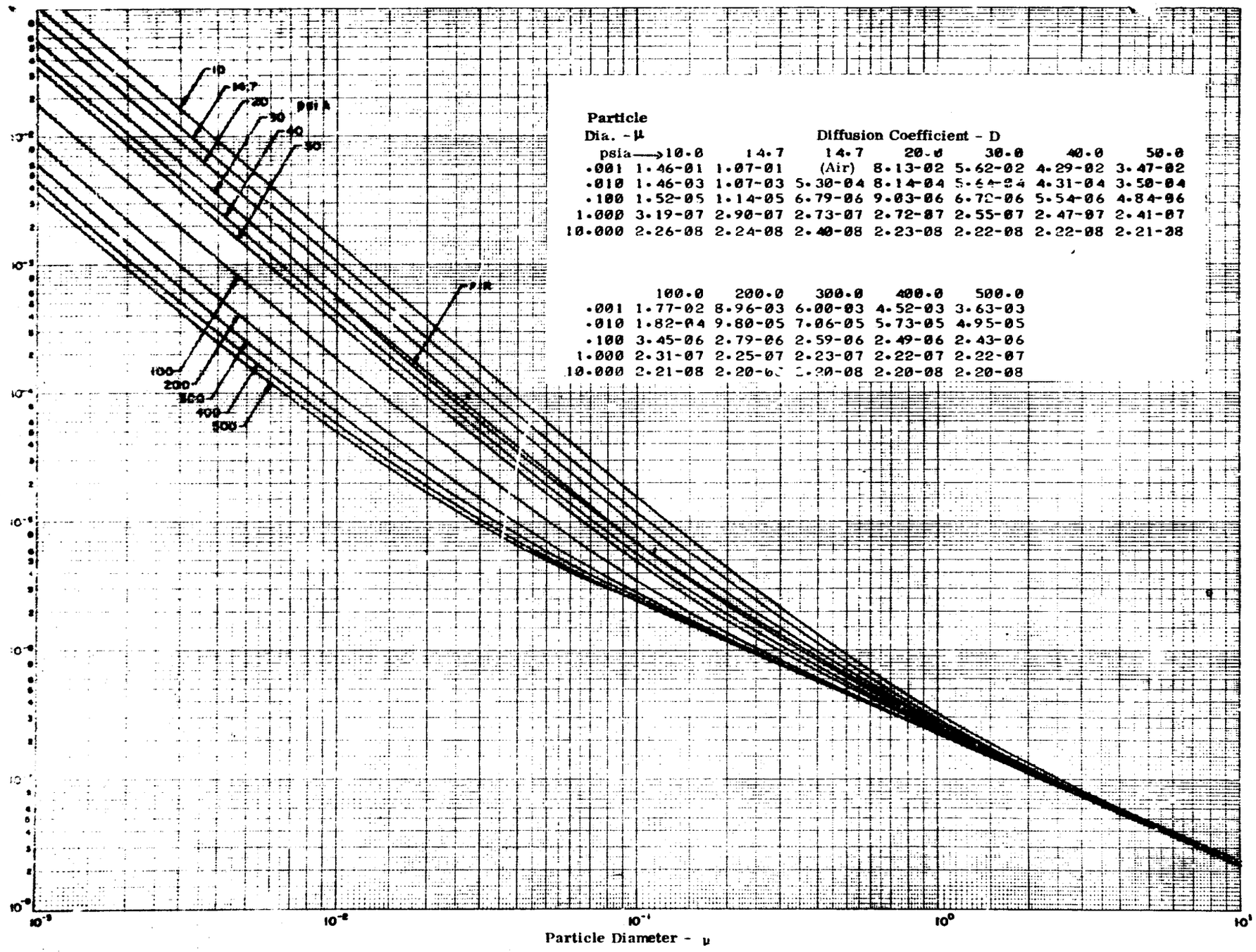

Figure 7. Particle Diffusion Coefficient vs Diameter (He - O_2; PO_2 = 160 mm Hg; T = 20°C)

Considering the reduction in numbers concentration in a confined spherical space due to diffusion, Fuchs[11] states the following equation in the form of an infinite series:

$$n = n_o \frac{6}{\pi^2} \sum_{\theta=1}^{\infty} \frac{1}{\theta^2} \exp\left(- D \pi^2 \theta^2 t/R^2\right) , \qquad (19)$$

where

n_o = initial concentration of particles,

n = concentration at time t,

D = diffusion coefficient,

t = time,

R = radius of sphere, and

θ = integer,

Actually, there are several relationships presented by Fuchs for different specific configurations in which: or to which, diffusion is occurring. The spherical one illustrates an example relationship and is presented because there are two possible spherical volumes of interest to this study: viz., deep submersible vessels and the alveoli of the lung.

5.4 AGGLOMERATION

Agglomeration is a continuous and spontaneous property found, to some degree, in all aerosols. In their random Brownian movements, aerosol particles

undergo numerous collisions with each other, depending upon the number concentration of the particles. Usually these collisions are "effective"; that is, when two particles touch, they remain together and form an agglomerate. The classical work on this subject was done by Whytlaw-Gray and Patterson[12] and the most recent concise reviews of all the factors that describe this mechanism are presented by Green and Lane[5] and Zebel.[13] In the simple case of a monodispersed aerosol, the equation describing the rate of concentration decrease is:

$$-\frac{dn}{dt} = \frac{2}{3}\frac{k\,T\,S}{\eta}\,n^2 \quad \text{(slip correction)} \quad , \tag{20}$$

where

$$\left[\frac{2}{3}\frac{k\,T\,S}{\eta}\right] = K = \text{coagulation coefficient,} \tag{21}$$

k = Boltzmann's constant,

T = absolute temperature,

η = viscosity of the fluid medium,

n = number concentration of particles,

S = ratio of particles sphere of influence to particle radius = 2 for "effective" collisions, and

t = time.

This equation does not account for any other losses in the system (e.g., diffusion to containing walls or sedimentation) and, therefore, measurements are generally done on aerosols for which these factors may be neglected.

The K factor varies among aerosols. However, if it is assumed that no other losses are present and that all collisions are "effective", then the above relationship may be integrated and a general equation for the coagulation coefficient may be written as:

$$\frac{1}{n} - \frac{1}{n_o} = \frac{4}{3} \frac{k\,T}{\eta}\, t \text{ (slip correction)} \quad , \tag{22}$$

where

n_o = initial concentration of particles, and

n = concentration at time t.

There are many factors that affect the rate of agglomeration, such as degree of heterodispersity (i.e., all the particles not being initially monodispersed) plus mixtures of particles of various sbustances, turbulence, particle shape, effects of the dispersion medium, differential settling, electrical effects, temperature, pressure and viscosity. All these factors have been dealt with to some degree and either increase or decrease the agglomeration rate. Specific data has been obtained for special cases; but, as a consequence of a review of these factors,[14] we have concluded that, for a specific case, the effect of interest must be evaluated and useful generalizations are very sparse.

For the purposes of this study, we have shown that changes in the medium's viscosity over the considered pressure range are slight and ~~that~~ therefore

the only direct effect on the coagulation rate will be due to the slip correction, which decreases with increasing pressure and increasing particle size to yield a net decrease in the agglomeration rate with increasing pressure. Indirect verification of this conclusion may be obtained from the studies of Cawood and Whytlaw-Gray;[15] they worked with reduced pressures that increased the slip correction and, therefore increased the agglomeration rate. These investigators were, in fact, able to demonstrate successfully the predicted increase in the agglomeration rate with decreasing pressure. For purposes of simple calculations, Figure 8, with the accompanying table for the helium-oxygen atmosphere, gives the K factor for the pressures and size ranges of interest.

5.5 COMBINED EFFECTS OF SEDIMENTATION, DIFFUSION AND AGGLOMERATION

The preceding discussions of sedimentation, diffusion, and agglomeration have shown that for other than the slip correction factor, there is little to be considered because of the high helium content of the atmosphere and the pressure range involved.

For the examination of the combined agglomeration, diffusion, and sedimentation, consider a spherical vessel containing an aerosol that ideally, is monodispersed. Within this sphere, the numbers concentration, n, is continuously decreasing due to (1) loss of particles settling to the floor (sedimentation), (2) loss of particles

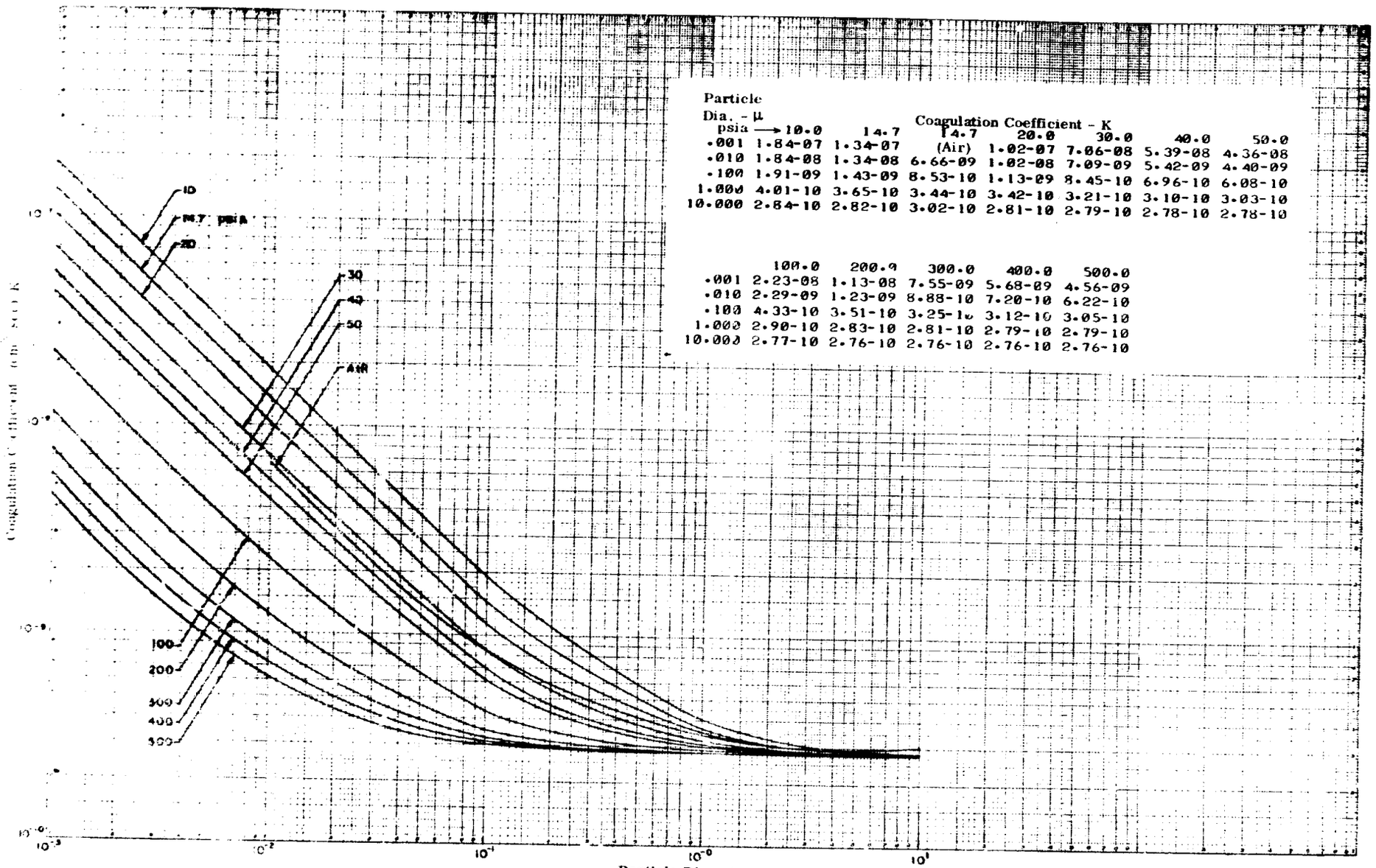

Figure 8. Coagulation Coefficient vs Particle Diameter (He - O_2; PO_2 = 160 mm Hg; T = 20°C)

migrating to all surfaces (diffusion), and (3) loss of particles sticking to each other subsequent to collision (agglomeration). While agglomeration does not strictly constitute a reduction in the mass of material airborne, it does mean a change in numbers concentration. Investigators seldom consider these three mechanisms in conjunction for reasons other than the difficulty involved. The diffusion mechansim is chiefly important for submicron aerosols in which the effects of sedimentation are very slight. Conversely, when the sedimentation rate of an aerosol is considered to be of importance, the diffusional mobility of the particles is generally quite small and may not be evaluated. Since agglomeration is a major function of the numbers concentration of the particles, it applies to both cases. (Other size-dependent factors do enter into the complex (real) situation.) Sinclair[11] considers combined coagulation and stirred settling by simply adding the differential equations for agglomeration and settling:

$$-\frac{dn}{dt} = K n^2 + \frac{v}{h} n \quad , \tag{23}$$

which directly integrates to the form:

$$\frac{1}{n} = \frac{Kh}{v} + \frac{Kh}{v} + \frac{1}{n_o} \exp(-vt/h) \quad . \tag{24}$$

It is difficult to state the precise particle size range over which it is possible for the effects of both diffusion and sedimentation to be of simultaneous importance such

that a combined equation must be considered. However, knowing that the effects of diffusion become quite small above 1 micron and the effects of sedimentation are (similarly) not significant below 1 micron, we may conclude that the approximate order of magnitude between 0.1 and 1 micron is worthy of consideration. Green and Lane[5] present the attempts of Davies to solve a combined equation for diffusion and sedimentation in a vessel in which it is assumed that there is no diffusional loss to the walls (i.e., infinitely wide) and the only losses are by sedimentation and diffusion to the floor and by diffusion to the ceiling. According to Green and Lane, the results are extremely complex and involve the reduction of all physical values to dimensionless units.

In view of the preceding difficulties and the highly ideal nature of the calculations, it is difficult to present a strong argument for proceeding with the development of a combined equation for the three mechanisms in a spherical vessel. Nevertheless, the references on submarine atmosphere reviewed to date indicate that a good deal of the mass present will be in the 0.1 to 1 micron size range and the final development of realistic equations have usually been observed to begin from idealized considerations.

In the preceding sections on diffusion, sedimentation and agglomeration, the rate equations for the reduction of particle number concentration have been stated. Before an attempt at combining these can be made, it should be noted that the

equation for the rate of sedimentation is for an infinitely wide container in which there is no deposition on the walls. A separate derivation is required for the sphere. Beginning with the basic relationship that the change in concentration is equal to the concentration in, minus the concentration out, the following development may be undertaken according to Billings.[16]

$$\Delta \text{ conc.} = \text{conc. in} - \text{conc. out}$$

where:

conc. in = 0 (no particles added to the environment.)

For the sphere containing a concentration of monodispersed particles undergoing stirred settling:

$$\left(\frac{4}{3}\pi R^3\right) \Delta n = 0 - (\pi R^2)\, nv\Delta t \tag{25}$$

$$-\frac{\Delta n}{n} = \frac{\pi R^2}{4/3\ \pi R^3}\, v\Delta t \tag{26}$$

$$-\frac{dn}{dt} = \frac{3}{4}\frac{v}{R}\, n \tag{27}$$

$$n = n_o \exp\ (-\ 3vt/4R) \tag{28}$$

The actual combination of the three rate equations is not amenable to direct addition and integration. This is due to the fact that the Fuch's equation for diffusion within a sphere is in the form of an infinite series and may not be put directly in integral form.

We have previously attempted such a combination, but, while moderately successful, we required computer approximations for its solution and, therefore judged the combination of little practical value.[17] Booth states, without proof, that Eq. 19 (Fuch's diffusion equation) may be reduced to a nonseries form provided that the time is sufficiently short so that 80% of the original concentration remains airborne (i.e., less than 20% of the original material is deposited on the walls due to diffusion). This solution is

$$1 - \frac{n}{n_0} = 6\sqrt{\frac{Dt}{\pi R^2}} - 3\frac{Dt}{R^2} . \qquad (29)$$

Before proceeding further with Eq. 29 we determine to ascertain the validity of the transformation, inasmuch as it is not readily apparent. This verification was accomplished in two ways: First, since Eq. 29 is stated as valid when the quantity $\pi^2 Dt/R^2 \leq 1$, we substituted $\pi^2 Dt/R^2$ into Eqs. 19 and 29 at values ranging from 0 to 1. This simple technique produced an almost perfect agreement between the two equations. Second, we decided to determine the method of transformation, because the approximation represented by Eq. 29 in simplifying a series equation seems of such real importance to aerosol physics. Although there is no way of knowing the original method, the following solution has been obtained.

Differentiate Eq. 19 with respect to time, obtaining

$$\left(-\frac{dn}{dt}\right)_{diff} = \frac{n_0 D}{R^2} \sum_{\theta=1}^{\infty} e^{-\beta^2 \theta^2} , \qquad (30)$$

defining:

$$\beta^2 = \frac{\pi^2 D t}{R^2} \tag{31}$$

The series may be evaluated by means of the Poisson summation formula,[18]

$$\sum_{\theta=-\infty}^{\infty} f(2\pi\theta) = \frac{1}{2\pi} \sum_{\theta=-\infty}^{\infty} \int_{-\infty}^{\infty} f(x) e^{-i\theta x} dx \ , \tag{32}$$

which is valid for any continuous and continuously differentiable function f(x). For an even function, Eq. 32 becomes

$$f(0) + 2 \sum_{\theta=1}^{\infty} f(2\pi\theta) = \frac{1}{\sqrt{2\pi}} \left[F(0) + 2 \sum_{\theta=1}^{\infty} F(\theta) \right] \ , \tag{33}$$

where F(k) is the Fourier cosine transform of f(x):

$$F(k) = \sqrt{2/\pi} \int_0^{\infty} f(x) \cos\theta x \ dx \ . \tag{34}$$

Applying Eq. 33 to the function $f(x)=\exp(-\beta^2 x^2/4\pi^2)$, yields

$$\sum_{\theta=1}^{\infty} e^{-\beta^2\theta^2} = \frac{\sqrt{\pi}}{2\beta} - \frac{1}{2} + S \ , \tag{35}$$

where

$$S = \frac{\sqrt{\pi}}{\beta} \sum_{\theta=1}^{\infty} \exp(-\pi^2\theta^2/\beta^2) \tag{36}$$

can be neglected for $\beta << 1$. Combining Eqs. 30 and 35 and integrating, yields the relationship expressed by Eq. 29.

Differentiating Eq. 29 and substituting for n_0 in terms of n, yields

$$\left(-\frac{dn}{dt}\right)_{diff} = \frac{3n\left(\sqrt{\frac{D}{\pi tR^2}} - \frac{D}{R^2}\right)}{1 - 6\sqrt{\frac{Dt}{\pi R^2}} + \frac{3Dt}{R^2}} . \qquad (37)$$

Since only the initial stages of the diffusion process are being considered when the quantity Dt/R^2 is very small, the denominator in Eq. 37 is sufficiently close to 1 so that it can be neglected and the equation reduced to

$$\left(-\frac{dn}{dt}\right)_{diff} = 3n\left(\sqrt{\frac{D}{\pi tR^2}} - \frac{D}{R^2}\right) . \qquad (38)$$

The equations for agglomeration (20), sedimentation (27), and diffusion (38) may now be summed to give this differential equation for the total concentration:

$$-\frac{dn}{dt} = Kn^2 + \frac{3vn}{4R} + 3n\left(\sqrt{\frac{D}{\pi tR^2}} - \frac{D}{R^2}\right) . \qquad (39)$$

Before proceeding with the solution of Eq. 39, it is necessary to estimate the range of variation of the constant coefficients. Pressures of interest range from 10 to 500 psia, particle diameters of 10^{-5} to 10^{-4} cm, and vessel radii of 1 to 100 cm.

Under these conditions, the orders of magnitude of v, D, and K are $v = 10^{-5}$ to 10^{-3} cm/sec, $D = 10^{-7}$ to 10^{-5} cm^2/sec, and $K = 10^{-10}$ to 10^{-9} cm^3/sec.

Expressing Eq. 39 in the form

$$\frac{dn}{dt} + g(t)n + Kn^2 = 0 \ , \tag{40}$$

with

$$g(t) \equiv p + \frac{1}{2} qt^{-\frac{1}{2}} \ , \tag{41}$$

where

$$p \equiv \frac{3}{4} \frac{v}{R} - \frac{3D}{R^2} \tag{42}$$

$$q \equiv 6 \sqrt{\frac{D}{\pi R^2}} \ . \tag{43}$$

This is an ordinary differential equation of the Bernoulli type and may be solved by standard methods.[19] Under the transformation $u=n^{-1}$, the equation becomes

$$\frac{du}{dt} - g(t)u = K \ , \tag{44}$$

whose solution in terms of quadratures is

$$u(t) = e^{\int g(t)dt} \left(c + \int_0^t K e^{-\int g(t)dt} \right) \ , \tag{45}$$

where A is an integration constant and

$$G(t) = \int_0^t g(t)dt = pt + qt^{\frac{1}{2}} \quad . \tag{46}$$

From the initial condition $u=1/n_o$ at $t=0$, it follows that $A=1/n_o$. With the transformation $y=i(p^{1/2}t^{1/2} + \frac{1}{2}qp^{-1/2})$, the integration in Eq. 45 can be performed, with the result

$$\frac{1}{n} = -\frac{K}{p} + \left\{\frac{K}{p}[1 + H(t)] + \frac{1}{n_0}\right\}e^{G(t)} \quad , \tag{47}$$

where

$$H(t) = \exp\left(-\frac{q^2}{4p^2}\right)\frac{q}{2}\sqrt{\frac{\pi}{p}}\left[\operatorname{erf}\left(\frac{q}{2\sqrt{p}}\right) - \operatorname{erf}\left(\frac{q}{2\sqrt{p}} + \sqrt{pt}\right)\right] \quad . \tag{48}$$

The function erf(x) is the standard error function

$$\operatorname{erf}(x) = \int_0^x e^{-z^2}dz$$

for which tabulated values exist.[20] Equation 47, together with Eqs. 46 and 48, represent the exact solution of Eq. 39.

Under the conditions stated above, the factor $q/2\sqrt{p}$ is of the order of magnitude of 10^{-2}. Therefore, take $\exp(-q^2/4p^2) \approx 1$ and use the small argument expansion[19] for erf(x),

$$\operatorname{erf}(x) = \frac{2}{\sqrt{\pi}}\left(x - \frac{x^3}{3} + \cdots\right) \quad ,$$

to obtain $H(t) \sim -q\sqrt{t}$. Since q is of the order of magnitude of 10^{-4} to 10^{-3}, note that $H(t) \ll 1$ for ordinary times, so that H(t) may be neglected in Eq. 47. The final result is

$$\frac{1}{n} = -\frac{4KR}{3v} + \left(\frac{4KR}{3v} + \frac{1}{n_0}\right) e^{G(t)} \tag{49}$$

where

$$G(t) = -\frac{3vt}{4R} + \frac{6}{R}\sqrt{\frac{Dt}{\pi}} \ . \tag{50}$$

For a very small t, it is possible to further approximate $\exp[G(t)] \simeq 1+G(t)$ to obtain

$$\frac{1}{n} \approx \frac{1}{n_0} + \left(\frac{1}{n_0} + \frac{4KR}{3v}\right) G(t) \ . \tag{51}$$

Note that with D=0 and 4R/3 replaced by h, the solution given by Eq. 49 reduces to that given by Sinclair[21] for the problem of combined coagulation and settling in a rectangular box of height h.

The approximations used to obtain Eq. 49 become more inexact as the vessel radius R decreases. For R less than a few centimeters, one should use the exact expression given by Eqs. 47 and 48.

As a final point, note that if the denominator in Eq. 37 is not approximated by unity, the integrations required to determine G(t) and $\int_0^t \exp[-G(t)]\, dt$ can still be performed by standard methods, although the result is much more complex than Eq. 48. However,

under the stated conditions the numerical results would not differ significantly, so that the more complex analytical form would not have more practical value than does Eq. 48.

SECTION 6.0: EVAPORATION, CONDENSATION AND NUCLEATION

The purpose of considering the evaporation, condensation, and nucleation of materials within the helium-oxygen environment is to permit a determination of the promotion or inhibition of aerosol existence due to the high-pressure, helium-rich atmosphere involved. While it would be desirable to examine a long list of materials and consider their propensity to exist as aerosols under the increasing pressure, we have observed a singular lack of the necessary information and a complexity in the computations that has restricted the consideration to water vapor.

The evaporation (condensation) rate of droplets is given varied presentation in modern literature, especially by Fuchs,[22] Orr,[23] Amelin,[24] and Green and Lane.[5] The basic equation is presented in various ways; however, all the developments may be stated in the following form:

$$-\frac{dm}{dt} = \frac{2\pi\, d\, M_1\, D_{1(23)}}{R\,T} \times \frac{(\delta\, p_t - p)}{\xi\, D_{1(23)}/d\upsilon\alpha + \dfrac{2}{d + 2\Delta}} \qquad (52)$$

where

d = droplet diameter - cm,

M_1 = molecular weight of the liquid vapor - g/mole,

$D_{1(23)}$ = diffusivity of the liquid vapor through the gas - cm^2/sec,

R = gas constant - 8.317×10^7 ergs/^oK-mole,

T = temperature - ^{o}K,

δ = degree of saturation (1 = 100% RH, this value used for all calculations),

p_t = vapor pressure of the liquid - dynes/cm^2 (see Appendix III)

p = vapor pressure of the droplet - dynes/cm^2 (see Appendix III)

$\upsilon = (RT/2\pi M_1)^{1/2}$ - cm/sec,

α = evaporation (condensation) coefficient - 0.04 for H_2O, and

$\Delta \approx \lambda$ the mean free path of the molecules - cm.

The Δ function given in the above equation is a development of Fuchs;[22] he found certain deficiencies in Langmuir's[5] relationship when the droplets considered were small or the pressure was low. Basically, Fuchs' theory considers that molecules are coming to or leaving a spherical shell that envelops the droplet and whose thickness equals approximately the mean free path length of a molecule (λ). Green and Lane report that this theory has been tested and found to account for the deficiencies in Langmuir's formula. While it is not a necessary correction over the entire size range considered, it is simpler, for machine computations, to use it in all cases. The results of these calculations are shown in Figure 9 and Table 6; these illustrations show that increasing pressure and an increasing mole fraction of helium results in decreased evaporation (condensation) rate. In addition, Figure 9, points up that the rate is nearly constant for the smallest size droplets considered but undergoes order of magnitude decreases for the larger particles when the pressure is increased.

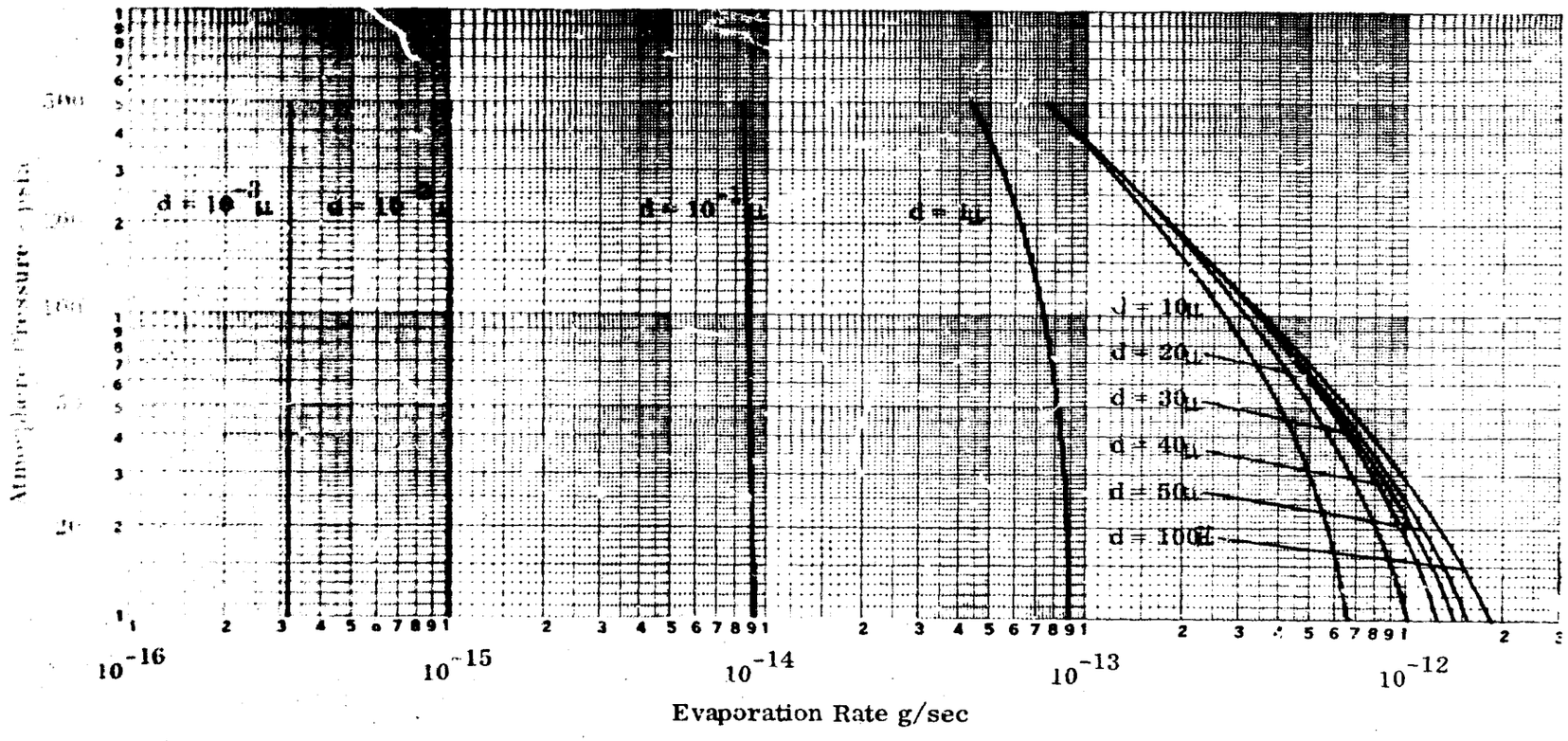

Figure 9. Oxygen-Helium Atmosphere Pressure vs H_2O Droplet Evaporation Rate. (PO_2 = 160 mm Hg; PH_2O = 23.37 mm Hg; T = 20°C)

Table 6. Oxygen Helium Atmosphere Pressure and Droplet Diameter vs:
Droplet Vapor Pressure
Droplet Temperature
Droplet Evaporation Rate
Droplet Evaporation Time

	P Atmosphere Pressure psia	p Droplet Vapor Pressure dynes/cm^2	T_d = 293- Droplet Temp. (depression) ^oK	dm/dt Droplet Evap. (cond.) Rate g/sec	t Droplet Evap. Time sec
$d = 10^{-3}\mu$	10.0	.26734572+06	.25711516-01	-.32181549-14	-.48703032-06
	14.7	.26733573+06	.20617039-01	-.32180186-14	-.48714447-06
	20.0	.26732983+06	.17590911-01	-.32179379-14	-.48721438-06
	30.0	.26732411+06	.14693715-01	-.32178590-14	-.48728037-06
	40.0	.26732122+06	.13206584-01	-.32178185-14	-.48731320-06
	50.0	.26731948+06	.12301578-01	-.32177935-14	-.48733185-06
	100.0	.26731578+06	.10462177-01	-.32177322-14	-.48736022-06
	200.0	.26731401+06	.95273826-02	-.32176667-14	-.48735094-06
	300.0	.26731337+06	.92133751-02	-.32175915-14	-.48733051-06
	400.0	.26731308+06	.90557902-02	-.32174977-14	-.48730972-06
	500.0	.26731291+06	.89609442-02	-.32173832-14	-.48729082-06
$d = 10^{-2}\mu$	10.0	.38622619+05	.81320512-02	-.10178396-13	-.15396663-03
	14.7	.38622573+05	.65209600-02	-.10178266-13	-.15399311-03
	20.0	.38622547+05	.55638927-02	-.10178132-13	-.15400762-03
	30.0	.38622520+05	.46475142-02	-.10177852-13	-.15401807-03
	40.0	.38622506+05	.41770608-02	-.10177517-13	-.15402074-03
	50.0	.38622499+05	.38906987-02	-.10177121-13	-.15402062-03
	100.0	.38622482+05	.33080700-02	-.10174252-13	-.15401534-03
	200.0	.38622473+05	.30098165-02	-.10165002-13	-.15403692-03
	300.0	.38622470+05	.29071068-02	-.10152504-13	-.15409549-03
	400.0	.38622469+05	.28533432-02	-.10137851-13	-.15417898-03
	500.0	.38622468+05	.28190629-02	-.10121708-13	-.15427959-03
$d = 10^{-1}\mu$	10.0	.31829084+05	.73626242-02	-.92153511-13	-.16983965-01
	14.7	.31829080+05	.59012367-02	-.92109685-13	-.16989034-01
	20.0	.31829078+05	.50320456-02	-.92052138-13	-.16994231-01
	30.0	.31829076+05	.41976395-02	-.91926463-13	-.17004547-01
	40.0	.31829075+05	.37670186-02	-.91784388-13	-.17016199-01
	50.0	.31829075+05	.35030392-02	-.91630981-13	-.17029089-01
	100.0	.31829073+05	.29515466-02	-.90777344-13	-.17103693-01
	200.0	.31829073+05	.26337934-02	-.88950656-13	-.17274407-01
	300.0	.31829072+05	.24930241-02	-.87133849-13	-.17454427-01
	400.0	.31829072+05	.24027696-02	-.85369751-13	-.17637929-01
	500.0	.31829072+05	.23302616-02	-.83666905-13	-.17823156-01

Table 6. Continued

	P Atmosphere Pressure psia	p Droplet Vapor Pressure dyner/cm^2	T_d 293-+ Droplet Temp. (depression) ^oK	dm/dt Droplet Evap. (cond.) Rate g/sec	t Droplet Evap. Time sec
d = 1μ	10.0	.31219245+05	.70975289-02	-.88835474-12	-.17346023+01
	14.7	.31219244+05	.56351613-02	-.87956636-12	-.17437458+01
	20.0	.31219244+05	.47545789-02	-.86976388-12	-.17539561+01
	30.0	.31219244+05	.38696379-02	-.85181363-12	-.17730528+01
	40.0	.31219244+05	.34252060-02	-.83456034-12	-.17921060+01
	50.0	.31219244+05	.31271420-02	-.81798425-12	-.18111464+01
	100.0	.31219243+05	.24192474-02	-.74406024-12	-.19063790+01
	200.0	.31219243+05	.18658367-02	-.63014583-12	-.20970136+01
	300.0	.31219243+05	.15648042-02	-.54647734-12	-.22877485+01
	400.0	.31219243+05	.13578010-02	-.48242301-12	-.24785182+01
	500.0	.31219243+05	.12026602-02	-.43180927-12	-.26693056+01
d = 10μ	10.0	.31158907+05	.52720059-02	-.65986506-11	-.20381115+03
	14.7	.31158907+05	.39349192-02	-.61418339-11	-.21275358+03
	20.0	.31158907+05	.31122174-02	-.56932364-11	-.22288624+03
	30.0	.31158907+05	.22841803-02	-.50022546-11	-.24199692+03
	40.0	.31158907+05	.18305571-02	-.44601993-11	-.26110725+03
	50.0	.31158907+05	.15383532-02	-.40239575-11	-.28021491+03
	100.0	.31158907+05	.10855145-03	-.27020598-11	-.37573626+03
	200.0	.31158907+05	.48280757-03	-.16305778-11	-.56675572+03
	300.0	.31158907+05	.33432673-03	-.11675708-11	-.75776997+03
	400.0	.31158907+05	.25594210-03	-.90935531-12	-.94878243+03
	500.0	.31158907+05	.20740208-03	-.74466699-12	-.11397944+04
d = 20μ	10.0	.31155558+05	.40924798-02	-.10244619-10	-.95226296+03
	14.7	.31155558+05	.29437147-02	-.91894169-11	-.10231020+04
	20.0	.31155558+05	.22475676-02	-.82230336-11	-.11037174+04
	30.0	.31155558+05	.15655905-02	-.68571471-11	-.12561728+04
	40.0	.31155558+05	.12063515-02	-.58786130-11	-.14088310+04
	50.0	.31155558+05	.98326646-03	-.51439701-11	-.15615584+04
	100.0	.31155558+05	.51453403-03	-.31649860-11	-.23254783+04
	200.0	.31155558+05	.26477478-03	-.17884382-11	-.38535703+04
	300.0	.31155558+05	.17843971-03	-.12463314-11	-.53817188+04
	400.0	.31155558+05	.13459428-03	-.95641939-12	-.69098767+04
	500.0	.31155558+05	.10805439-03	-.77592781-12	-.84380391+04
d = 30μ	10.0	.31154442+05	.33439820-02	-.12556374-10	-.24512836+04
	14.7	.31154442+05	.23512966-02	-.11018092-10	-.26894520+04
	20.0	.31154442+05	.17588581-02	-.96525346-11	-.29609552+04
	30.0	.31154442+05	.11909196-02	-.78241852-11	-.34749311+04
	40.0	.31154442+05	.89959353-03	-.65756483-11	-.39898603+04
	50.0	.31154442+05	.72254784-03	-.56700280-11	-.45051380+04
	100.0	.31154442+05	.36379908-03	-.33566842-11	-.70830391+04
	200.0	.31154442+05	.18240318-03	-.18480885-11	-.12240247+05
	300.0	.31154442+05	.12169637-03	-.12750020-11	-.17397780+05
	400.0	.31154442+05	.91304780-04	-.97320980-12	-.22555375+05
	500.0	.31154442+05	.73058635-04	-.78694083-12	-.27712999+05

Table 6. Continued

	P Atmosphere Pressure psia	p Droplet Vapor Pressure dynes/cm^2	T_d = 293 - Droplet Temp. (depression) ^oK	dm/dt Droplet Evap. (cond.) Rate g/sec	t Droplet Evap. Time sec
d = 40μ	10.0	.31153884+05	.28268928-02	-.14153003-10	-.49068336+04
	14.7	.31153884+05	.19573590-02	-.12220606-10	-.54702338+04
	20.0	.31153884+05	.14447128-02	-.10571353-10	-.61130765+04
	30.0	.31153884+05	.96094698-03	-.84177250-11	-.73306918+04
	40.0	.31153884+05	.71721514-03	-.69900493-11	-.85508987+04
	50.0	.31153884+05	.57111354-03	-.59755762-11	-.97720744+04
	100.0	.31153884+05	.28137065-03	-.34615181-11	-.15882219+05
	200.0	.31153884+05	.13912223-03	-.18794194-11	-.28106589+05
	300.0	.31153884+05	.92334443-04	-.12898401-11	-.40331820+05
	400.0	.31153884+05	.69085094-04	-.98182985-12	-.52557281+05
	500.0	.31153884+05	.55185658-04	-.79256518-12	-.64782864+05
d = 50μ	10.0	.31153549+05	.24482906-02	-.15321886-10	-.85248769+04
	14.7	.31153549+05	.16764736-02	-.13083643-10	-.96238957+04
	20.0	.31153549+05	.12657769-02	-.11211682-10	-.10878552+05
	30.0	.31153549+05	.80541634-03	-.88191322-11	-.13255867+05
	40.0	.31153549+05	.59631987-03	-.72647391-11	-.15638657+05
	50.0	.31153549+05	.47215689-03	-.61752333-11	-.18023503+05
	100.0	.31153549+05	.22939509-03	-.35276201-11	-.29956848+05
	200.0	.31153549+05	.11244174-03	-.18987365-11	-.53832455+05
	300.0	.31153549+05	.74386848-04	-.12989078-11	-.77709901+05
	400.0	.31153549+05	.55563267-04	-.98707390-12	-.10158785+06
	500.0	.31153549+05	.44338630-04	-.79597842-12	-.12546599+06
d = 100μ	10.0	.31152880+05	.14663280-02	-.18353114-10	-.51261526+05
	14.7	.31152880+05	.97609804-03	-.15235465-10	-.60030483+05
	20.0	.31152880+05	.69736633-03	-.12757033-10	-.70053303+05
	30.0	.31152880+05	.44516237-03	-.97488467-11	-.89057971+05
	40.0	.31152880+05	.32359262-03	-.78844071-11	-.10811278+06
	50.0	.31152880+05	.25298412-03	-.66174395-11	-.12718718+06
	100.0	.31152880+05	.11925196-03	-.36676961-11	-.22264536+06
	200.0	.31152880+05	.57400923-04	-.19385916-11	-.41364704+06
	300.0	.31152880+05	.37723878-04	-.13174328-11	-.60466740+06
	400.0	.31152880+05	.28081644-04	-.99773178-12	-.79569349+06
	500.0	.31152880+05	.22361924-04	-.80289396-12	-.98671915+06

Two formulas determine the lifetime of a given size droplet. One is according to Langmuir; the other is derived from Fuchs and includes his expression for the vapor shell (Δ) surrounding the droplet. According to Green and Lane,[5] the difference between the two becomes significant below 1 micron initial droplet diameter and therefore the Fuchs relationship has been utilized as being correct for all purposes. The net effect of utilizing the Fuchs expression is that longer droplet lifetimes are found than with the Langmuir expression:

$$t = \frac{d\, R\, T\, \rho_L}{2 \alpha\, \nu (\delta p_t - p) M_1} + \frac{R\, T\, \rho_L}{D_{1(23)} (\delta p_t - p) M_1} \left[\frac{d^2}{8} - \frac{d}{2} \Delta + \Delta^2 \log \left(1 + \frac{d}{2\Delta}\right) \right] , \qquad (53)$$

where

ρ_L = liquid density - g/cm^3,

Figure 10 and Table 6 show that, for increasing pressures, the droplet lifetime will be increased and the evaporation rate depressed. This will significantly increase the existence time for aerosols formed from the bulk liquid in the high pressure environment.

The "critical diameter" of a droplet is the particle size that, for a given saturation value, will grow by condensation to a larger size. Particles below the critical diameter in size will not grow and their mass will be lost to the

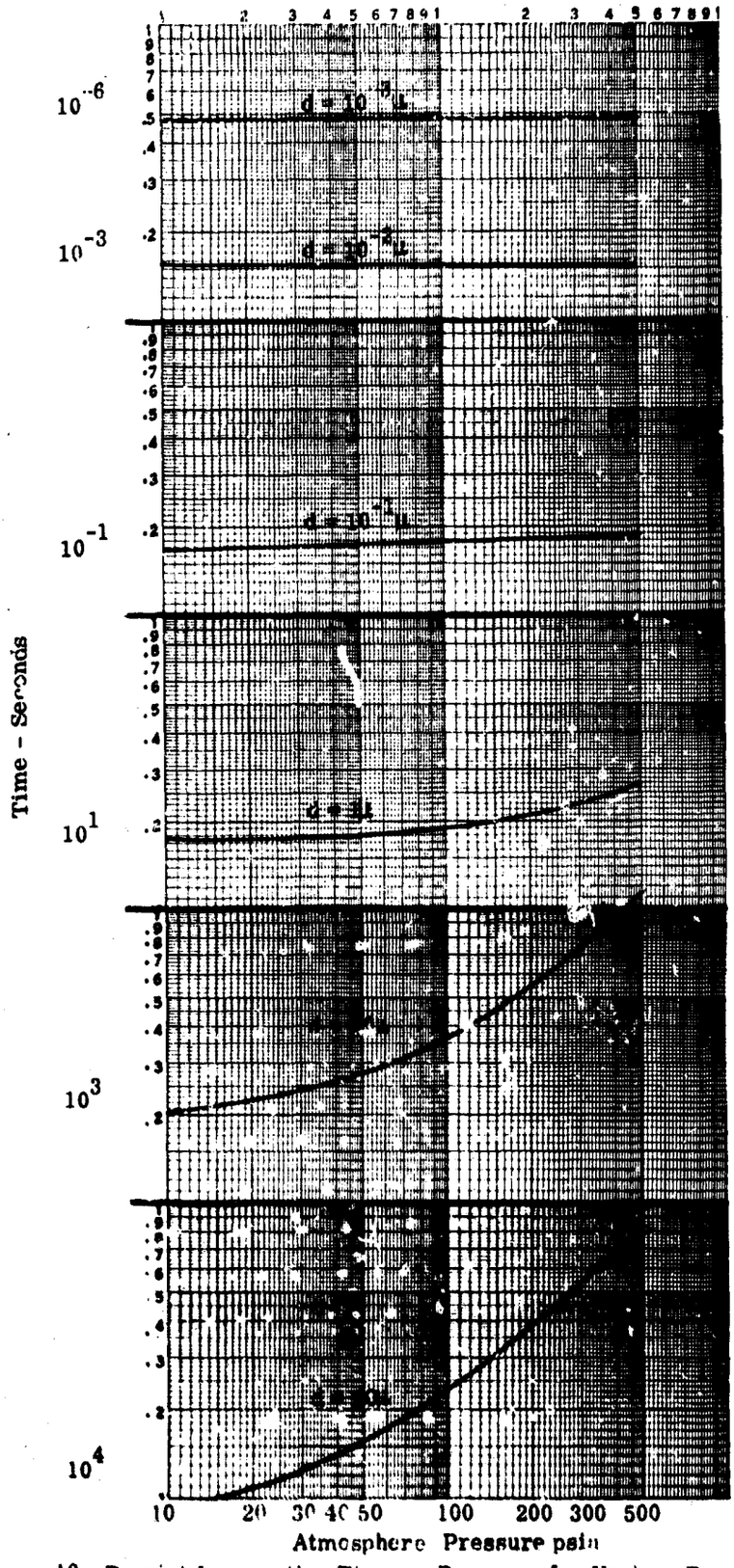

Figure 10. Droplet Evaporation Time vs Pressure for Various Droplet Diameters (PO_2 = 160 mm Hg; PH_2O = 23.37 mm Hg· T = 20°C.

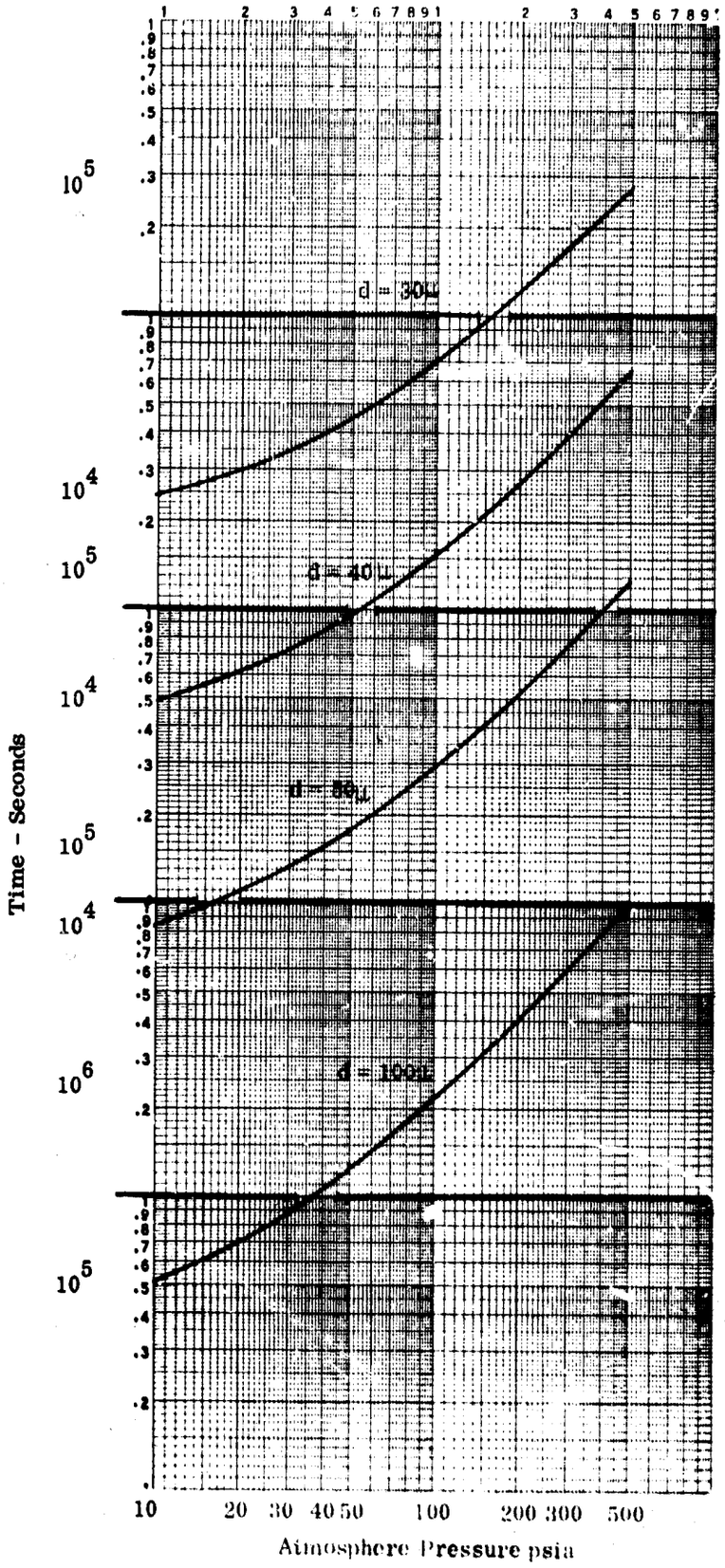

Figure 10. Continued

growth of the larger particles.[23] According to Bradley's work on high pressure nucleation, the critical radius is determined from the formula:[25]

$$d_c = \frac{4\gamma M_1}{\rho_L (r T \ln S - P' V_L)} \qquad (54)$$

where

d_c = critical diameter - cm,

γ = surface tension of the liquid - dyne/cm,

S = saturation (S = 1 = 100% RH)

V_L = molecular volume - cm^3/g-mole, and

P' = environment pressure - dynes/cm^2

An S value of 2 (200% relative humidity) has been selected for illustrative purposes only. This supersaturation could be achieved in a saturated atmosphere during a sudden, 16% decrease in pressure. While this condition is not likely, it does indicate the slight pressure fluctuations that will cause relatively high saturations and promote droplet growth.[26] Table 7 presents the results of these calculations for the environment and demonstrates that the critical diameter increases with increasing pressure; however, the change is far too slight to be of importance.

The net results of the preceding series of calculations can be simply stated in the following way. The propensity of aerosols to form by condensation

P Atmosphere Pressure psia	$D_{1(23)}$ Diffusion Coefficient cm^2/sec	K_{123} Thermal Conductivity cal/sec-cm-^oK	d_c Critical Diameter μ
10.0	.7362+00	1.165-04	.31033-02
14.7	.5867+00	1.453-04	.31044-02
20.0	.4761+00	1.703-04	.31056-02
30.0	.3507+00	2.039-04	.31079-02
40.0	.2774+00	2.268-04	.31102-02
50.0	.2294+00	2.435-04	.31124-02
100.0	.1229+00	2.863-04	.31240-02
200.0	.6372-01	3.144-04	.31473-02
300.0	.4301-01	3.251-04	.31709-02
400.0	.3246-01	3.307-04	.31949-02
500.0	.2606-01	3.342-04	.32193-02

Table 7. Oxygen-Helium Atmosphere Pressure vs:
H_2O Vapor Diffusivity
Atmosphere Thermal Conductivity
Critical Droplet Diameter (S = 2)
(PO_2 = 160 mm Hg; T = 20°C)

processes is retarded by the composition of the He-O_2 atmosphere and increasing pressure. However, aerosols once formed should be found to have a longer lifetime with increasing pressure of the environment.

SECTION 7.0: EXPERIMENTAL DETERMINATIONS OF THE PRODUCTION OF AEROSOLS FROM HEATED SURFACES IN HELIUM-OXYGEN ATMOSPHERES AT VARIOUS PRESSURES.

The purpose of this series of experiements was to determine how the size distribution and number concentration of aerosols produced by heating elements vary with pressure in a helium-oxygen environment. Because resistance heating is a technique used in deep-submersible vessels (where smoking is virtually impossible), heating and cooking activities seem to be the main identifiable sources of aerosols arising within such environments. Duscussions of the production of particles from nichrome, tungsten, and other resistance heating elements are numerous. The more recent observations are typified by Refs. 27, 28, 29, and 30. Generally, the literature presents data on the particle size distributions and number concentrations obtained from various wires that have been brought to a red heat under stable flow conditions. Electron microscopy is the most common technique for the analysis of solid submicron aerosol samples. Occasionally, new information has been obtained such as that pointed out by Goldsmith et. al., [30] who performed a chemical analysis of the particles produced from a heated nichrome wire. They determined that the composition of the aerosol was almost entirely chromium - a marked contrast to the initial composition, which was 80% nickel and 20% chromium. The process by which aerosols are formed in the vicinity of a heated wire is apparently simple; molecules boil off the surface of the wire in great numbers, and upon entering into the cooler air surrounding the wire, the condense from the vapor phase and agglomerate into

particles in the submicron size range (in air at ambient pressure). When one considers the decrease in percentage oxygen concentration with the increase in depth and takes into account the high heat transfer rate in helium, it is logical that the number concentrations and particle dimensions produced in deep-submersible vessels will vary from those produced in air at ambient pressure. Further, since our initial studies have indicated relatively greater lower pulmonary deposition for submicron aerosol particles, it is of prime importance to couple real measurement data on aerosol generation with postualted pulmonary deposition.

7.1 APPARATUS AND PROCEDURES

The test chamber used for generation and thermal deposition of aerosol particles from a heated nichrome wire is shown in Figure 11. Pressure chamber (A) is closed by a removeable cap (B) containing two electrodes (3.34 cm spacing) holding a 20 mil (0.05 cm) nichrome wire (C). A cassette is mounted in the chamber to position a standard glass cover slip (D) 0.47 cm below the wire ($\Delta T/\Delta x = 2500^{o}C/cm$). A new clean wire was installed prior to each test and heated for 0.2 min (3V at 8.8 amp) in helium at 15 psia to clean the surface. Carbon coated electron microscope specimen grids, when used, were placed directly on the steel surface for collection of an aerosol particle sample. The chamber was pressurized with the test gas mixture and the wire was heated (4 to 15 VDC at 3.8 to 9.5 amp) for a brief period (0.24 to 1.23 min). Voltage, current, and time were selected to provide a wire surface temperature of ~1200°C and deposition of a suitable particle population. The entire

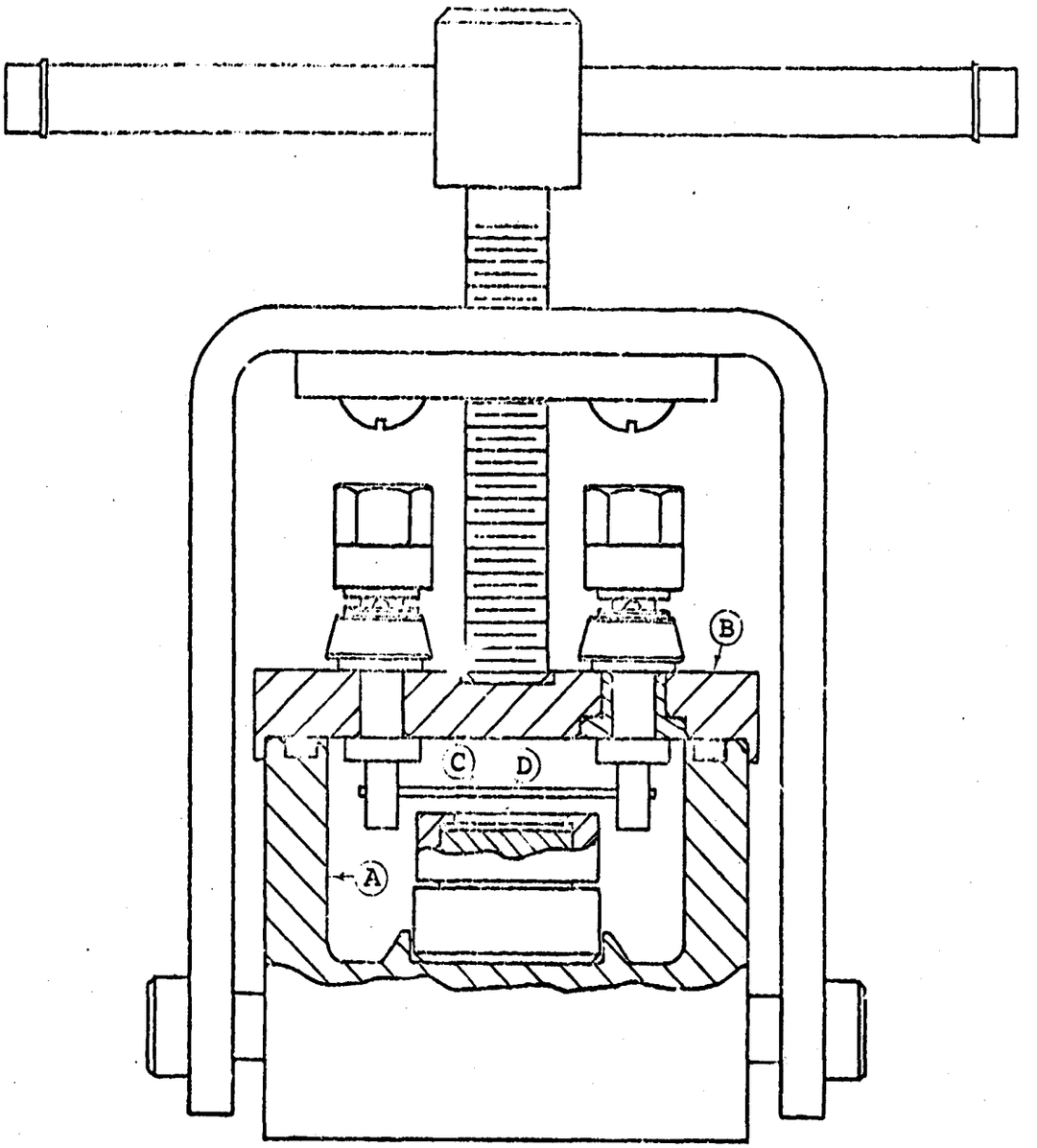

A - Pressure Chamber
B - Removeable Cap
C - Nichrome Emitter
D - Deposition Surface

0 1 inch

Figure 11. Sectional View of Aerosol Test Vessel

experimental apparatus is shown in Figure 12. The operating parameters at each experimental pressure are given in Table 8.

Samples deposited on the carbon coated grids were removed and examined in a transmission electron microscope. Photographs of representative fields were obtained for analysis of particle size and number concentration. Particle size was determined from photographs by means of a transparent overlay of a Porton graticule (projected area diameter). The number of particles in each size interval was tabulated and the count median diameter (M_g) and mass median diameter (M'_g) were calculated by the method suggested by Corn.[31] Count and mass size distribution were not log-normal (i.e. non-parallel curves on log-probability paper) so an apparent geometric standard deviation was estimated from the size ratio (M'_g/M_g) and the Hatch-Choate relation.[32]

7.2 RESULTS

Photomicrographs of representative particles are shown in Figures 13a and 13b. Particles deposited at lower pressures are smaller and more numerous that at higher pressures. Generally particle form at low pressures is similar to that shown by Megaw and Wiffen, consisting of small, relatively, compact nuclei. Extended chained aggregates form at higher pressures.

Table 9 presents the operating conditions for each test, and the calculated particle distribution parameters. Values of the count median diameter (M_g) and the mass

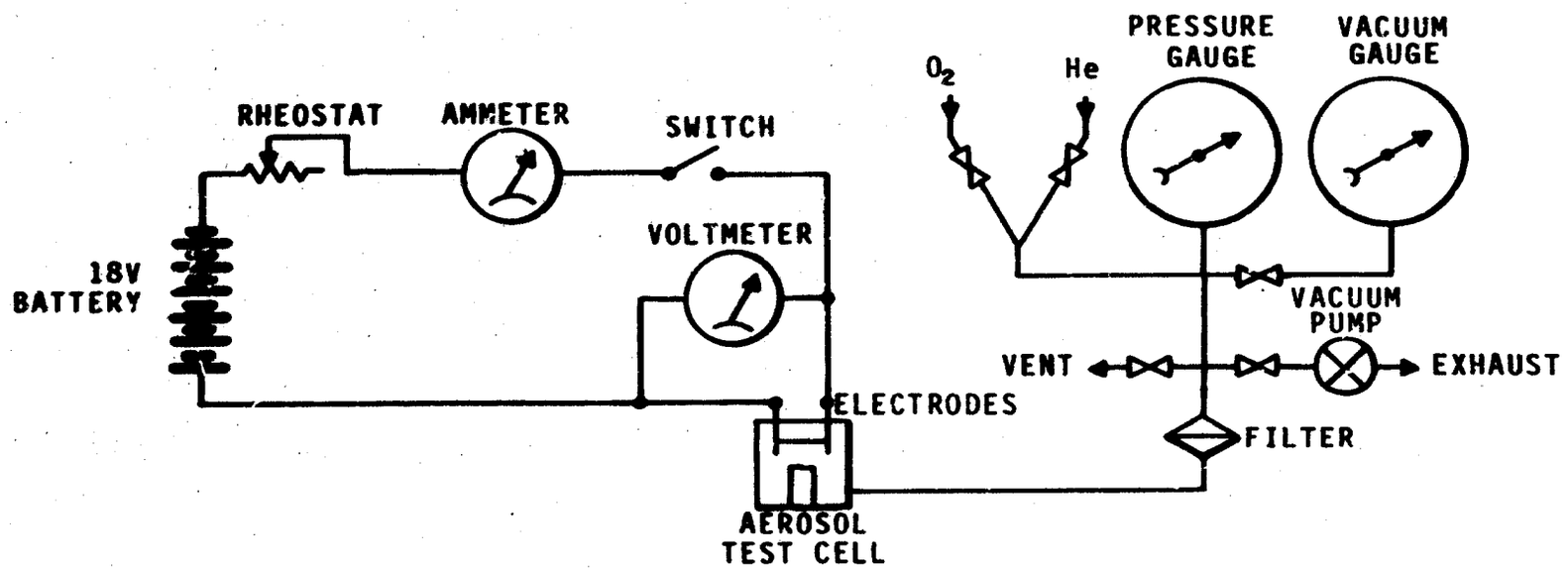

Figure 12. Schematic Diagram of Aerosol Generation and Sampling Apparatus

Table 8. Operating Parameters for Nichrome Wire at 2200°F in a He-O_2 Gas Mixture (PO_2 = 160 mm Hg)*

Pressure psia	Current Amps-I	Power Watts-IE	Energy Watt-Seconds IEt	Duration Seconds
10	10.6	42.7	1160	27.2
14.7	11.2	47.8	1160	24.3
20	11.8	53.0	1160	21.9
30	12.8	61.0	1160	19.02
40	13.4	64.9	1160	17.89
50	13.8	71.0	1160	16.34
100	15.0	78.5	1160	14.8
200	16.1	89.5	1160	12.98
300	17.4	103.0	1160	12.7
400	17.7	116.0	1160	10.0
500	18.8	133.0	1160	8.72
14.7 (air)	9.5	31.5	1160	36.9

*wire diameter = 0.020 in., L = 1-5/16 in.

Pressure = 10 psia Magnification = 80,000X

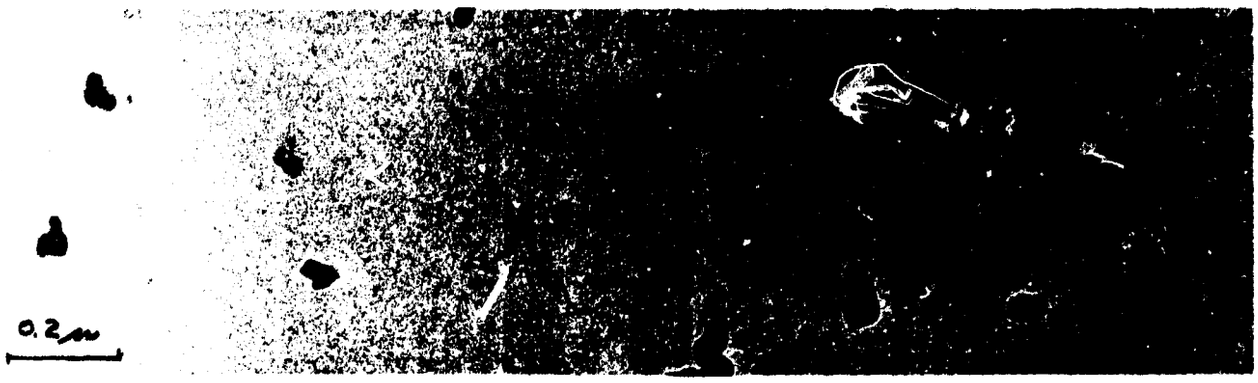

Pressure = 50 psia Magnification = 80,000X

Pressure = 100 psia Magnification = 70,000X

Pressure = 200 psia Magnification = 75,500X

Figure 13a. Electron Photomicrographs of Particles Thermally Precipitated from a Heated Nichrome Wire in an He-O_2 Atmosphere. -- Pressures and Magnifications as noted.

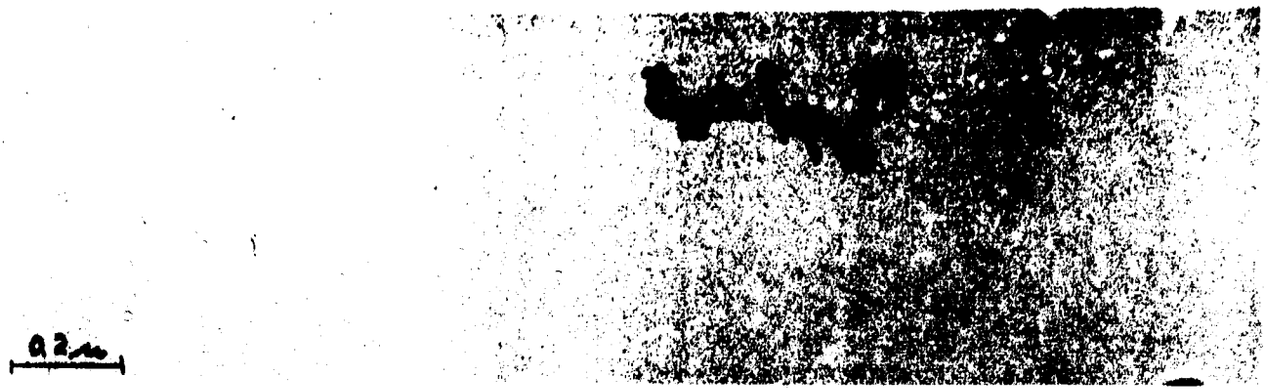

Pressure = 300 psia Magnification = 75,000X

Pressure = 400 psia Magnification = 80,000X

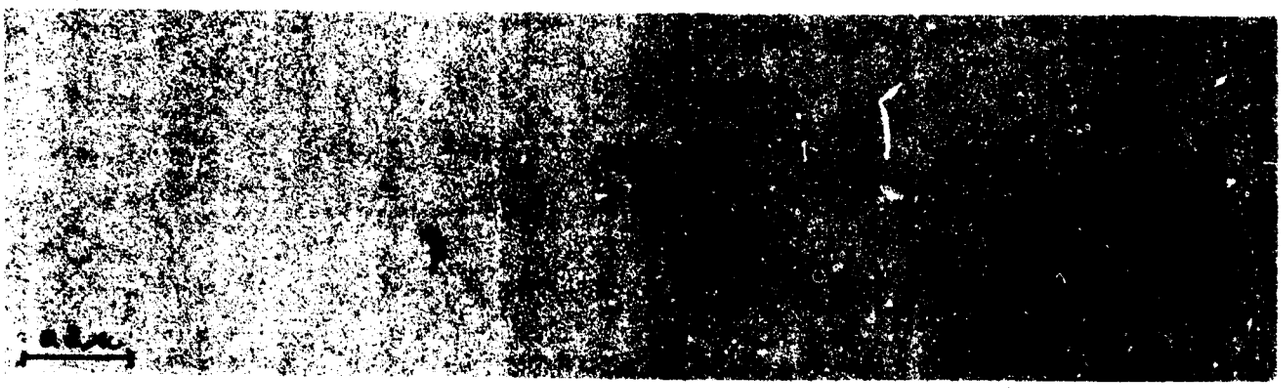

Pressure = 500 psia Magnification = 75,500X

Pressure = 14.7 psia (air) Magnification = 80,000X

Figure 13b. Electron Photomicrographs of Particles Thermally Precipitated from a Heated Nichrome Wire in an He-O_2 Atmosphere. -- Pressures and Magnifications as noted.

Table 9. Effect of Pressure on Aerosol Particle Size Generated by 80:20 Nichrome Wire* at 1200°C.

Absolute Pressure** psia	Voltage (E) volts	Current (I) amp	Time (t) min.	Energy (EIt) watts-seconds	Count Median Diameter	Mass Median Diameter	Apparent Geometric Standard Deviation $\sigma_{g(i)}$
10	10.6	3.8	0.453	1097	0.0134	0.104	2.27
14.7	11.2	4.0	0.404	1090	0.0160	0.084	2.10
20	11.8	4.2	0.365	1086	0.0205	0.115	2.13
30	12.8	4.6	0.317	1123	0.0183	0.120	2.20
40	13.4	4.9	0.298	1175	0.030	0.125	2.00
50	13.8	5.0	0.273	1130	0.035	0.099	1.81
60	14.1	5.1	0.269	1151	0.037	0.112	1.84
70	14.3	5.2	0.260	1160	0.0328	0.100	1.85
80	14.5	5.3	0.252	1161	0.0365	0.091	1.74
90	14.8	5.4	0.242	1161	0.0254	0.125	2.07
100	15.0	5.5	0.494	2450	0.0370	0.116	1.86
200	16.1	5.4	0.648	3380	0.0410	0.077	1.58
300	17.4	6.0	0.636	3990	0.102	0.280	1.78
400	17.7	6.3	0.501	3350	0.0463	0.150	1.87
500	18.8	6.5	0.438	3210	0.066	0.127	1.60
Air	3.6	9.5	1.232	2530	0.0435	0.111	1.75

*High purity wire 0.02 in. diameter
**He + 160 mm Hg P_{O2} = total pressure. "Air" indicates filtered room air @ 14.7 psia.

median diameter (M'_g) are plotted in Figure 14 as a function of pressure. The solid lines shown were determined by a least squares regression analysis. The count median diameter increases with increasing pressure according to the relationship:

$$M_g = 0.0057\ P^{0.40} \quad . \tag{55}$$

The mass median diameter increases slightly, with increasing pressure, according to the relationship:

$$M'_g = 0.071\ P^{0.11} \quad . \tag{56}$$

Physically, the reasons for the differing slopes can be explained. Examination of the photomicrographs indicates that the number of smaller particles is reduced as pressure increases. There is no indication of an increase in deposition of very large particles, merely a reduction in the quantity of smaller ones. This observation is supported by the decreasing trend (with increasing pressure) of the values of $\sigma_{g(i)}$ (Table 9) and by the convergence of the M_g and M'_g curves shown in Figure 14.

A second feature apparent from an examination of the photomicrographs in Figures 13a and 13b, is the marked reduction in the total number of particles produced. In the performance of these experiments approximately five to seven photomicrographs of the grid area were examined per test. At each pressure, counts were normalized to a common area and further normalized to an energy level of 1160 watt-secs by

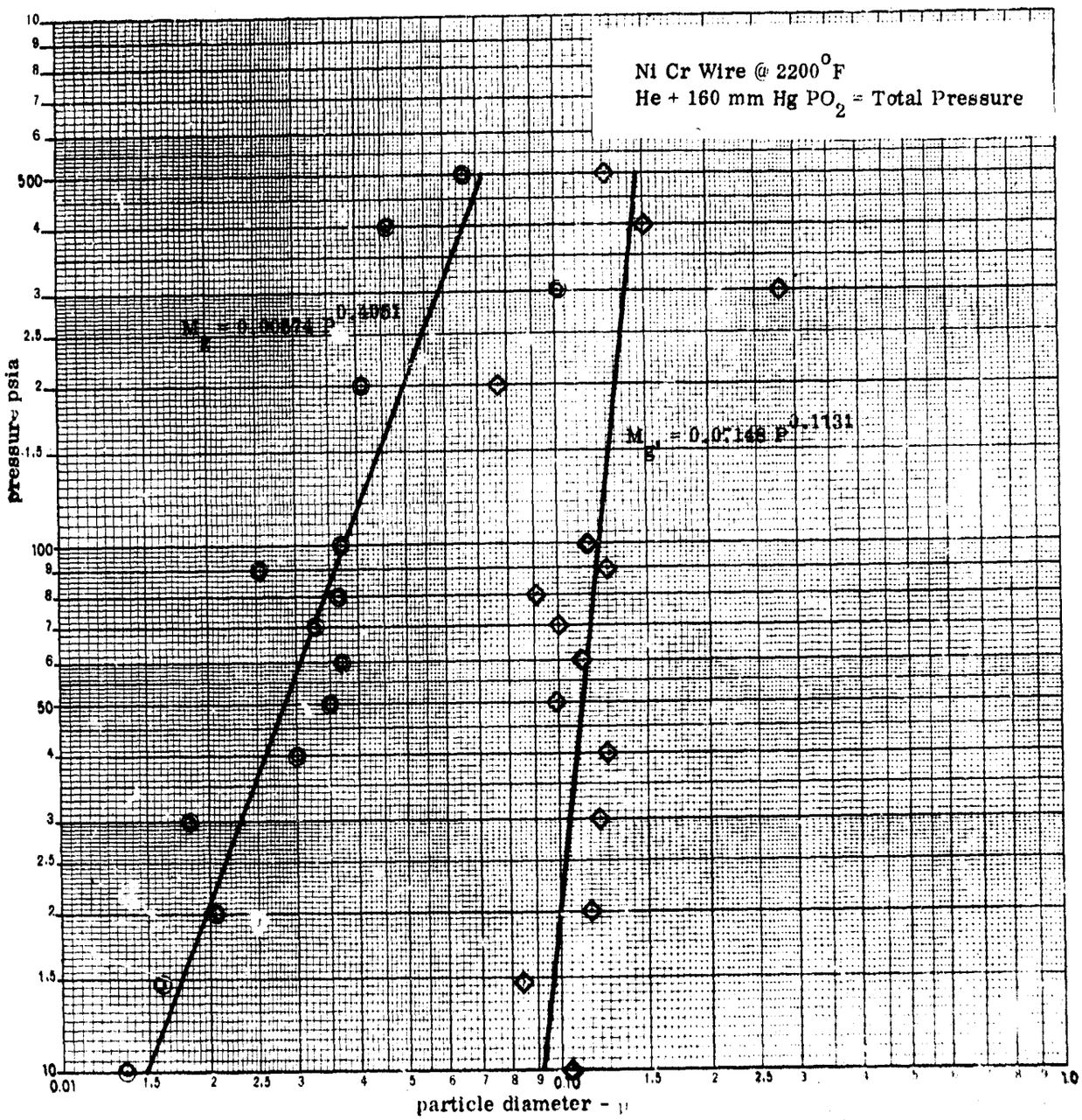

Figure 14. Count (M_g) and Mass ($M_{g'}$) Median Diameters vs Pressure.

multiplying by the ratio of 1160 to the test energy. Number of particles per square micron vs pressure has been plotted in Figure 15 and yields a relative indication of number concentration vs pressure. The variation in concentration between 10 and 500 psia amounts to a reduction of approximately 300 times (60 p/μm^2 vs 0.2 p/μm^2; respectively). Particle deposit density was low at high pressures, even with increased operating energy.

7.3 CONCLUSIONS

1. Under fixed energy and temperature conditions the median diameter of particles produced from a heated wire increases with increasing pressure. The count median diameter increases more rapidly than the mass median diameter and the nature of the increase is such that fewer fine particles are observed. This observed change may be due to the decreasing weight percentage of oxygen available as pressure increases but is more likely attributable to alterations in mobility, diffusivity, and higher heat transfer rates with the increased quantity of helium at increased pressure (1.2×10^{-4} cal/sec-cm^2-(^oK/cm) at 10 psia to 3.3×10^{-4} at 500 psia). Particles produced within the apparatus in air at ambient pressure do not directly relate to those produced in the He-O_2 environment as M_g (0.044 μm) equals the He-O_2 results at 50 psia. M_g for air (0.111 μm) corresponds to the He-O_2 size at 150 psia.

2. The number concentration decreases with increased pressure. Gross investigation of the data indicates that there is not only a loss of smaller particles,

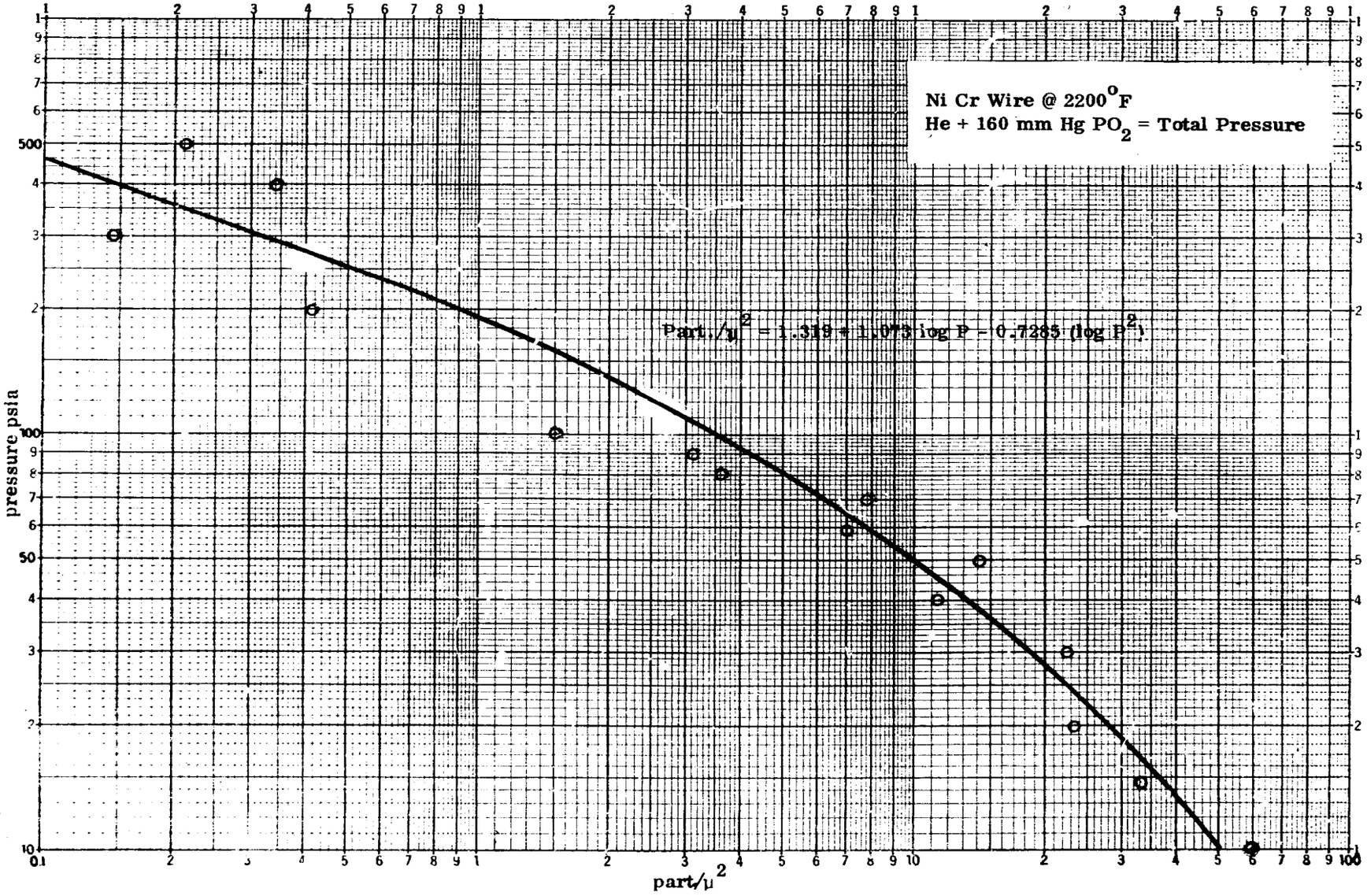

Figure 15. Particle Concentration vs Pressure.

possibly to the larger ones, but there also is a distinct reduction in the total number of particles generated, that is, a reduction in the total quantity of mass released from the wire. The number of particles/$_{\mu}m^2$ produced in air (0.91) corresponds to the He-O_2 result at 200 psia.

SECTION 8.0: FORMATION OF LIQUID AEROSOLS

At the present time the existence of liquid aerosols in high pressure environments has been neither proven or disproven. The question of aerosol formation and disappearance by the processes of condensation and evaporation was discussed in Section 6.0. However, evaporation and condensation processes do not account for the formation of liquid aerosols by what might be termed "mechanical processes." This means the application of mechanical energy to a quantity of liquid to produce a system of droplets comprising "an aerosol." In classical terms the mechanical process may be in the form of shearing energy (hydraulic or two-fluid nozzle), vibrational energy (ultrasonic nozzles), vibrating reeds, vibrating capillaries, and variations of these themes such as centrifugal energy (spinning disk generator).

While there would be no purposely formed liquid aerosols in the high pressure environment, there is always the possibility that the accidential juxtaposition of liquids and mechanical forces will produce liquid aerosols. Ready examples would be speaking, coughing, washing, etc., or associated with personnel and equipment in and out of the habitat-sea interface.

8.1 APPARATUS AND PROCEDURE

An ultrasonic spray nozzle was used to study the effect of high pressure environments on liquid aerosol formation. Figure 16 illustrates the test apparatus constructed for aerosol generation and particle deposition. The ultrasonic spray

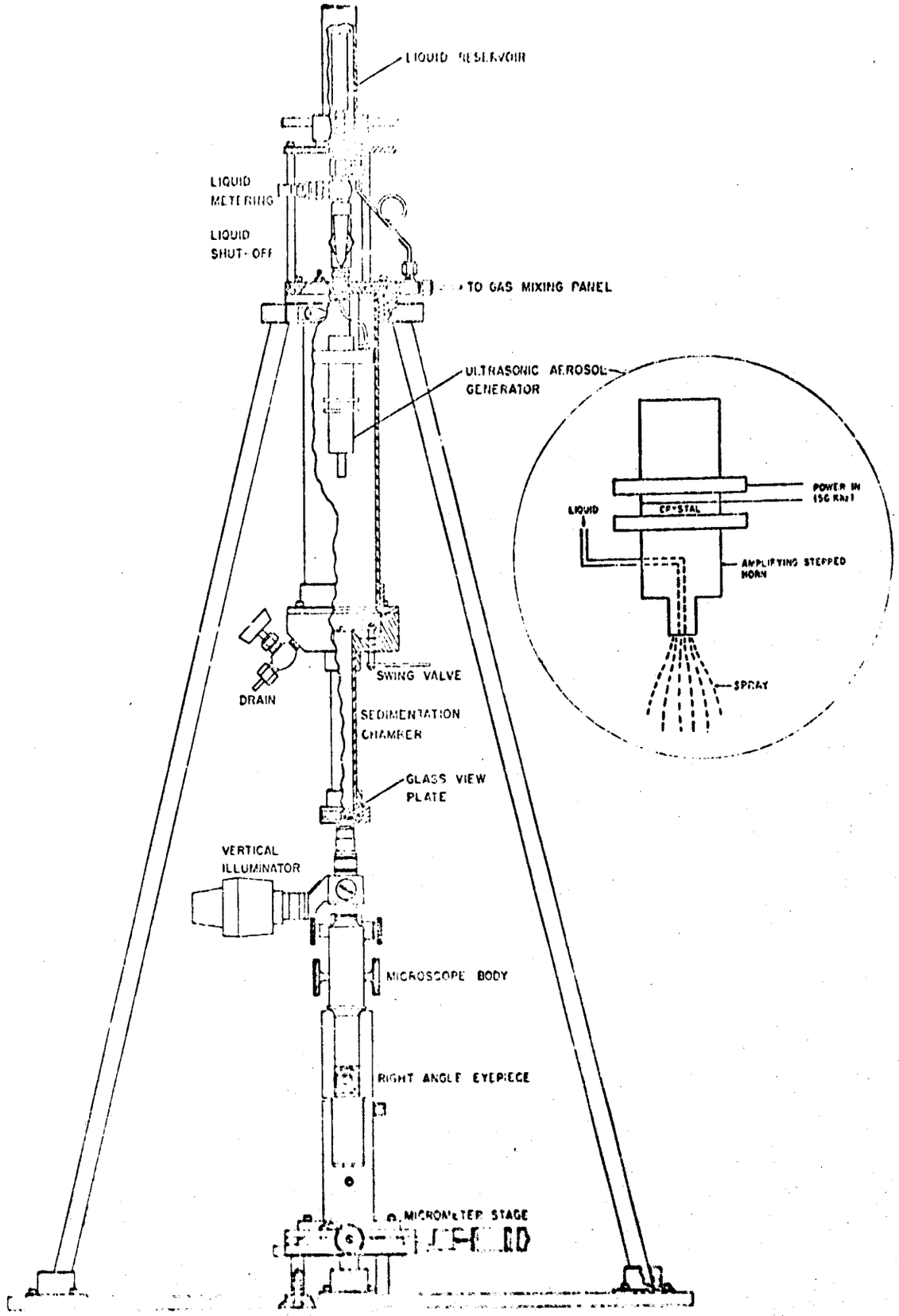

Figure 16. Schematic Diagram of High Pressure Ultrasonic Atomization Test Apparatus.

generator[33] shown in the inset of Figure 16 and 17 consists of a piezoelectric crystal and a 56 kHz driver oscillator. A solid stepped horn amplifier is attached to one side of the oscillating crystal with a liquid channel drilled through the amplifier to a nodal aperture, as shown. Liquid passed through the channel is forced through the hole and spreads out as a film on the lower surface. Oscillations of the solid surface produce waves in the liquid film leading to formation of ligaments at the fluid-gas interface, which subsequently collapse and produce droplets and satellites, in a similar manner to drop formation from the bottom edge of a wetted vertical plate, or from a spinning disc generator.[34]

Empirical equations for the mean droplet diameter produced by ultrasonic atomizers were developed by Perron et al.[35] A more consistent theory developed by Peskin and Raco,[36] relates particulate diameter to liquid surface tension, density, and driving frequency. Peskin's equation is:

$$d = (\pi\gamma/\rho\omega^2)^{1/3} \tag{57}$$

where

d = droplet diameter, cm

γ = liquid surface tension, dynes/cm

ρ = liquid density, gm/cm^3

ω = oscillator frequency, Hz

The Peskin equation has been empirically modified to include the effect of liquid flow rate[33] as:

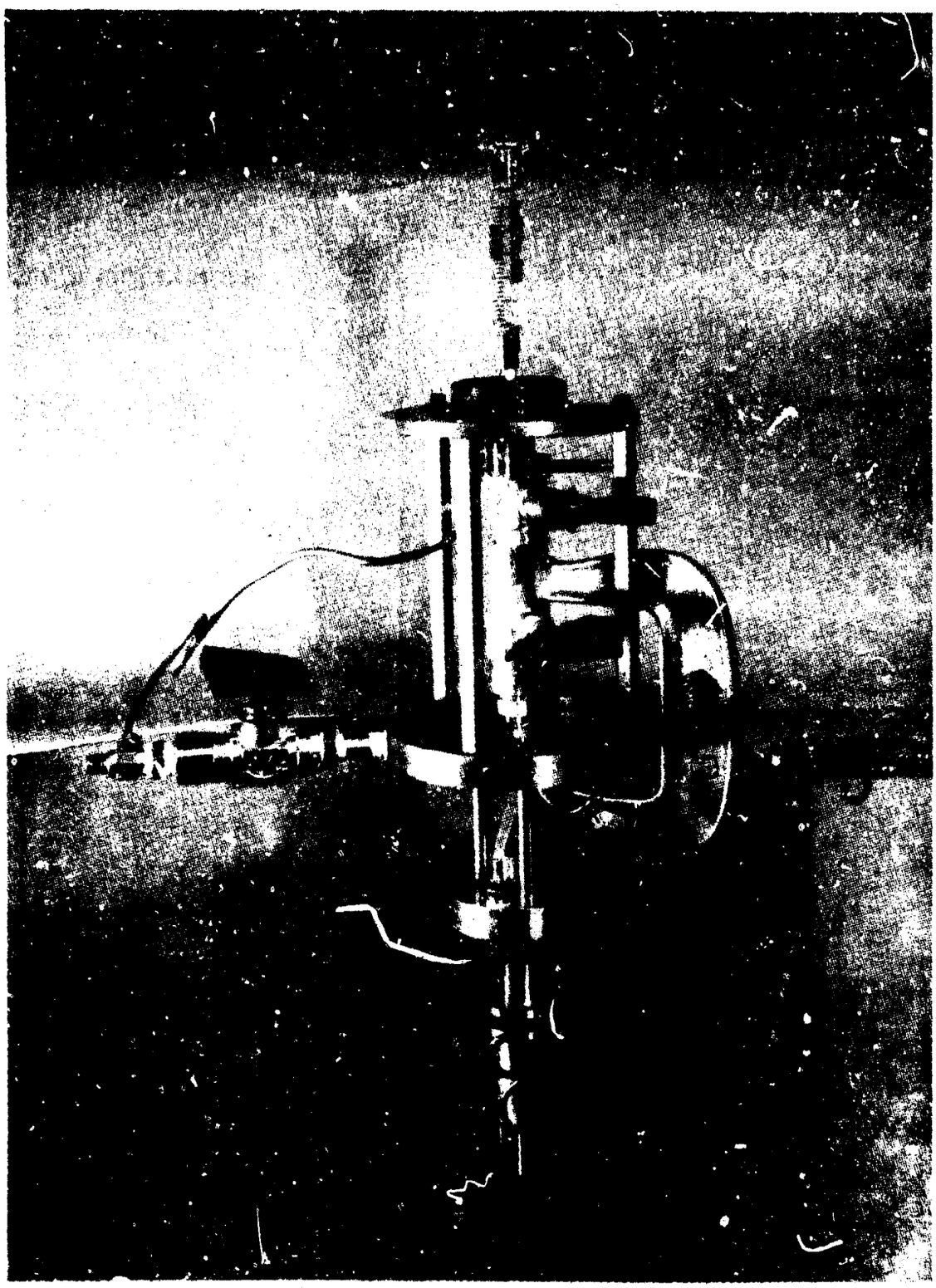

Figure 17. Ultrasonic Atomizer

$$M_g = 0.95Q^{0.2}(\pi\gamma/\rho\omega^2)^{1/3} \quad (58)$$

where Q is the liquid flow rate, cm^3/min. Effects of oscillator and hole geometry, liquid viscosity, etc. have not been studied. The apparatus constructed for housing the generator and for obtaining a sample aerosol deposit is also shown schematically in Figure 16. Liquid to be aerosolized is contained in the receptacle half of a 5 cc syringe. A shut off valve and a needle valve control liquid flow. A pressure cover over the liquid container permits this chamber to be pressurized separately from the balance of the apparatus (+20 psia), to yield uniform flow (1.6 cm^3/min). Samples of the aerosol generated are obtained for analysis by opening the swing gate valve shown. Particles generated by the ultrasonic nozzle pass into the lower pressure chamber (3/4 in. i.d. x 6 in.), and settle onto a transparent surface to be evaluated by light microscopy. The inner transparent collection surface of the lower chamber was coated with a thin (25 μm) layer of Teflon^R to increase the interfacial contact angle and control deposited droplet spreading. Selected tests were also run with a humid atmosphere by placing damp plotting paper in the large upper generation chamber.

In operation, the liquid reservoir was filled with ethylene glycol,* the system was sealed, pumped down, and pressurized with the He-O_2 test mixture. An aerosol

* $\rho = 1.113\ g/cm^3$
$\gamma = 47.7$ dynes/cm @ 20^oC
$\eta = 0.19$ gm/cm-sec @ 20^oC

was generated and, upon achieving equilibrium, the swing gate was opened briefly and closed to secure a sample.

Deposited droplets were sized (at test pressure) with a Porton graticule at 100X (projected area diameter). The particle observed through the microscope was flattened, and the diameter measured was that of the lens formed by the droplet when deposited on the plate. The lens diameter was corrected to the diameter of the original droplet by the application of a spreading coefficient according to the method of May.[37] Particle sizes reported below are airborne droplet diameters (corrected for spreading after deposition).

8.2 RESULTS

Particle size distributions were found to be bimodal, arising from the simultaneous production of large droplets and small satellites. Each data set was truncated and used to construct two size distributions for the smaller and larger droplet populations, respectively, from which particle count and mass median diameters were derived, by the method suggested by Corn.[31] Test results are presented in Table 10 in terms of count median diameters for the lower and upper branches (M_g^{ℓ}, M_g^{h}), and mass median diameters ($M_g^{\ell'}, M_g^{h'}$), for dry and humid atmospheres. Figures 18 and 19 indicate the variation of median diameters for main and satellite droplet populations with pressures from 15 to 500 psia (1-34 atm). The solid lines shown were developed from a regression analysis. Examination of these lines indicates approximately parallel slopes between count median diameter in the low and high

Table 10. Effect of Pressure on Aerosol Particle Size Generated by Ultrasonic Sprayer*

Absolute Pressure** psia	Dry				Wet (P_{H_2O} = 23.23 mm Hg)			
	M_g^{ℓ}	M_g^{h}	M_g^{ℓ},	M_g^{h},	M_g^{ℓ}	M_g^{h}	M_g^{ℓ},	M_g^{h},
15					3.16	23.30	5.50	41.00
					2.82	22.80	5.30	56.00
					2.80	17.50	4.75	53.50
20	1.60	15.00	3.22	1.83	2.45	25.60	4.95	39.50
	2.24	15.00	4.13	18.70	2.52	22.20	4.95	52.00
30	1.34	16.70	4.50	35.40	2.07	22.50	5.90	51.50
	1.73	20.30	2.76	50.00	1.81	24.40	8.00	42.00
					3.00	30.50	5.20	50.00
40	1.62	13.40	2.58	33.20	7.00	38.00	17.40	81.00
	1.32	14.50	3.05	19.70	3.40	41.50	14.30	57.00
					7.60	37.80	16.70	60.00
50	4.70	14.20	6.00	26.50	3.70	19.70	5.40	35.30
	2.65	16.10	43.50	42.70	3.95	18.50	5.50	40.00
	1.80	17.20	4.25	26.00				
100	2.65	13.80	4.25	23.00				
	2.45	18.20	3.85	28.20				
200	3.05	17.50	5.30	75.00	4.55	14.50	8.00	56.50
	2.40	16.80	5.50	47.00	3.37	29.30	8.80	38.80
300	3.05	18.20	6.70	40.50	3.60	29.00	11.20	58.00
	3.95	25.00	7.80	60.00	3.35	26.50	5.50	37.00
	1.62	17.00	5.30	52.00				
400	2.95	29.00	6.10	62.00	2.95	22.00	6.35	35.30
	3.20	31.50	6.70	56.00	2.50	11.00	6.20	74.00
					3.37	11.80	4.55	55.00
					3.85	12.60	5.45	13.80
					3.85	15.30	6.40	61.00
500	3.80	23.50	9.30	41.50	3.20	22.70	5.60	26.80
	4.30	51.00	19.00	69.00	2.92	21.00	6.10	26.30
Air	1.80	10.60	2.84	32.00				
	1.67	12.30	2.75	63.00				

*Ethylene glycol spray liquid, 56 kHz, 1.6 cm^3/min flow rate.
**He + 160 mm Hg P_{O_2} = total pressure. "Air" indicates filtered room air at 14.7 psi.

Figure 18. High Pressure Ultrasonic Atomization Tests of Ethylene Glycol into Dry Oxygen-Helium Atmosphere.

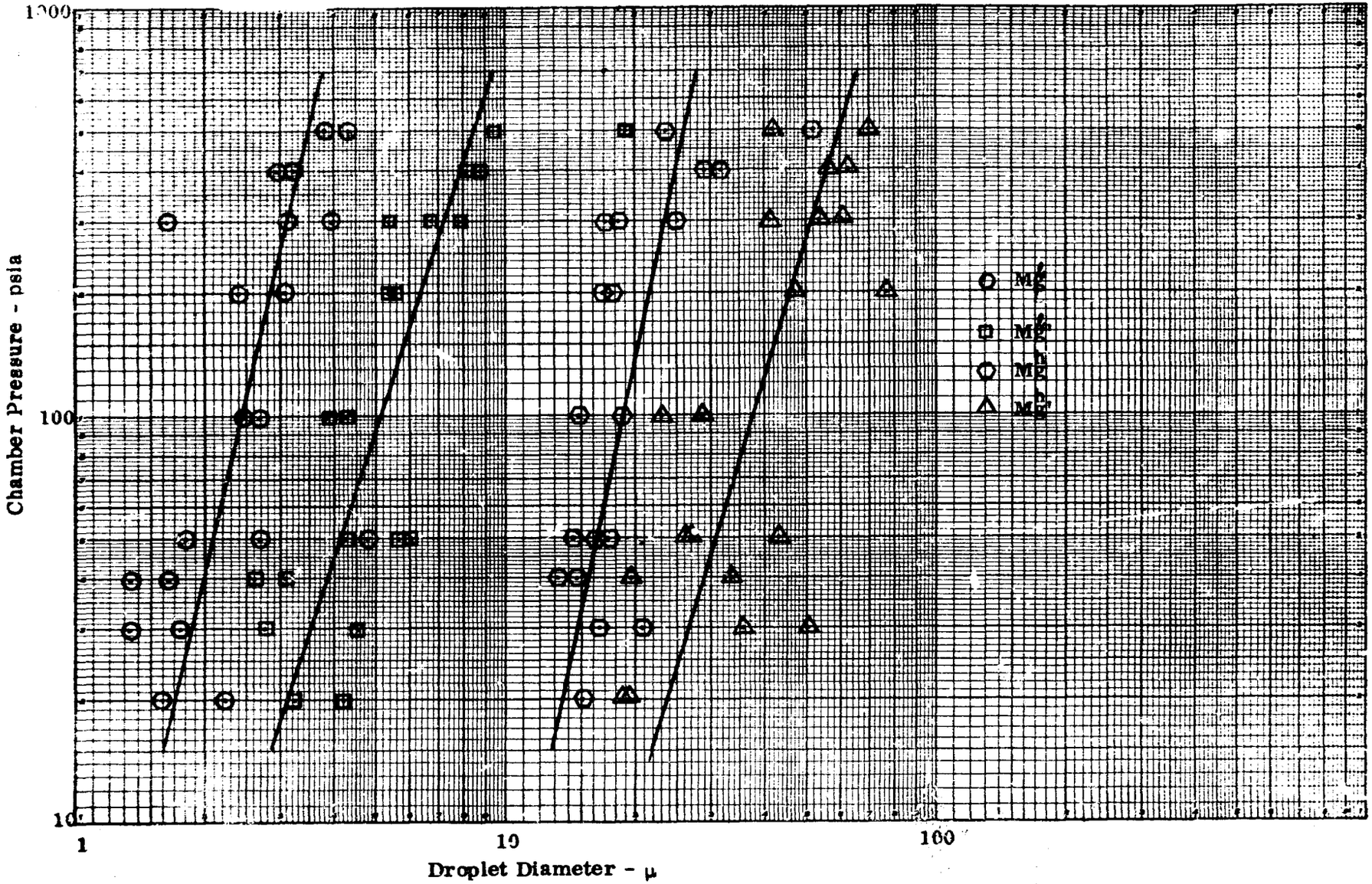

Figure 19. High Pressure Ultrasonic Atomization Tests of Ethylene Glycol into Humid Oxygen-Helium Atmosphere

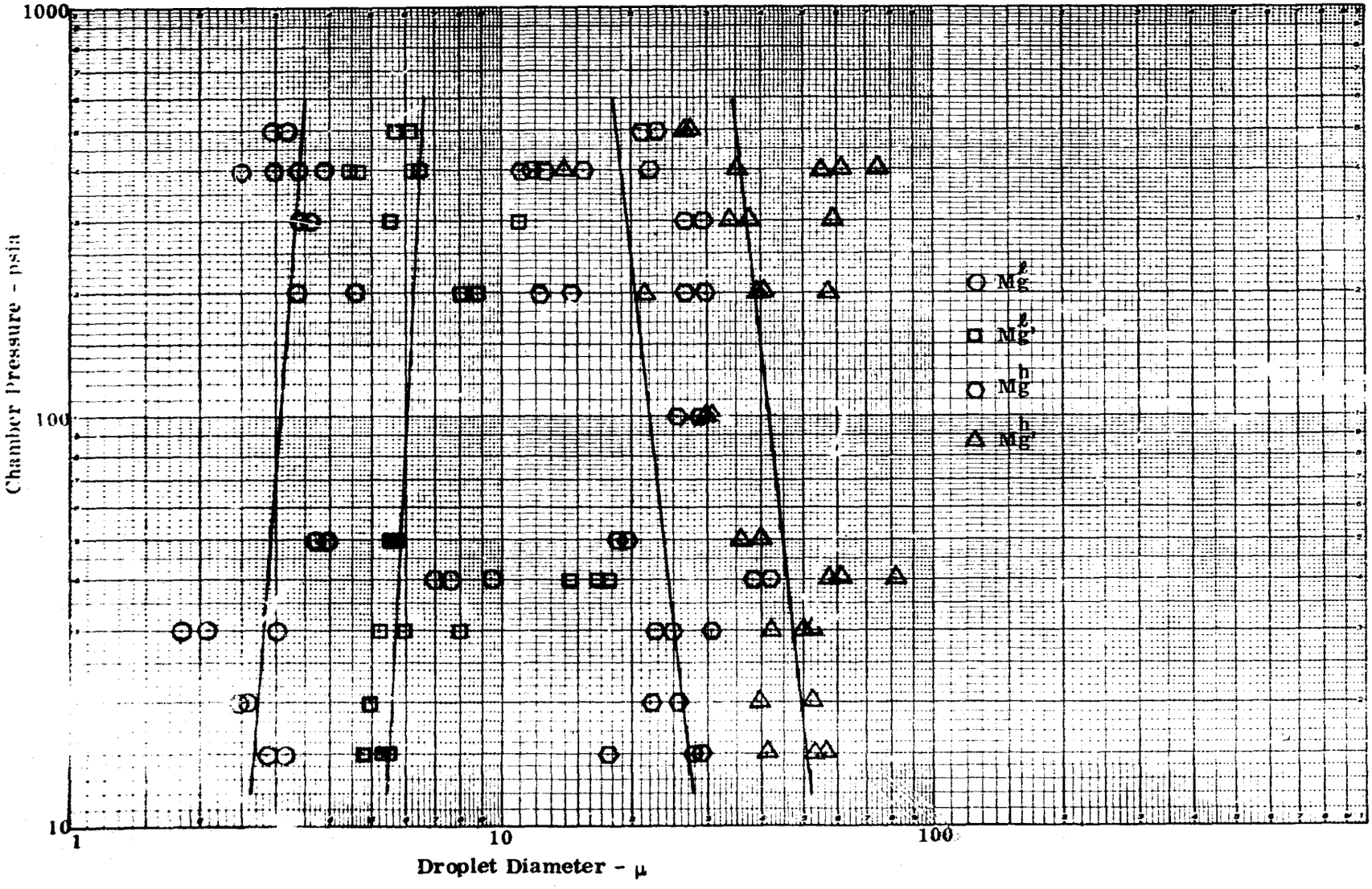

mode and between mass median diameter in the high and low mode. It is also observed that the count and mass median diameters diverge as pressure increases. This divergence is a significant measure of the width of the particle size distribution. The distributions in the high and low modes observed in this study were found to be approximately log-normal. The width of a log-normal distribution can be described by the geometric standard deviation (σ_g). If σ_g has been constant over the full pressure range, then the relationship between M_g and M_g' would be constant, and the slopes of the two cumulative distribution lines parallel. In this case, the slopes diverge, indicating that the distributions are becoming increasingly polydisperse with increasing pressure.

The general nature of the results above are similar to those observed for the emission of submicron particles from heated wires, i.e., moderate increases in particle size with increasing pressure. Since the slopes of the high and low modes are nearly parallel, an averaging process has been utilized and the equation presented above for the output of the ultrasonic generator[17] has been modified to include effect of environmental pressure for helium-oxygen atmospheres. For the high and low mode count median diameter, the following empirical relationships are proposed.

$$M_g^h = 1.935 \times 10^3 \left(\pi\gamma/\rho\omega^2\right)^{1/3} Q^{0.211} P^{0.208} \qquad (58)$$

$$M_g^\ell = 2.35 \times 10^2 \left(\pi\gamma/\rho\omega^2\right)^{1/3} Q^{0.211} P^{0.208} \qquad (59)$$

for P = absolute pressure, psia; $1 \leq P \leq 34$ atm. Bimodal particle size distributions from ultrasonic spray nozzles were reported previously[33] to be affected by surface tension and viscosity.

Increasing pressure and changing gas composition may have some effect on liquid properties such as surface viscosity, but for $1 \leq P \leq 34$ atm, compressibility effects on bulk viscosity are presumed small (i.e., < 1%). Increasing solubility of He in the liquid might have an effect on surface tension or viscosity.

Water vapor present at ~23 mm Hg in humid tests (Figure 19) undoubtedly produced a change in ethylene glycol properties affecting droplet generation and settling.

8.3 CONCLUSIONS

1. The influence of environmental pressure on the particle size spectrum produced by a standard quantity of ultrasonic energy applied to a fixed quantity of fluid is slight.

2. The influence of humidity will depend on the hygroscopic properties of the liquid being aerosolized and may decrease the particle size produced.

SECTION 9.0: FILTRATION - THEORY

9.1 INTRODUCTION

When a particle-laden air stream is forced to flow through an array of fine fibers, the particles are removed from the air stream by one or a combination of six mechanisms defined by Pich.[13] These mechanisms may be listed as:

1) diffusional deposition,
2) direct interception,
3) inertial deposition,
4) electrostatic deposition,
5) gravitational deposition, and
6) deposition influenced by molecular (Van der Waals') forces.

Pich further lists three factors to be considered in a filtration situation: "The dispersed particles, the dispersion medium (represented by the gas in the present case) and the porous substance."

A large number of theories have been presented for the various filtration mechanisms and for combinations of the mechanisms. Each has its proponents and detractors, armed with supporting evidence. These theories were first summarized in a conference report published in 1960;[38] the most recent work can be found in two chapters of the book, edited by Davies, Aerosol Science.[13] Here again, several theories and variations are presented and it still remains for the individual investigator to make his own selection.

Determination of the overall efficiency of fibrous filters requires a consideration of the six individual filtration mechanisms mentioned above and their contribution to the total efficiency. Since various mechanistic efficiencies are usually calculated on the basis of an individual fiber, the effect of many fibers in close proximity must also be accounted for (interference effect). Inasmuch as the relationships for considering the interference effect and for the summation of efficiencies are not, in their present form, affected by the pressure of the environment, they will not be treated in detail here - except for some precautionary notes regarding the balance of this discussion.

A large number of efficiency terms will be referred to in the following section. The subscript nomenclature includes:

E = efficiency of the complete intact filter

E_D = single fiber collection efficiency due to diffusion

E_R = single fiber collection efficiency due to direct interception

E_I = single fiber collection efficiency due to inertial deposition

E_G = single fiber collection efficiency due to gravitational deposition

E_M = single fiber collection efficiency due to Van der Waals' forces

E_{Qq} = single fiber collection efficiency due to electrostatic deposition (This notation indicates that both the fiber and the particles are charged. When the particle is charged and the fiber is not, the nomenclature is E_{Oq}; when the fiber is charged and the particle is not, then E_{QO}.)

E_j = efficiency due to all mechanisms (j = ERIGMQq)

$E_{\beta j}$ = single fiber collection efficiency for all mechanisms when the interference effect of other fibers is being considered. (This is not to be confused with E, where the efficiency of the total filter mat is being considered.)

For each of the filtration mechanisms, there is a filtration parameter, N, that becomes an important descriptor in a first approximation of a filter's efficiency. Pich[13] states that "by a simple summation of partial efficiencies, as used by some authors, not even approximate results can be obtained as may be demonstrated by the simplest of cases." Further, according to Ranz and Wong, (Pich, 13) "The main mechanism is that having the greatest parameter" (N).

9.2 DIRECT INTERCEPTION

For this deposition mechanism, the number of equations are more limited. While the equations are solely a function of Reynolds number and the interception parameter (N_R), Langmuir and Natanson present relationships with Reynolds number in the denominator while Friedlander places Reynolds number in the numerator.[13] However, because of the nature of the algebra involved in the equations and the fact that the Reynolds number is usually less than 1, the result should always be a reduction in the efficiency value due to an increase in the density term of the Reynolds number with increasing pressure.

Previous calculations on submicron aerosols and fibers ranging from 25-130 microns indicate that the efficiency due to direct interception is so small as to be zero or negligible.[39] The descriptive parameter for direct interception is simply defined as:

$$N_R = d_p/d_f \quad . \tag{60}$$

9.3 INERTIAL DEPOSITION

The efficiency of removal by impaction of particles from a flowing gas stream is generally held to be not directly calculable from an equation and therefore is deduced from theoretical and experimental curves of target efficiency and the impaction parameter (Stk).[13] The literature gives various curves and compilations of curves, but it is difficult to select one for a given set of conditions since they are rather specific and depend upon the Reynolds number. The impaction parameter (N_I) is also known as the Stokes number and is given by the equation:

$$Stk = \frac{\tau V}{d_f} \quad , \tag{61}$$

where

τ = relaxation time = $\frac{d_p^2 \rho}{18\eta}$ (slip factor) and

ρ = particle density.

For a rough evaluation of the magnitude of impaction efficiency, Landahl and Hermann have obtained an empirical formula for $R_e = 10$:

$$E_I = \frac{Stk^3}{Stk^3 + 0.77\ Stk^2 + 0.22} \tag{62}$$

Therefore, for this mechanism, an appreciation of the effects of increased pressures and atmospheric composition can be gained by examining the equation directly for the parameter of the mechanism. Inasmuch as none of the terms of the equation for the impaction parameter are much affected by the atmosphere in question, the principal alteration will be in terms of the slip factor. Taking a tenth micron particle as an example, the correction factor will reduce from a value of five for helium-oxygen at ambient pressures to very nearly one at the 500 psia condition.

9.4 ELECTROSTATIC DEPOSITION

The effect of electrostatic charge present on either the particles, filters fibers or both are that the charge will make the particles adhere more strongly to the fiber surface once they are deposited and that the particles may be attracted (or repelled) from a greater distance.

In discussing electrostatic deposition, there are three separate cases to consider: charged particle, charged fiber (E_{Qq}); charged fiber, neutral particle (E_{Qo}); and neutral fiber, charged particle (E_{oq}). The collection parameter and efficiency equation for each of these mechanisms is somewhat different and, inasmuch as this material is lengthy and very clearly discussed by Pich,[13] only the affected parameters will be treated here. For particles

or fibers small enough to be affected by the slip correction, this parameter will certainly apply and the magnitude of that change has already been stated several times in this discussion; i.e., its effect will be small at the elevated pressure and it may be neglected. The same finding holds for the efficiency equations and the only other consideration is one of how the particles and/or the fibers become charged. A simple relationship exists for the decrease in ionic mobility with increasing pressure, which is given as:(Whitby, 13)

$$Z_r = \frac{Z}{P} \quad , \tag{63}$$

where

Z = ionic mobility

Z_r = reduced mobility, and

P = pressure in atmospheres.

Since there will be a 34-fold reduction at the 500 psia (34 atmosphere) condition, beneficial deposition effects from charged particles are not likely. On the other hand, an efficient method of fiber charging might be sought. Experimental evidence by Silverman et.al.[40] describes an improvement in filtration when the fibers are charged.

9.5 GRAVITATIONAL DEPOSITION

Gravitational deposition to a fiber (horizontal) is simply given by the relationship:[13]

$$E_G = \frac{v}{V} = N_G \quad , \tag{64}$$

where

v = sedimentation velocity.

It is also pointed out[12] that, for particles with a diameter of less than 0.6 microns, the mechanism is of little importance and therefore we will not consider it further.

9.6 VAN DER WAALS' FORCES

Van der Waals' or molecular forces resemble electrostatic forces in that they may influence the process of deposition and also tend to keep the particle on the fiber. The constants given in the equation for the characteristic parameters and the efficiency are apparently unaffected by pressure except for the usual slip correction factor and for the viscous flow regime, for which a Reynolds number term is presented.[13]

9.7 DIFFUSION DEPOSITION

There are at least nine equations[13] that describe diffusional deposition of particles on a fiber. To be sure, the choice is not truly that broad and may be somewhat reduced by considering the flow regime involved. Nevertheless, all the equations involve the Peclet number (P_e) and, usually, the Reynolds

number (R_e). Since there are no other components of the equations affected by pressure or environmental composition, an appreciation of the effects may be obtained by directly examining these two numbers.

$$P_e = \frac{d_f V}{D} \quad , \tag{65}$$

where

V = gas velocity at a great distance from the fiber and

d_f = fiber diameter.

$$R_e = \frac{V d_f \rho'}{\eta} \quad , \tag{66}$$

where

ρ' = gas density, and

η = viscosity of the fluid medium.

The diffusion coefficient is unaffected by pressure or composition, but does require the application of the slip correction. For a 0.1 micron diameter particle, the magnitude of this correction varies from approximately 5 at 14.7 psia in the helium-oxygen mixture to 1.1 at 500 psia; that is, as pressure increases, the magnitude of the correction decreases and may be virtually ignored at 500 psia.

The value of Reynolds number will increase with increasing pressure, due to the rise in density of the mixture and the fact that the viscosity is relatively

unaffected and not remarkably different from that of air from ambient pressure to the 500 psia condition. However, the density increases and therefore the value of Reynolds number increase amounts to approximately one order of magnitude.

Because of the diversified ways in which the Peclet and Reynolds numbers are utilized in the diffusion equations, it is difficult to present a more quantitative discussion of the magnitude of the pressure affect on the diffusion mechanism. Pich[13] discusses the experimental work of Stern et. al. at low pressures and finds a remarkable increase in efficiency at very low pressures in which the mean free path of the gas molecules has become very long, i.e., the particles are highly mobile. Extrapolating Stern's work to increased pressures shows that the curve is quite flat in the vicinity of atmospheric pressures and would seem to indicate no further change with increasing pressure. Apart from this being theoretically unlikely, concern is expressed over "some obscurities in the work of Stern et. al." A plot of one of the diffusion equations is presented by Pich demonstrating efficiency to be falling asymptotically as the curve passes through ambient pressure. The particular equation favored by Fuchs and Pich is given as:[13]

$$E_D = \frac{2.86}{Y^{1/3} P_e^{2/3}} \left(1 + \frac{0.388 \chi P_e^{1/3}}{Y^{1/3}} \right) \qquad (67)$$

where:

$$Y = -\frac{1}{2} \ln \beta - C + 1.996 \chi (-1/2 \ln \beta - C + 1/2)$$

where:

χ = fiber Knudsen number $\frac{\lambda}{d_f}$

λ = mean free path of the gas molecules

β = volume fraction of fibers

C = a constant 0.5 or 0.75*

This equation is derived from considerations of the Kuwabara-Happel velocity field surrounding the fiber. The range of Knudsen numbers for a variety of fiber diameters over the pressure regime involved is plotted in Figure 20. When the Knudsen number is small (10^{-3} to 0.25) then equ. no. (67) is utilized. When slip may be neglected ($\chi \rightarrow 0$) the expression for Y reduces to $Y = -1/2 \ln \beta - C$ and the whole equation reduces to:

$$E_D = \frac{2.86\ P_e^{-2/3}}{(-1/2 \ln \beta - C)^{1/3}} \qquad (68)$$

Equations (67 & 68) characterize only the diffusional deposition efficiency for a single fiber. They do, however, because they are derived from considerations of the Kuwabara-Happel field, include the interference effect of other fibers.

---

*NOTE: There is no physical basis for choice but rather, different authors (13) arriving at almost the same equation. We have elected to use 0.75.

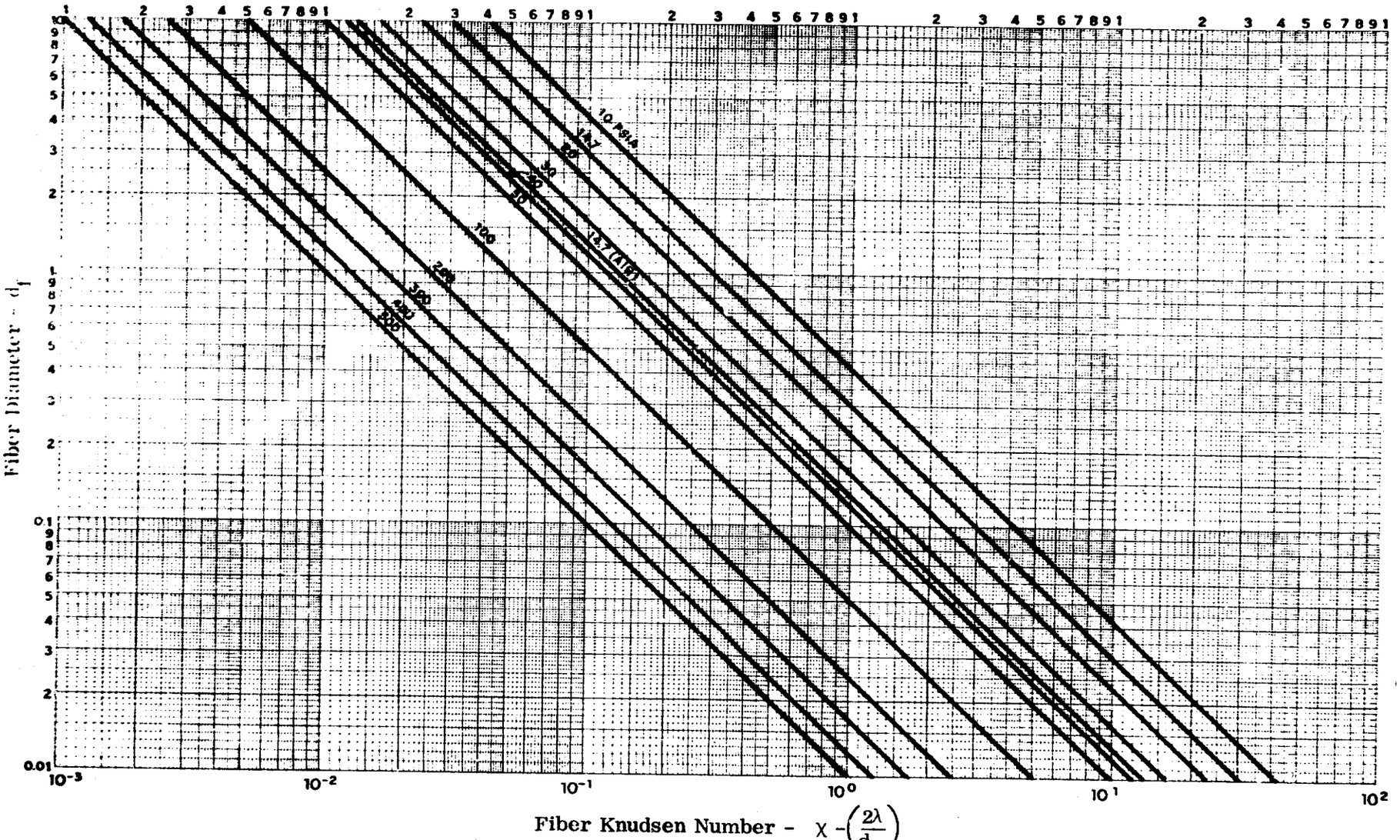

Figure 26. Fiber Knudsen Number vs Fiber Diameter at Various Pressures of an Oxygen–Helium Atmosphere. (PO_2 = 160 mm Hg; T = 20°C).

In order to determine the total filter efficiency the following equation is utilized[13]

$$E = 1 - e^{\alpha} \tag{69}$$

where:

$$\alpha = \frac{4}{\pi} \cdot E_D \cdot \frac{\beta}{1 - \beta} \cdot \frac{L}{d_f}$$

where:

α = coefficient of adsorption through the filter

L = thickness of filter material

Since only the Peclet number is affected by pressure in the diffusion equation, then for the five-fold reduction in the slip correction (for a 0.1 micron particle) owing to the increase in pressure to 500 psia, the net effect will be to reduce the single fiber efficiency by a factor of approximately 0.3 (as demonstrated in the next section).

The parameter that describes diffusional deposition (N_D) is given as being equal to the reciprocal of the Peclet Number.

Equation (67), above, has been utilized in a series of computer calculations to estimate the diffusional collection efficiency of an actual fiber mat. Subsequent to the completion of the aforementioned calculations additional theoretical material was published in the open literature and should be noted at this time.

A paper by Kirsh and Fuchs[41] has expanded earlier work by Fuchs on diffusional deposition of aerosols in fiber filters. Equations (67) and (68) presented above and attributed to both Fuchs and Pich[13] are repeated in this new paper with slight modification of coefficients. The purpose of this paper is to carry their theoretical and experimental work from a system of regular parallel cylinders to ones of random array more nearly simulating actual filters. The results of their study with real and simulated fiber filters in the diffusional range is that the efficiency is <u>not</u> dependent upon the packing density of the filter. No firm reason for this finding is given although some suppositions are presented. Based upon their findings two equations for total filter efficiency are presented; one for general conditions and one for low values of packing density. These equations have been transposed into the nomenclature used here and are given as:

$$E_{T(D)} = 1 - \exp\left(d_f \Delta_p E_D^b / F_b^* V \eta\right) \tag{70}$$

where

$E_{T(D)}$ = total collection efficiency of the filter (by diffusion)

d_f = fiber diameter

Δ_p = pressure drop across the filter

V = filter face velocity

η = gas viscosity

E_D^b = single fiber efficiency due to diffusion for this equation

$= 2.7\ P_e^{-2/3}$

P_e = Peclet number $= \frac{D}{V d_f}$

D = diffusion coefficient

F_b^* = dimensionless force acting on a unit fiber length

$= 4\pi \left[-0.5\ \ell n\ (2\alpha/\pi) + 2\alpha/\pi - (\alpha/\pi)^2 - 0.75\right]^{-1}$

α = packing density.

For low values of packing density

$$E_{T(D)} = 1 - \exp\left\{-0.685\ \Delta p\ d_f \left[-0.5\ \ell n\ (2\alpha/\pi) - 0.75\right]/\pi P_e^{2/3}\ V\eta\right\} \quad (71)$$

SECTION 10.0: FILTRATION - EXPERIMENTAL

Inasmuch as the review of the submarine literature and experiments on aerosol formation from heated surfaces indicated a rather fine structure to be expected in any aerosol distribution existing in the environment, the actual filtration studies have been based upon the diffusion mechanism only. The particle size of interest to this study is less than 0.1μ and it is expected that only this mechanism will be active (with the possible exception of electrostatics). To support this decision a brief examination of the characteristic parameters (N) for impaction, direct interception and diffusion was conducted for further assurance that major mechanisms other than diffusion would be negligible. This consideration necessitates the establishment of the media to be used, the characterisitcs of which are given in Table 11. The characteristic parameter for direct interception (N_R) is given as:

$$N_R = \frac{d_p}{d_f} \tag{72}$$

where:

d_p = particle diameter

d_f = fiber diameter

The parameter will have a minimum value of 1.5×10^{-2} for 0.1μ particles with a fiber diameter of 0.64μ. The largest possible value is 0.32 for a particle diameter of 0.1μ and a fiber diameter of 0.31μ. The parameter as stated is uneffected by pressure.

Table 11. Characteristics of Actual "Absolute" Type Filter Media*

Name:	All glass fiber media, non-water-proof #475	Area Density:	9.46×10^{-3} g/cm^2
Fiber Diameter:	1) Surface Volume Dia. = 0.64μ 2) Number Diameter = 0.31μ	Packing Density:	0.205 g/cm^3
Thickness (L):	0.046 cm	Solids Fraction (β):	0.0816

*All data furnished by Naval Research Laboratory.

Table 12. Extreme Values of Characteristic Filtration Parameters for 0.01μ and 0.1μ Aerosols.

Filtration Parameter	Impaction N_I	Direct Interception N_R	Diffusion N_D
	$\rho_p = 7.1$ (Cr)		
Smallest Value	1.75×10^{-4} ($P = 500$ psia, $d_p = 0.01\mu$, $d_f = 0.34\mu$)	1.56×10^{-2} ($d_p = 0.01\mu$, $d_f = 0.64\mu$)	1.5×10^{-2} ($P = 500$ psia, $d_p = 0.1\mu$, $d_f = 0.64\mu$)
Largest Value	1.1×10^{-1} ($P = 10$ psia, $d_p = 0.1\mu$, $d_f = 0.31\mu$)	3.21×10^{-1} ($d_p = 0.1\mu$, $d_f = 0.31\mu$)	19.2 ($P = 10$ psia, $d_p = 0.01\mu$, $d_f = 0.31\mu$)

The impaction parameter is given as:

$$N_I = \frac{v\,V}{g\,d_f} \tag{73}$$

where:

v = sedimentation velocity

V = gas stream velocity

g = gravitational constant.

The smallest value of the impaction parameter will be 2.5×10^{-5} for 0.01μ particles and 0.64μ fibers at 500 psia. Also at 500 psia, 0.1μ particles and 0.31μ fibers yield a parameter value of 2.5×10^{-3}. Both of these values are substantially below those for direct interception and this mechanism is of no interest for the particle size in question.

The descriptive parameter for diffusion is simply stated as the inverse of the Peclet (P_e) number:

$$N_D = \frac{1}{P_e} = \frac{D}{V\,d_f} \tag{74}$$

where.

D = diffusion coefficient corrected for slip.

N_D has a minimum value of 1.5×10^{-2} at 500 psi for a particle diameter of 0.1μ and a fiber diameter of 0.64μ. At 10 psi where the particles will have a maximum mobility the parameter has a value of 19.2 for a 0.01μ particle and a 0.31μ fiber. Note that the largest diffusion parameter value dominates the largest direct interception value but the two smallest values for both diffusion and direct interception are equal. Nevertheless, the direct interception low value is for a 0.01μ particle

and the effects of diffusion for that particle size will be the predominating ones. The basis for these conclusions are reiterated in Table 12.

The Fuch's-Pich diffusion equation (no. 67) has been written into a computer program and several runs have been made using the media specified in Table 11. Both the surface-volume fiber diameter (0.64μ) and the count median fiber diameter (0.31μ) have been considered as it is not clear which of these numbers (or possibly the intervening descriptors) is truly applicable to diffusional filtration mechanisms. The particle diameters considered are 0.1μ and 0.01μ. These sizes essentially bracket those found in the experiment on the generation of particles from heated surfaces. An additional set of computer calculations were made utilizing actual count median diameter (M_g) sizes found in the heated wire experiments (Figure 14). The results of these calculations are summarized in Table 13 and plotted in Figure 21. It should be noted that the calculations, are in some areas outside the limits of Eq. (67) in that some of the Knudsen numbers are too large (Figure 20) and some of the Peclet numbers are greater than 1 which is an upper limit for the application of Eq. (67). Further theoretical calculations have not been carried out to reduce the Knudsen number and Peclet number problem for two reasons. First, it is highly probable that an additional calculation covering the areas in question will not yield figures matching the balance of the calculations and secondly, there is a wide number of equations to pick from in the high Knudsen number range but only one in the low Peclet number range. Therefore, it was felt that further calculation would only

Table 13. Filter Efficiency Calculations for the Diffusional Mechanism in a Helium-Oxygen Environment (PO_2 = 160 mm Hg).* (V = 2.46 cm/sec).

	Pressure psia	Peclet Number	E_D	E_T
d_f = 0.31μ	10.0	.1138	9.68	1.00000000
d_p = actual	14.7	.2112	6.99	1.00000000
(Fig. 2)	20.0	.3631	5.21	1.00000000
	30.0	.7461	3.61	1.00000000
	40.0	1.1732	2.72	1.00000000
	50.0	1.6226	2.26	1.00000000
	100.0	4.5665	1.23	1.00000000
	200.0	10.5917	.73	.99999937
	300.0	15.5633	.57	.99995095
	400.0	18.1571	.52	.99969000
	500.0	23.1091	.44	.99810884
d_f = 0.64μ	10.0	.2350	6.96	1.00000000
	14.7	.4373	4.94	1.00000000
d_p = actual	20.0	.7497	3.63	1.00000000
(Fig. 2)	30.0	1.4578	2.47	1.00000000
	40.0	2.4222	1.83	1.00000000
	50.0	3.3498	1.50	.99999999
	100.0	9.4275	.79	.99980303
	200.0	21.8667	.46	.98700379
	300.0	32.1306	.36	.95001472
	400.0	37.4857	.32	.91206253
	500.0	47.7091	.28	.84774230
d_f = 0.31μ	10.0	.0522	15.72	1.00000000
	14.7	.0713	13.83	1.00000000
d_p = 0.01μ	20.0	.0937	12.21	1.00000000
(Fig. 2)	30.0	.1352	10.27	1.00000000
	40.0	.1769	9.05	1.00000000
	50.0	.2179	8.11	1.00000000
	100.0	.4190	5.79	1.00000000
	200.0	.7182	4.09	1.00000000
	300.0	1.0202	3.28	1.00000000
	400.0	1.3209	2.89	1.00000000
	500.0	1.5496	2.64	1.00000000

*See Equation 72, Table 11, Figure 20.

Table13- continued

	Pressure psia	Peclet Number	E_D	E_T
$d_f = 0.64\mu$	10.0	.1078	11.39	1.00000000
	14.7	.1471	9.87	1.00000000
$d_p = 0.01\mu$	20.0	.1934	8.62	1.00000000
	30.0	.2791	7.13	1.00000000
	40.0	.3653	6.17	1.00000000
	50.0	.4498	5.48	1.00000000
	100.0	.8651	3.74	1.00000000
	200.0	1.6065	2.55	1.00000000
	300.0	2.2300	2.07	.99999997
	400.0	2.7476	1.81	.99999881
	500.0	3.1806	1.65	.99998725
$d_f = 0.31\mu$	10.0	5.0171	1.06	1.00000000
	14.7	6.6895	.91	1.00000000
$d_p = 0.1\mu$	20.0	8.4452	.80	1.00000000
	30.0	11.3482	.68	1.00000000
	40.0	13.7653	.61	1.00000000
	50.0	15.7562	.56	.99999959
	100.0	22.1043	.46	.99996423
	200.0	27.3333	.40	.99958687
	300.0	29.4440	.38	.99860651
	400.0	30.6265	.37	.99682542
	500.0	31.3827	.36	.99411576
$d_f = 0.64\mu$	10.0	10.3579	.72	1.00000000
	14.7	13.8105	.61	1.00000000
$d_p = 0.1\mu$	20.0	17.4352	.53	.99999878
	30.0	23.4286	.45	.99979453
	40.0	28.4188	.39	.99751159
	50.0	32.5289	.36	.98968523
	100.0	45.6348	.29	.95597108
	200.0	56.4391	.25	.90461374
	300.0	60.7816	.24	.86142486
	400.0	63.2259	.23	.82192288
	500.0	64.7901	.23	.78543258

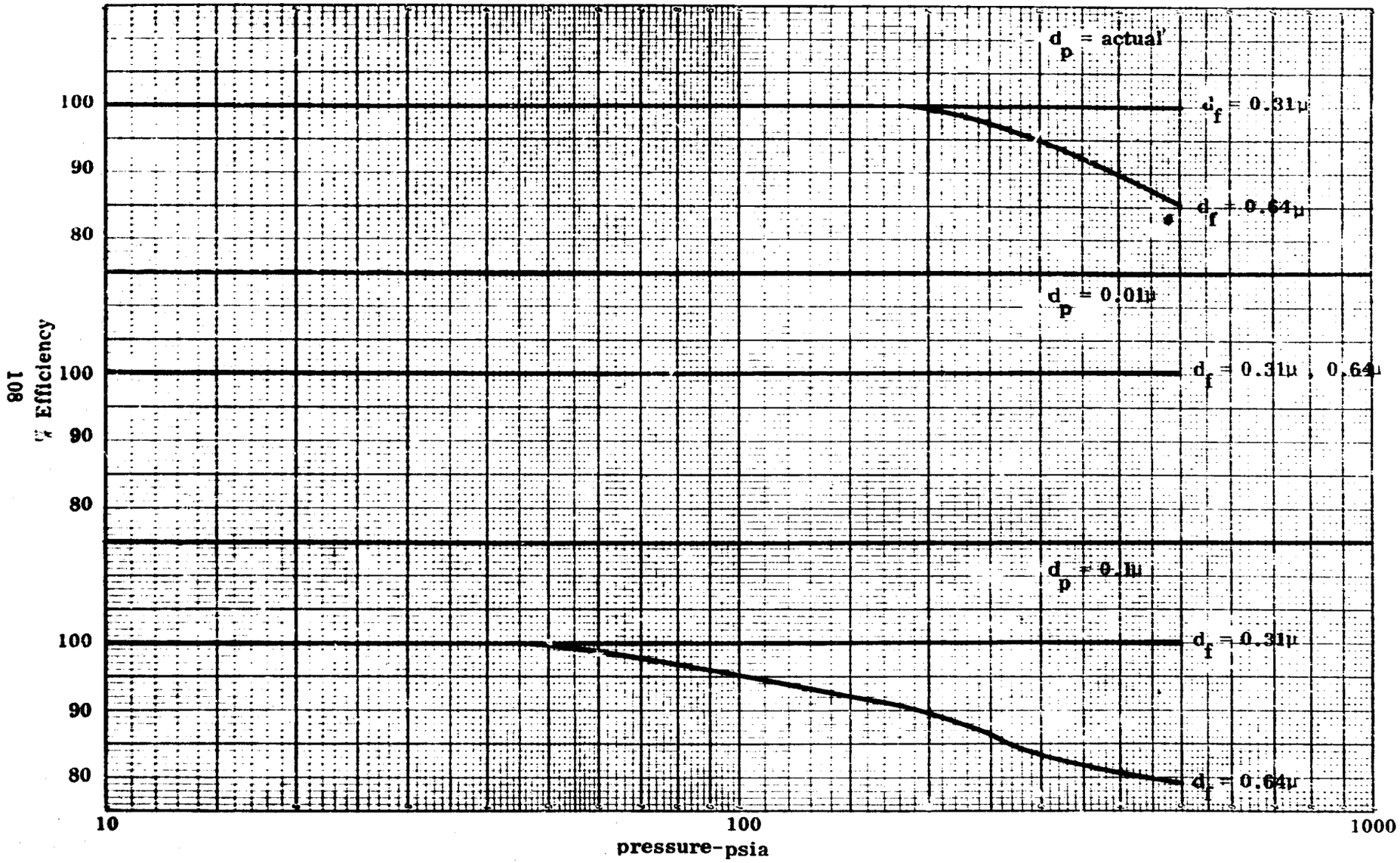

Figure 21. Calcula. l Filter Efficiency vs Pressure for the Diffusional Mechanism in a He-O_2 Environment.*

***See Table 13.**

confuse the presentation and since the difficulty lies in the lower pressure ranges considered, the theoretical results would be of little interest or usefulness to this study.

It is possible in the conduct of an actual experiment to utilize Eq. (67) to determine a theoretical curve with the insertion of one item of real data from the experiment, namely, the observed upstream particle size. In this way one can determine whether the observed efficiency is solely due to the diffusional mechanism or is being effected by additional factors.

10.1 EXPERIMENTAL APPARATUS

The experimental apparatus for any filtration experiment generally consists of a source of aerosol, an upstream sampling apparatus, the filter holder, and a downstream sampling apparatus. In view of the necessity to sample at pressures up to 500 psia, several additional factors must be considered. The gas mixture to be used for all experiments is helium and oxygen in the proportions of 160 mm mercury Hg partial pressure oxygen and the balance to the total pressure, helium. Four working pressures were selected: 50, 100, 300, and 500 psia. The equipment initially designed for this experiment is shown in Figures 22 and 23. Flow control may be achieved by initially setting the high pressure tank regulator to the desired pressure level. The gas will flow through the entire length of the system and exit through a needle valve which will permit pressure reduction to ambient conditions.

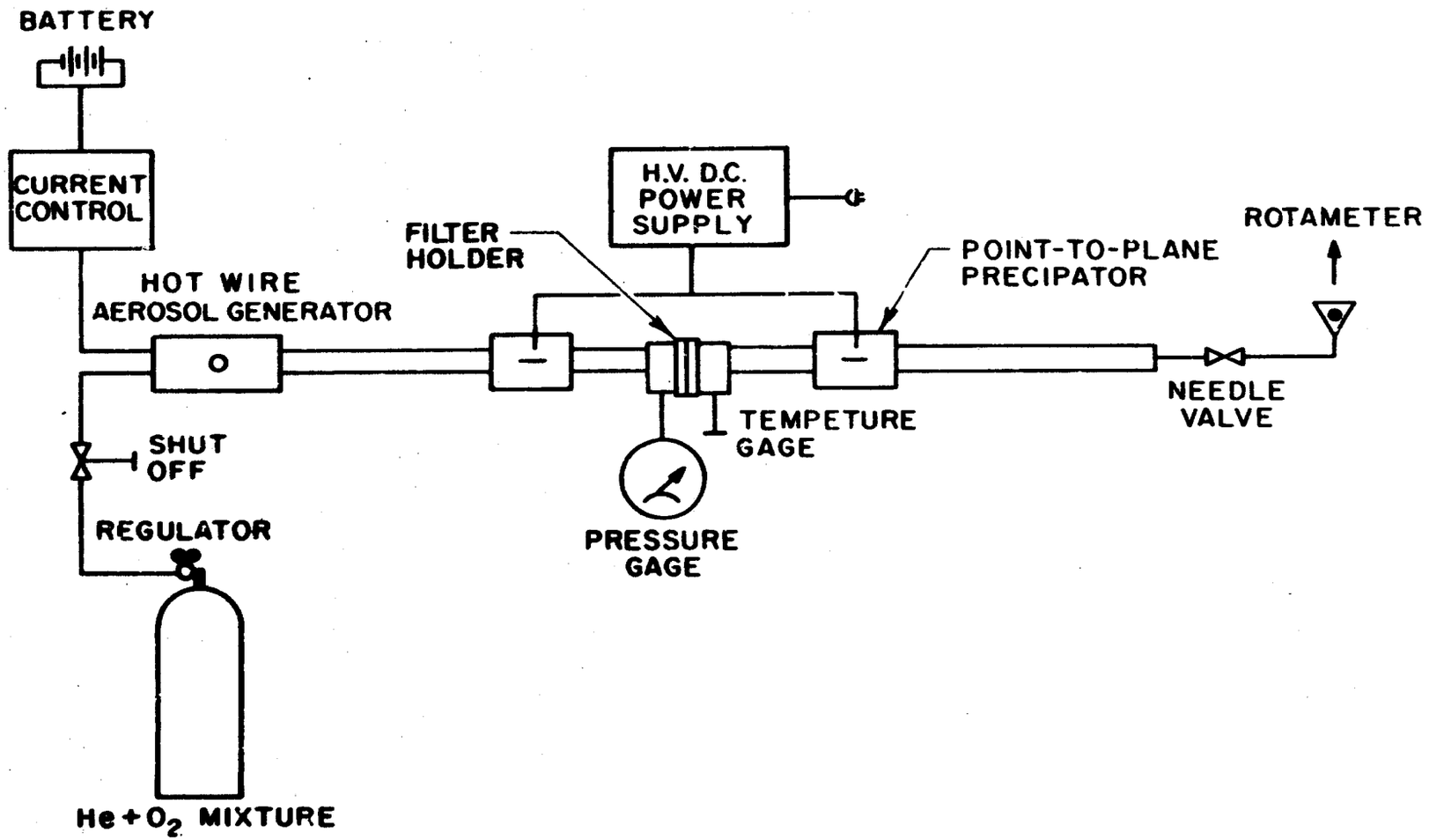

FIG. 22. SCHEMATIC DIAGRAM OF HIGH PRESSURE FILTRATION TEST APARATUS

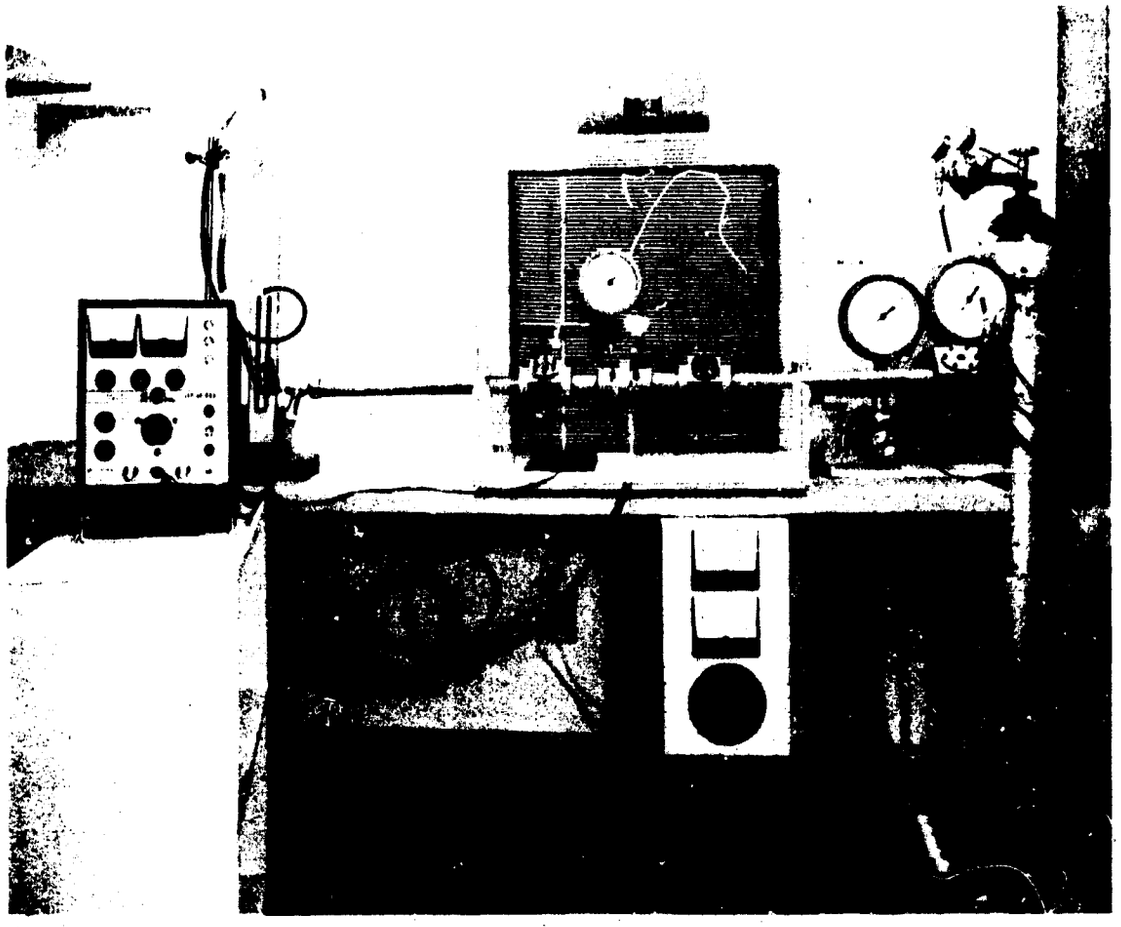

Figure 23. Filter Test Apparatus

The quantity of flow is monitored by a rotameter calibrated for the gas being used. Pressure in the system is monitored with an accurate test gauge upstream of the filter face. The various corrections for density and flow conditions are given in Table 14. The dimensions and flow rates for this system were arrived at by assuming that the filter media would be operated at its most commonly used velocity when employed for personnel protection and containment operations, i.e., 4.85 fpm (2.46 cm/sec). It was desired to work with a filter diameter of 1 in. or greater and yet be conservative in the quantity of gas consumed. The final inside diameter of the system was fixed at 1.125 inches and the desired velocity of 2.46 cm/sec is achieved for the flow rate of 1 lpm (at pressure).

The aerosol generator consists of a series of up to eight, half millimeter nichrome wires inserted in the apparatus shown in Figure 24. An additional pair of output leads were installed in the end cap for the insertion of a thermocouple welded directly to one of the wires for constant temperature monitoring. A half inch thick glass window is provided on the side of the aerosol generator section so that the condition of the wires may be observed.

The up- and downstream sampling points are identical in construction (Figures 25 and 26). The sampling method is via point to plane electrostatic precipitation directly on a carbon-coated electron microscope grid.[42] Four radial holes have been bored in the faces of a brass block. Two of these holes contain phenolic plugs

Table 14. Selected Operating Conditions for High Pressure Filtration Experiment*

Pressure psia	Pressure atm.	Density @ Pressure g/l	Density @ 14.7 psia g/l	Flow @ Pressure - lpm	Flow @ 14.7 psia - lpm
50	3.4	0.809	0.237	1.0	3.4
100	6.8	1.374	0.200	1.0	6.8
300	20.4	3.633	0.177	1.0	20.4
500	34.0	6.091	0.17	1.0	34.0

*V = 2.46 cm/sec (4.85 fpm)

He + 160 mm Hg PO_2 = Total Pressure

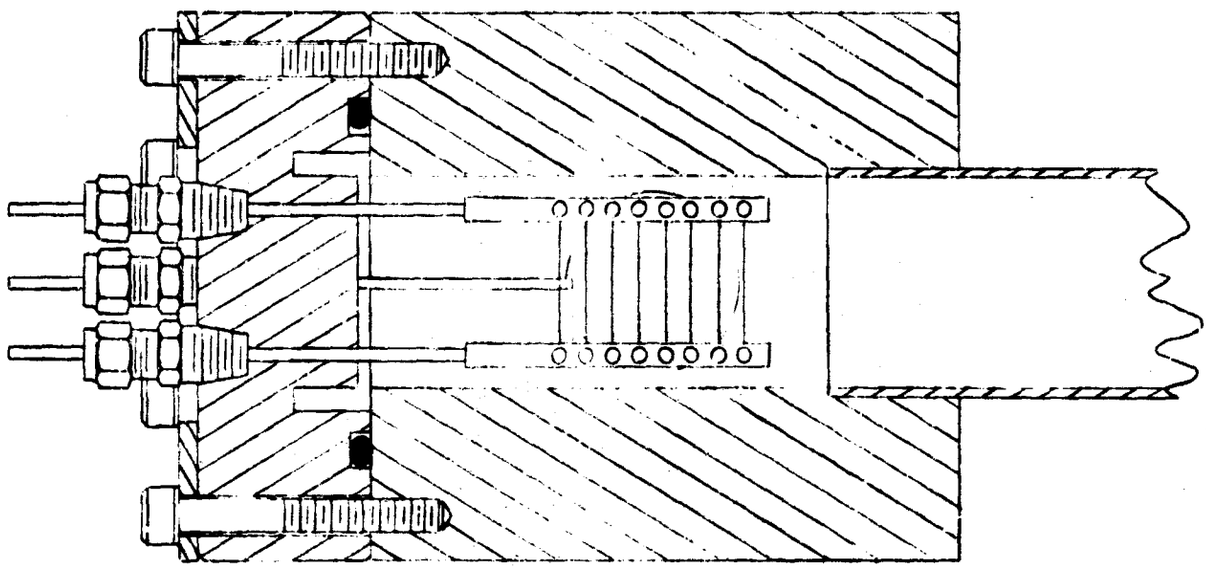

Figure 24. Sectional View of Hot-Wire Aerosol Generator.

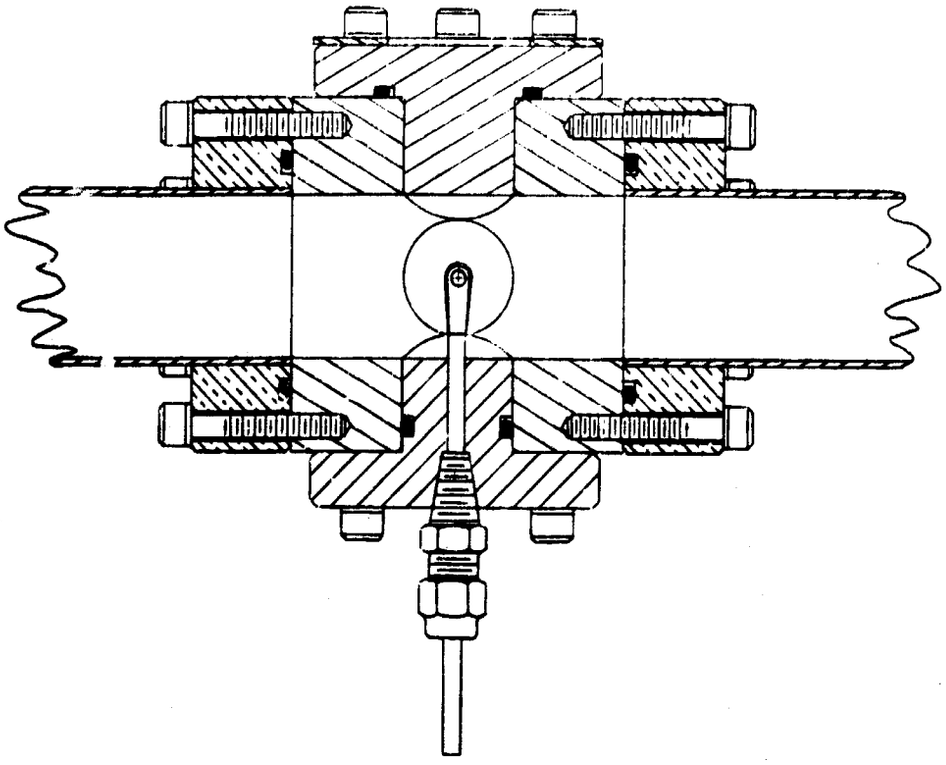

Figure 25. Sectional View of Up- and Downstream Sampling Apparatus.

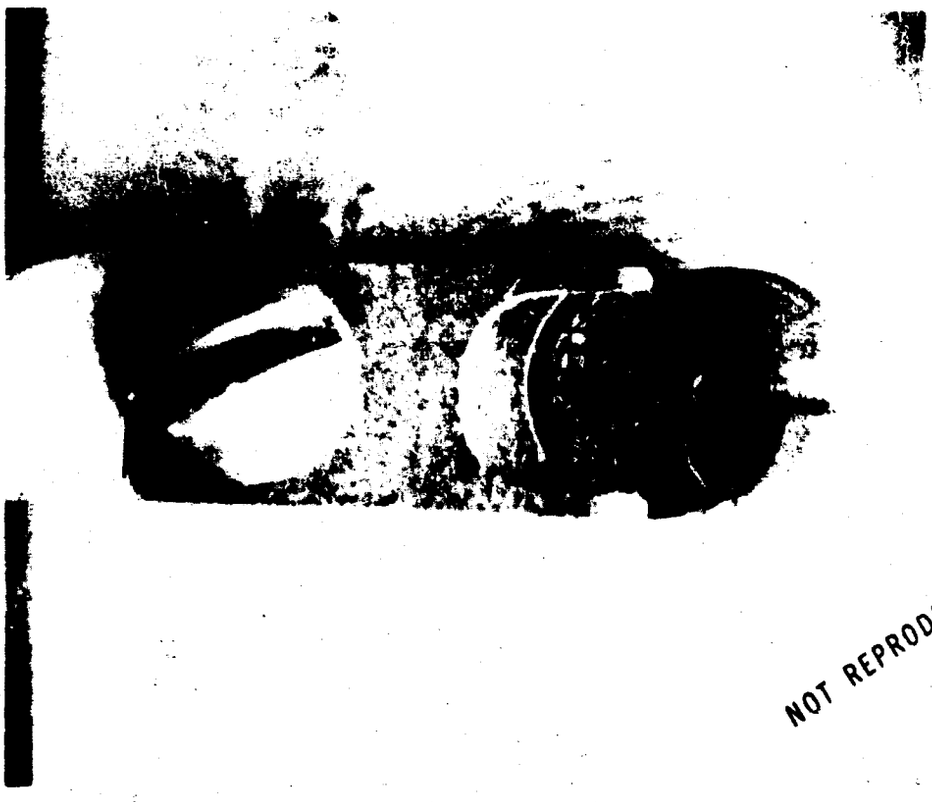

Figure 26. Final Design of ESP Grid Holder

mounting the precipitator elements. The electron microscope grid is contained in a brass holder (Figure 25) which presents a thin edge profile to the airstream creating a minimum disturbance. The opposite electrode is a fine piece of platium wire. The remaining two radial holes in the block contain clear plastic plugs which serve as windows to permit observation of the condition of the corona discharge. The block has been line-bored so that all four plugs present no disturbance to the airstream through this section.

The filter holder section consists of two flanges with provision for a backer screen and over-lapping gasket (Figure 27). The over-lapping gasket technique is one which has proved highly successful in the past under a wide variety of conditions.[43] The backer screen consists of an electro-deposited 60 mesh nickel media.

10.2 INITIAL EXPERIMENTATION

In the performance of any experiments which are intended to elucidate the collection efficiency of a device, it is necessary that the initial experiment be the generation of the test aerosol with both samplers operating but the collection mechanism rendered inoperative or removed. Under ideal circumstances a collection efficiency of 0% will be determined (100% penetration). Due to factors such as human and experimental error and unsuspected constructional anomalies a 0% efficiency is usually not obtained on the first try. Most often a series of tests under "no filter" conditions yields a slight positive or negative efficiency. These results, assuming

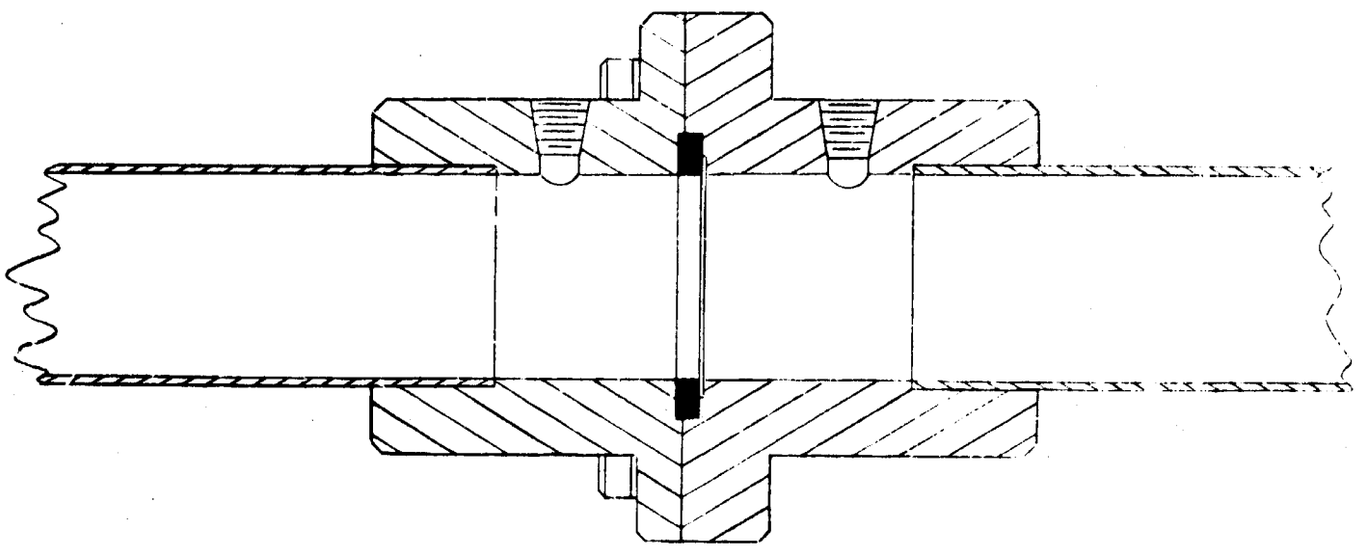

Figure 27. Sectional View of Filter Holder.

corrections, adjustments, and repairs have been made, yield the level of accuracy to be expected from the experimental series. In these studies the initial experiments were all conducted with highly filtered air at atmospheric pressure utilizing no filter media but with the filter support screen installed. The set flow rate was 1 liter per minute. Three to four, 3/4-inch long 0.020-inch diameter nichrome wires were used in all tests. Dry bottled air was passed through a grade VF Millipore filter which is the finest pore size available. Having no initial background information, a wide range of parameters were tried in order to find the most favorable sampling situation. An initial series of 12 runs were made wherein the generation and sampling time was varied from 0.2 to 30 minutes. The corona voltage was varied from 3250 volts to 6000 volts. The corona current was constant at 0.03 milliamps. Up- and downstream samples were taken in each case. The test conditions are summarized in Table 15.

Nickel, 400 mesh electron microscope, grids were used. These grids were coated with carbon and recieved no other preparation either prior to or after the sampling event.

The first set of runs are numbered 1 thru 12. In this set an attempt was made to cover all possible variables of sampling time and sampling conditions in order to yield information suitable for the main body of work. While the generator temperatures were not directly measured, our past experience indicated that a high red

TABLE 15. Summary of High Pressure Filtration Test Conditions

Test No.	Sampling Time-min	Sampling ESP Voltage	Sampling ESP Current ma	Generator Voltage	Generator Current amps
1	1.0	3250	0.03	-	-
2	1.0	3250	0.03	1.3	25+
3	0.5	3650	0.03	1.3	25+
4	0.2	3650	0.03	1.3	25+
5	0	-	-	-	-
6	1.0	3650	0.03	1.3	25+
7	1.0	3650	0.03	-	-
8	1.0	3650	0.03	-	-
9	30.0	6000	0.03	2.0	35
10	20.0	6000	0.03	2.0	35
11	10.0	6000	0.03	2.0	35
12	5.0	6000	0.03	2.0	35
13	30.0	6000	0.03	2.0	37
14	20.0	6000	0.03	2.0	37
15	10.0	6000	0.03	2.0	37
16	5.0	6000	0.03	2.0	37
17	25.0	6000	0.03	2.0	37
18	5.0	6000	0.03	2.0	37
19	25.0	6000	0.06	2.0	37
20	5.0	6000	0.06	2.0	37
21	1.0	6000	0.06	2.0	37
22	35.0	6000	2.6	2.4	37
23	5.0	6000	2.6	2.4	37
24	1.0	6000	2.6	2.4	37
25	25.0	6000	2.8	2.4	37
26	5.0	6000	2.8	2.4	37
27	1.0	6000	2.8	2.4	37
28	6.0	6000	0.07	2.4	32
29	0.5	6000	0.07	1.2	27
30	0.25	6000	0.07	1.2	27
31	1.0	6000	0.07	1.2	27
32	2.0	6000	0.07	1.2	27

heat would provide sufficient particles in the submicron size range. After the 8th test it was observed that there was some difficulty in maintaining a stable corona in the sampling apparatus as there was very little difference between corona and breakdown voltage. Therefore, the distance from the grid to the discharge electrode was increased from 0.25 inch to 0.375 inch.

The results from this initial series of runs was extremely poor. Sample photomicrographs demonstrated only random accumulations of extraneous material. This was determined to be due to handling errors, consequently, more rigirous procedures were instituted.

In view of the lack of any clear, visible nichrome aerosol collected in runs 1 thru 12, a change in the aerosol generator was effected. In the original design the air was admitted to the chamber around the annulus of the apparatus. Because Reynolds number varies only from 20 to approximately 200 over the entire range of flows being utilized for this experiment, the flow is laminar and it was considered possible that a certain degree of stratification existed. Therefore, the modification to the apparatus consisted of plugging the annular gas opening and directing a 1 millimeter jet directly at the heater wires. The series of tests under these conditions are summarized in runs number 13 thru 16. While some aerosol particles were observed in the photomicrographs, the samples were so sparse as to be meaningless and are not suitable for reproduction here.

At this point it was decided that there may be difficulty due to stray electrical currents within the instrument causing preferential deposition at some location. Consequently, a new series of tests were made, itemized as numbers 19 thru 27. Originally all tests to this point had been run with negative corona discharge, the collection electrode being positively grounded through the high voltage generator. The filtration apparatus had been essentially in a condition of "floating" ground. For Tests 19 thru 21 the unit was grounded and it was noted at this point that the corona current increased from 0.3 milliamps to 0.6 milliamps. Only one clear set of samples was obtained from this run and the upstream concentration was much higher than downstream. On runs 22 to 24 the unit ground was disconnected but placed at the same potential as the negative discharge electrode. Under these conditions the corona current rose to 2.6 milliamps but only one sample was obtained on the upstream collector. Nothing was observed downstream. Runs 25 thru 27 were run with a positive discharge electrode and the entire urit connected again to the discharge electrode as in runs 22 thru 24. Under these conditions no positive results were obtained and no aerosol was visible on the collection surfaces.

At this point several conclusions could be clearly drawn from the results obtained. The quantity of aerosol produced by the heated wire technique under flow conditions was rather sparse for the purposes of this test and a great deal of difficulty was being encountered in obtaining a uniform distribution of aerosol across the diameter of the tube. There is also a strong indication that the upstream sampler is

preferentially removing large quantities of the available aerosol and significantly denuding the stream. It was decided at this point that much heavier concentrations of aerosol were necessary and that if they could be generated at a constant rate, it would be entirely possible to cycle the up- and downstream samplers sequentially rather than simultaneously in order to avoid any preferential removal of aerosol from the stream. Inasmuch as salt ($NaC\ell$) particles are solid material which might be found in a submarine atmosphere and are readily generated, it was determined that this material would be suitable for the continuation of the tests. Accordingly, the nichrome wires were coated with a thin layer of salt and the series resumed with 6 more tests numbered from 28 thru 32. A negative discharge corona was used with the unit separately grounded. Under these conditions no difficulty was found in generating sufficient aerosol and the heater current had to be significantly reduced in order to prevent complete saturation of the sampling surface. Selected photomicrographs from this series are shown in Figures 28 and 29. While a cubical crystal is expected from this method of aerosol generation it is possible for the crystals to be degraded under the electron microscope beam so that the slight rounding observed in the photomicrographs occurs during analysis and the crystals were originally cubic.[44] The technique at this point appears successful with two important reservations. It is now definitely observed that the upstream sampler denudes the airstream of large quantities of aerosols so that a filter efficiency could not be determined with both samplers operating

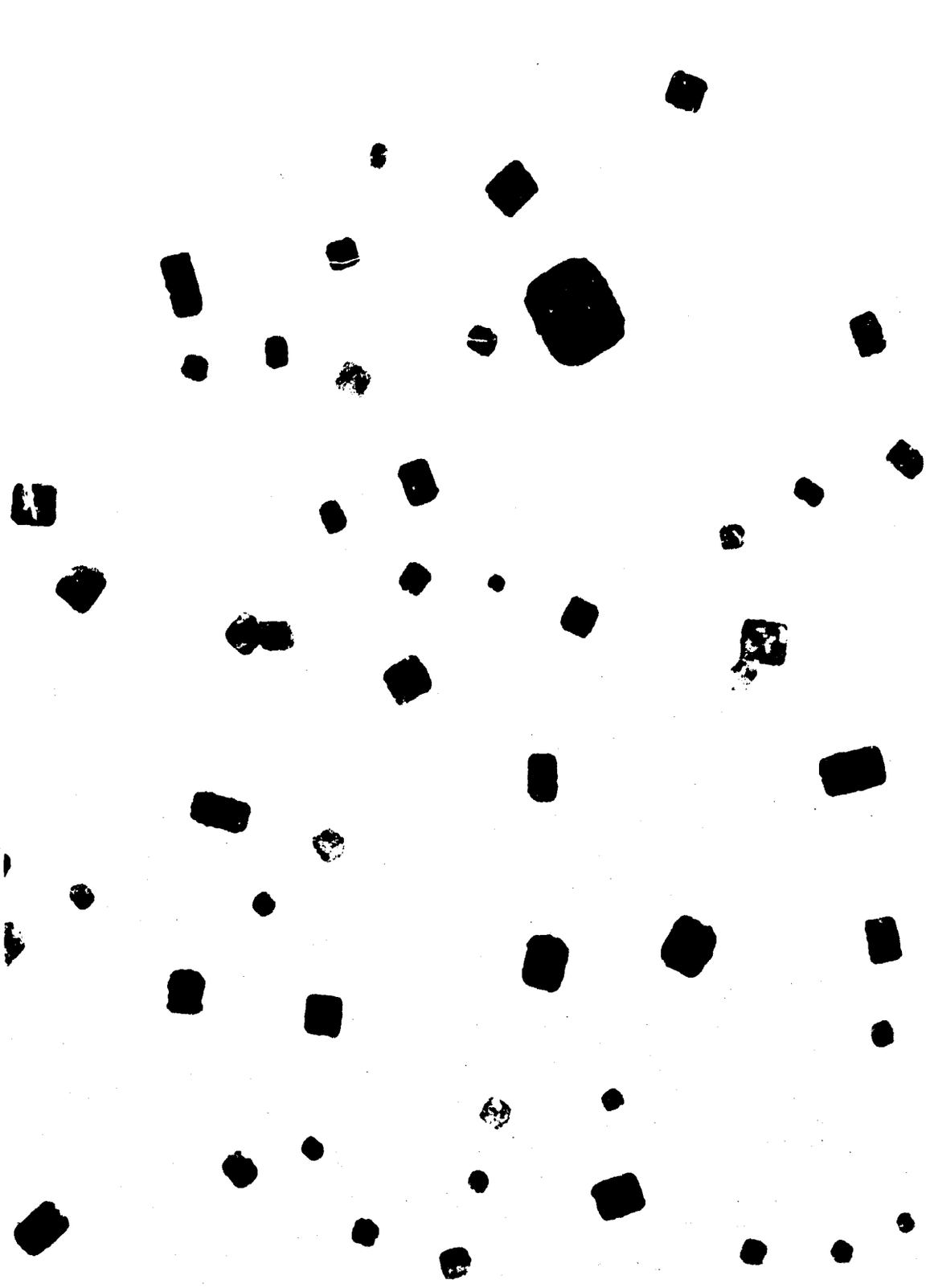

Figure 28. Typical Salt Crystals Generated and Collected in a Filtration System

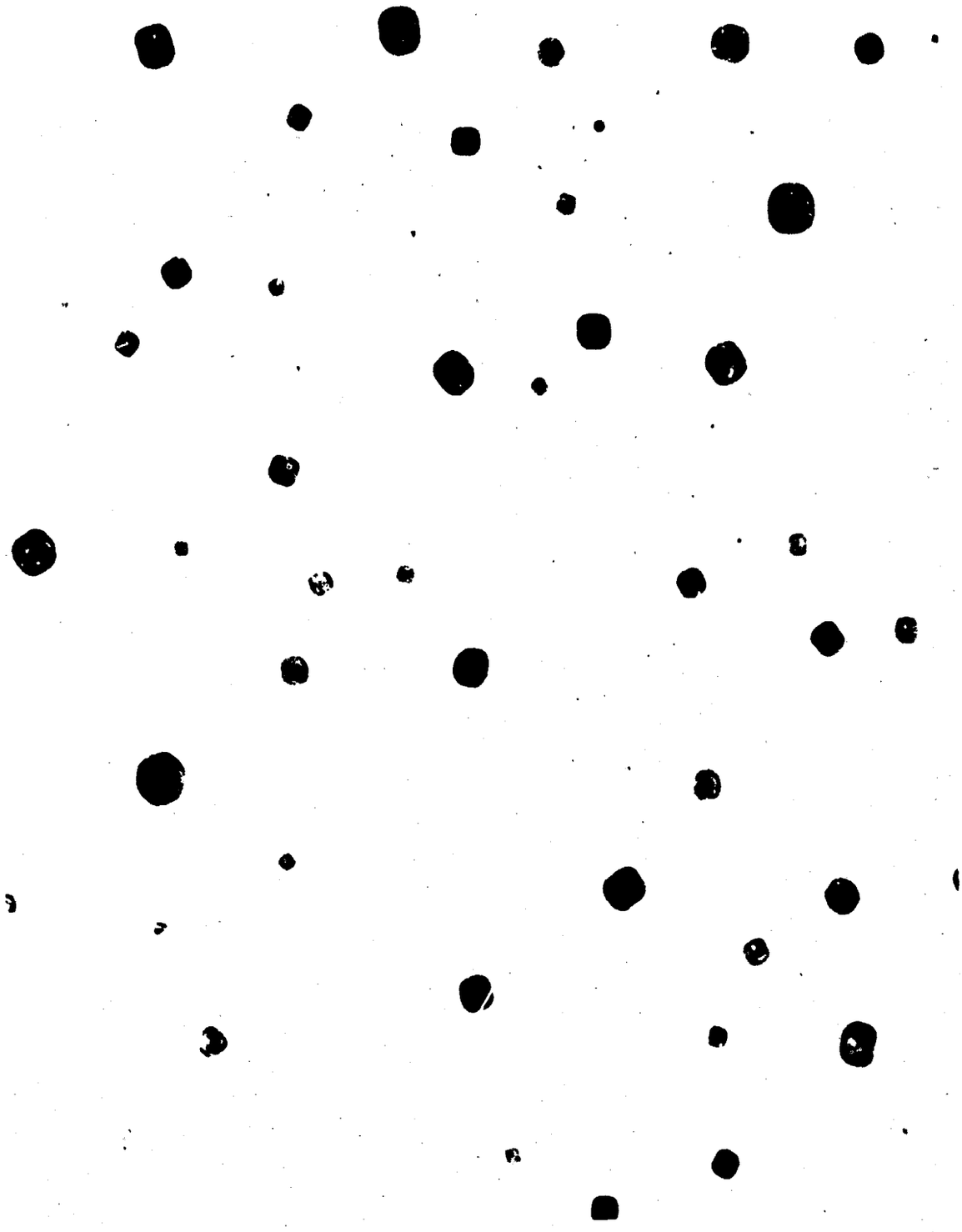

Figure 29. Degradation of Crystals Generated and Collected in a Filtration System.

simultaneously as the anomaly is too great to calculate out. Also it was found to be very difficult to maintain a constant generator output. However, this was probably due to the salt coating of the wires, the surface of which was constantly changing due to the flow of the material under the high temperatures to which it was subjected.

10.3 EXPERIMENTAL MODIFICATIONS

At this point the series was terminated. However, it is possible to detail a series of modifications necessary for the continuance of the study.

1. A uniform distribution of aerosol across the entire tube diameter must be achieved.
2. The aerosol must be generated at a constant rate.
3. If No. 2 can be achieved successfully, sampling will be carried out sequentially from upstream to down. Ideally a number of cycles can be made between the up- and downstream samplers to eliminate slight anomallies in the generator output. If output constancy cannot be satisfactorily achieved, then the upstream sample must be withdrawn from the airstream using a small sampling probe so that the electrostatic field will not remove too much of the test aerosol.

The achievement of uniform aerosol distribution across the diameter of the tube and constancy of output may be dealt with as a single problem. A proposed design is shown in Figure 30. The features of this system include a large diameter chamber with the generation source located a significant distance from the entrance

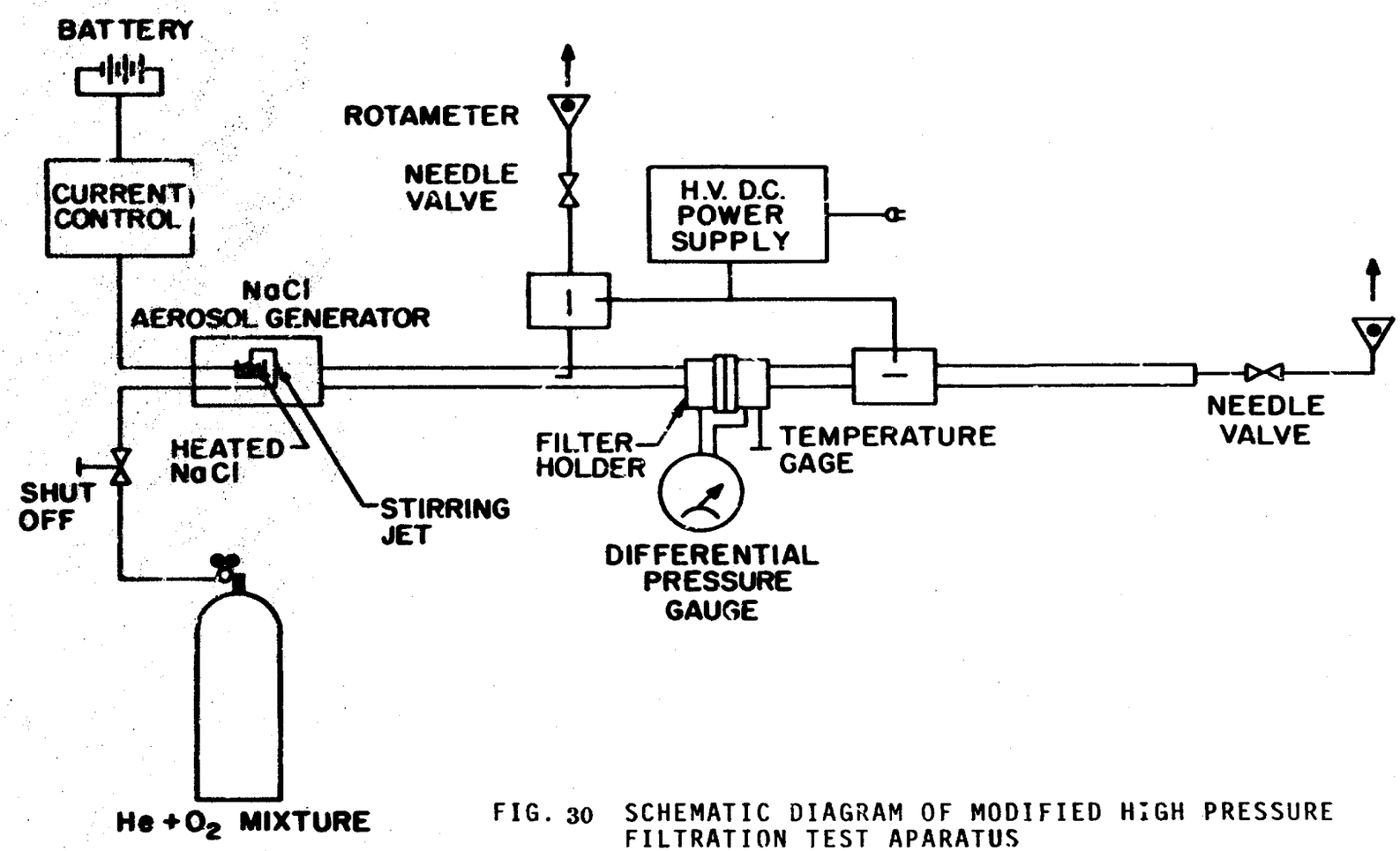

FIG. 30 SCHEMATIC DIAGRAM OF MODIFIED HIGH PRESSURE FILTRATION TEST APARATUS

to the flow tube. By generating the aerosol in a turbulent mode a uniform distribution of aerosol should be insured. The salt would be contained in a small crucible, heated externally by nichrome elements. The incoming gas jet may be directed downward into the salt cup to insure maximum turbulence and mixing. If further testing indicates the need to insert a probe for the removal of the upstream sample from the gas stream, so that the upstream corona discharge will not overly denude the air stream, then the apparatus shown schematically in Figure 30 and detailed in Figure 31 may be constructed and installed.

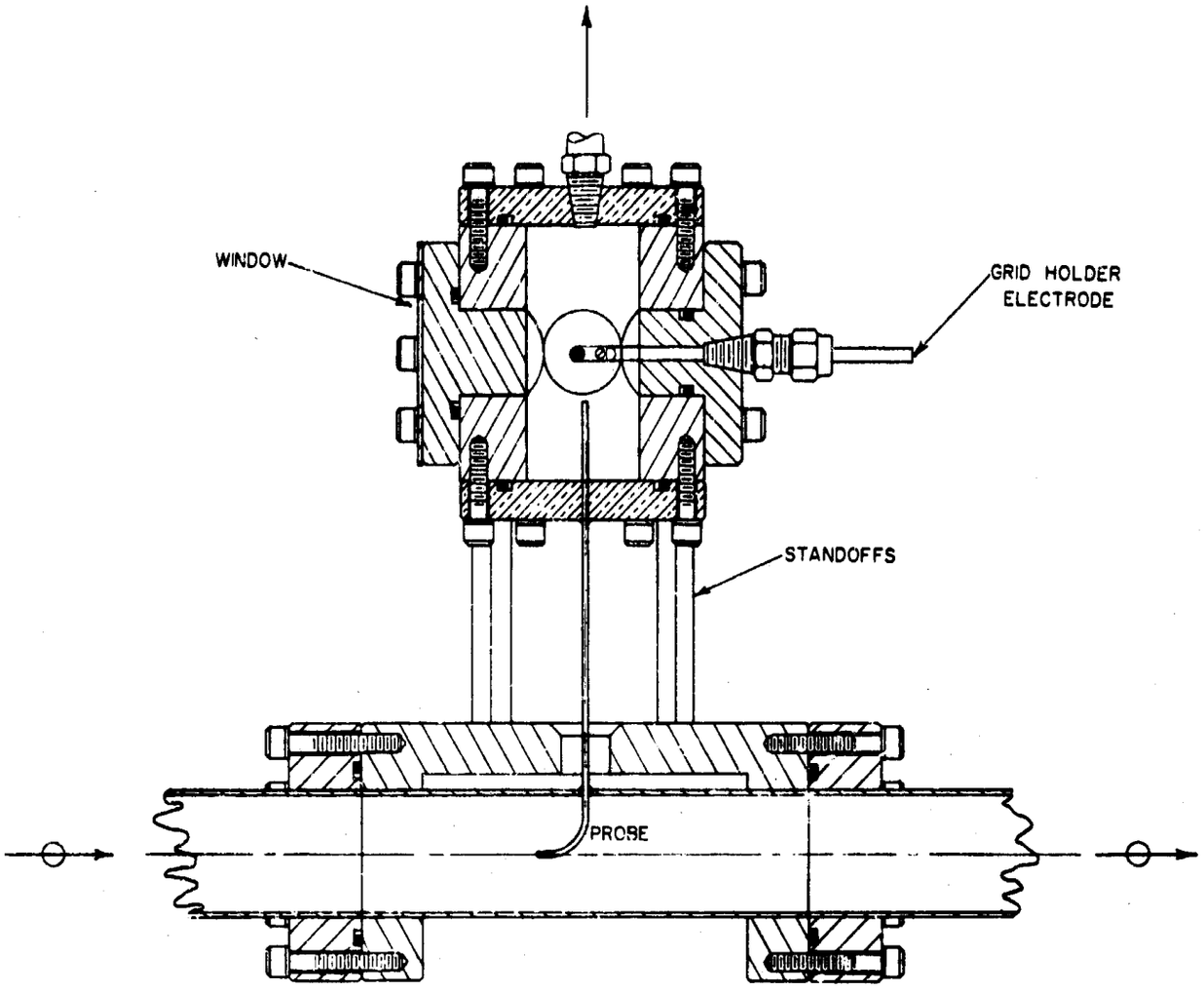

MODIFIED UPSTREAM SAMPLER
(HIGH PRESSURE FILTRATION STUDY)

Figure 31

SECTION 11.0: ELECTRIFICATION AND PRECIPITATION OF AEROSOLS - THEORY

11.1 THEORY

The electrification of aerosol particles is of great importance in aerosol mechanics and to the general subject of this study. The force that can be exerted on a charged particle in an electric field may be many times that of gravity and this one force may override other considerations. Also, the device most successfully used for the cleansing of submarine atmospheres has been the electrostatic precipitator and it therefore becomes of vital importance to determine its projected operating characteristics in the helium-oxygen atmosphere and at the pressures to be considered. Because both particle charging and precipitation are considered in this discussion and because of the complex terminology involved in considering electrification, it is felt that the subject will be more understandable if presented in what is usually considered a "reverse" order. To this end, the first relationship presented is a statement of the efficiency equation for electrostatic precipitation. From there the development proceeds backwards, introducing the terms required and the effects of the helium-oxygen atmosphere.

Consider an electrostatic precipitator to be a simple rod and tube device in which a fine wire or rod is concentrically contained in a cylindrical shell of some length, l. A positive or negative potential may be applied to the center wire electrode while maintaining the tube at ground conditions. Aerosol

laden gas is passed axially through this configuration and the aerosol will be found to deposit, with some efficiency, on the inside walls of the tube. The expression for the efficiency of this collection is given by White[45] as

$$M = 1 - \exp\left(-\frac{2\,u\,l}{R\,V}\right), \tag{75}$$

where

M = collection efficiency,

u = drift velocity of the particles,

l = length of precipitator,

R = radius of the tube, and

V = axial velocity of the particles (generally taken as the gas velocity).

All of the terms in the above equation are readily determinable in the design situation with the exception of the drift velocity of the particles, which is dependent upon several conditions (including the applied potential with its resultant field, particle size, gas composition, temperature, and pressure). Particle charging occurs by two basic mechanisms. In diffusion charging, the process occurs without the presence of an applied electric field, that is, the particles were charged from collisions with ions* undergoing random thermal

*According to Whitby,[13] "Thus, a small ion will be defined here as any molecule or atom which has a net electric charge or any charged molecular cluster which will disintegrate upon loss of charge. Any charge carrier in a gas which is not a small ion will simply be called a charged particle. The boundary between these two kinds of charge carriers will be taken as corresponding to a particle diameter of about 15Å and a mobility of about 0.1 cm^2/volt-sec."

motion. In the field charging process, the aerosols are in an applied electric field and the ions are thought to be driven along the electric force lines onto the particles. Summarizing the work of several investigators, Green and Lane[5] state that when the particles are less than 1 micron in size, charging is thought to be by diffusion rather than the field mechanism. Larger particles in an applied field are charged by the field mechanism although they may also be charged by diffusion in the absence of an applied field. After an extensive series of experiments, Liu and Yeh[46] have accepted this conclusion and developed a charge theory containing both terms in which the diffusion term predominates as the particle size decreases. Inasmuch as this theory is complex and capable of solution only by numerical integration, only the separate relationships for diffusion and field charging are presented here The simpler approach is adopted because at the present time the variation of ionic mobility with pressure and composition in their theory has not been clarified.

Returning to the efficiency equation, the drift velocity for field charging is given as:

$$u = \frac{(ne)\,E}{3\pi\,\eta\,d} \quad \text{(slip correction)}, \tag{76}$$

where

n = number of electronic charges, e,

note: the product ne is the charge q, acquired in time, t.

E = collection field strength,

η = viscosity of the gas, and

d = diameter of the particles.

For the above equation the quantity not directly available is the amount of charge (q) acquired in time (t). The relationship for the value of this charge is given by Green and Lane[5] as:

$$q = n_s e = p E_o \frac{d^2}{4} \quad , \tag{77}$$

where

n_s = total or saturation charge,

E_o = charging field strength, and

p = a factor equal to 3 for conducting particles and for insulating particles:

$$p = 1 + 2 \frac{\varepsilon - 1}{\varepsilon + 2} \tag{78}$$

where

ε = dielectric constant.

Note: Actually, the above equation is for the total charge (n_s) that may be placed on the particle regardless of the time. When time is considered, then the actual charge which may be placed on the particle is somewhat less than

the limiting value n_s indicated above. The relationship between n and n_s is given by White[45] as:

$$\frac{n}{n_s} = \frac{\pi N_o e Z t}{\pi N_o e Z t + 1} \quad , \tag{79}$$

where

N_o = ion concentration at a large distance from the particle,

Z = electric mobility of the ions, and

t = charging time.

The preceding equations may now be directly substituted and applied to the relationship for q.

$$q = ne = \frac{E_o d^2}{4} \left[\frac{\pi N_o e Z t}{\pi N_o e Z t + 1} \right] \left[1 + 2 \frac{\varepsilon - 1}{\varepsilon + 2} \right] \quad . \tag{80}$$

This relationship may then be substituted into the equation for the drift velocity (u) of the particles due to the applied field in the presence of the collecting field which takes the form:

$$u = \left[\frac{E E_o d}{12\pi \eta} \right] \left[\frac{\pi N_o e Z t}{\pi N_o e Z t + 1} \right] \left[1 + 2 \frac{\varepsilon - 1}{\varepsilon + 2} \right] \text{ (slip correction)} \quad . \tag{81}$$

Hence, for the field charging situation, the above expression for the drift velocity of the particles may be inserted into the efficiency equation; for particles significantly greater than 1 micron, a reasonable prediction of efficiency is available.

Of the texts investigated, the collection efficiency for particles charged by the diffusion mechanism is not specifically developed and this is so for certain practical reasons since the field charging mechanism stemming from the corona existing in industrial electrostatic precipitators is far more effective for charging purposes than the diffusion method. Further, the aerosols treated generally consist of both micron and submicron particles and, as was stated earlier, equations for both processes are neither readily combinable nor has experiment shown it possible to do so directly. However, re-examining the equation for the drift velocity given above, the term for the rate of charge acquisition with time has been developed by White, as quoted by Liu and Yeh:

$$q = ne = \frac{d\,k\,T}{2e} \ln\left(1 + \frac{\pi\, e\, \bar{c}\, d\, N_o\, t}{2\,k\,T}\right) , \qquad (82)$$

where

k = Boltzmann's constant,

T = absolute temperature, and

$\bar{c}$ = R.M.S. velocity of the ions.

This relationship may then be substituted into the drift velocity expression giving a final equation for the diffusion case as:

$$u = \frac{E k T}{6 e} \ln \left[1 + \frac{\pi e \bar{c} d N_o t}{2 k T} \right] . \qquad (83)$$

Having expressed the relationships for the collection efficiency of a precipitator and the methods by which the particles are charged, we may now investigate the individual components of these equations to determine the effects of the high-pressure helium-oxygen environment. Concerning the mobility of the ions (Z), Whitby[13] states that the mobility of the small ions is reduced linearly with increasing pressure according to the relationship:

$$Z_r = \frac{Z}{P} \quad , \qquad (84)$$

where

Z_r = reduced mobility, and

P = pressure in atmospheres.

At the 500 psia (34 atmosphere) condition, there will be a 34-fold reduction in the mobility of the ions, thus greatly reducing the drift velocity of the particles. This problem is further complicated by the fact that, according to White,[45] negative corona will not exist in pure helium and, when the voltage is raised to a point that would correspond to corona onset, spark-over will occur. Oxygen, on the other hand, has a strong electron affinity and will

produce a very stable negative corona. White[45] states that these determinations of collection efficiency under various abnormal circumstances of composition, pressure, and temperature are not amenable to theoretical treatment and are properly dealt with on a direct experimental basis.

Concerning the relationship for charge acquired by the diffusion process, it is even more difficult to stipulate the effects of the high-pressure environment. The RMS speed of the ions may be calculated according to Loeb[3] from the expression:

$$\bar{c}^2 = \frac{4}{\pi k m} \quad , \tag{85}$$

where

m = ion mass.

Seemingly, the speed is constant since the Boltzmann's constant will not vary under the conditions assumed, nor would the mass. However, in the Liu and Yeh[46] verification of White's equation for diffusion charging, they found that the experimental data could only be verified when the mean thermal speed of the ions was taken as a value considerably smaller than the mean thermal speed of air molecules. Quoting Liu and Yeh, "it was suggested that the discrepancy in the mean thermal speeds of the ions and the air molecules could be explained if it was assumed that the ions produced by a corona discharge were actually molecular clusters with an effective molecular weight equal to sixteen times the molecular weight of air." Actually, it can be seen

that Liu and Yeh are investigating diffusional charging of submicron particles and the charging is taking place in the field of a corona discharge. This is entirely correct, since they are dealing with submicron particles in a corona discharge that have been found to receive their charge via the diffusion process only.

SECTION 12.0: CORONA STUDIES

Inasmuch as White[45] specifically states that the existence of negative corona discharge in pure helium is not possible and because of the potential utility and importance of precipitator applications in undersea vessels, it was considered necessary to perform experiments in this area to determine if the small quantities of oxygen present at the higher pressures would be sufficient to maintain a corona discharge. The experimental apparatus designed for this purpose is shown in Figures 32 and 33. A heavy wall brass tube was constructed with a 3/4 in. precision bore diameter (1.915 cm). The collecting electrode was a 1/16 in. diameter polished brass rod (0.159 cm) with an effective length of 11.7 cm. The rod was supported by the high voltage input attachment fixture (Figure 32) and the free end was rounded. Potential gradients were provided by a stabilized dc power supply (Sorensen Model 230-6P) with a capability of 0 to 32,000 volts, 0 to 8 milliamps. Pressures below 1 atmosphere were measured with a vertical mercury manometer; above 1 atmosphere, up to 500 psi, with a precision Ashcroft test gauge. The balance of the equipment attached to the test apparatus in Figure 33 consisted of the numerous needle and latch-type valves necessary to the test procedure described below. Also not shown was a vacuum pump with a capability to 15 microns Hg.

Helium and oxygen was withdrawn from purchased cylinder gas, the oxygen being USP grade and the helium, standard high purity type (99.995% pure).

Four series of runs were made at pressures ranging from 0 to 500 psig (514.7 psia). A negative corona test was run of pure helium followed by similar tests

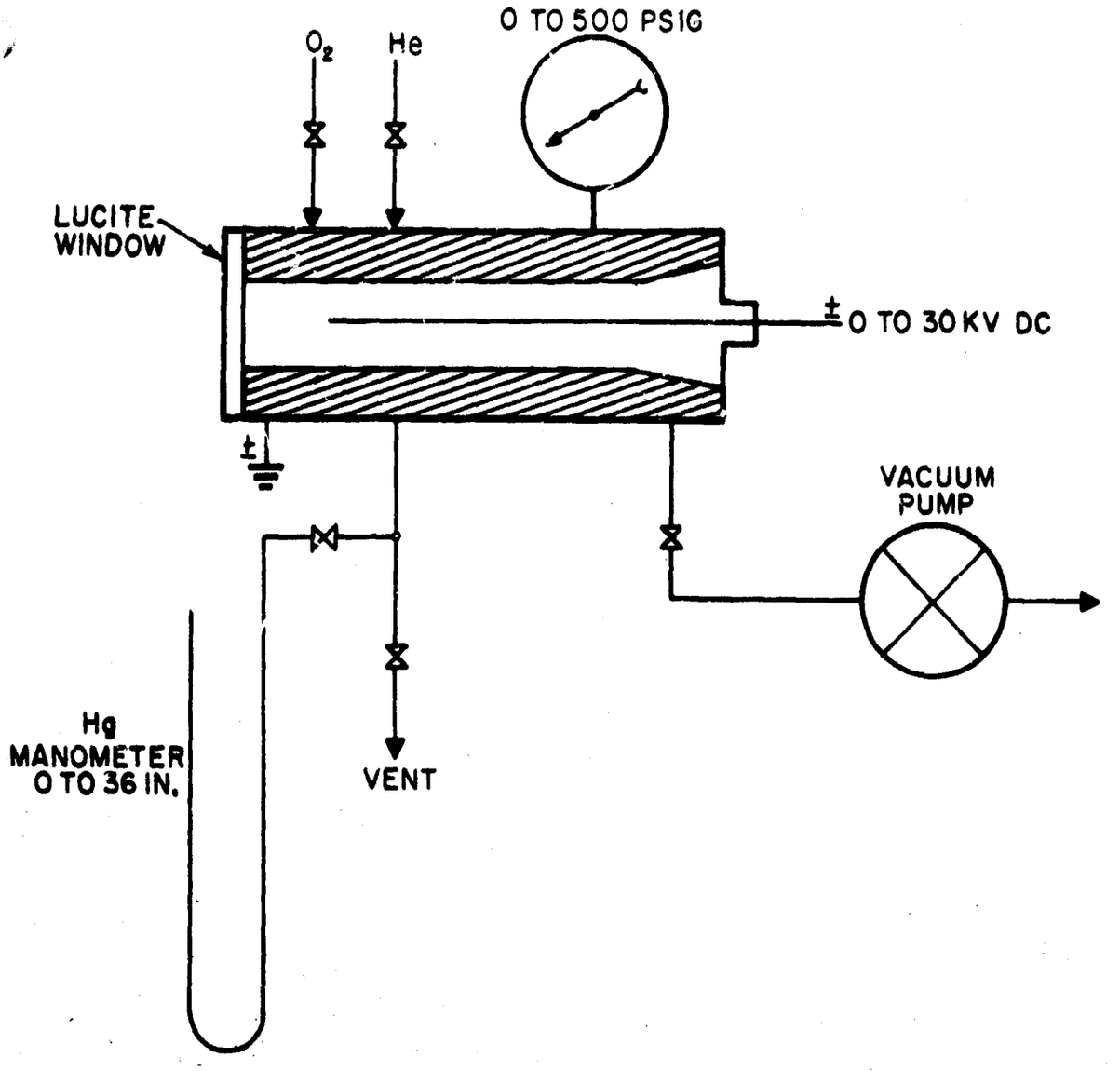

Figure 32. Schematic of Electrostatic Precipitator Experimental Apparatus.

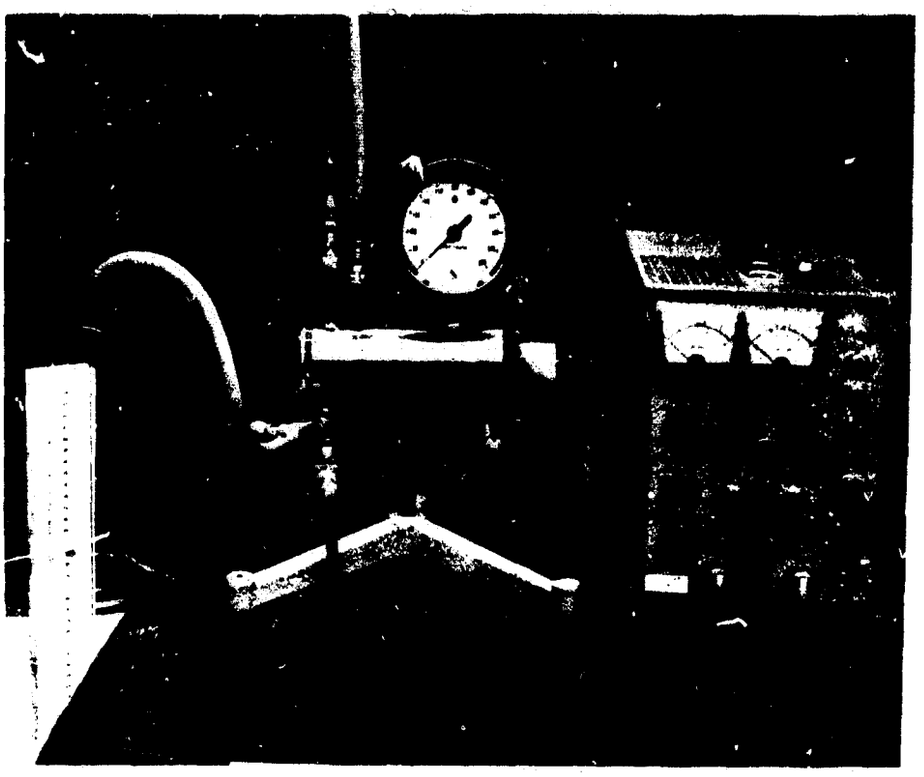

NOT REPRODUCIBLE

Figure 33. Electrostatic Precipitator Experimental Apparatus

with an oxygen constant partial pressure of 160 mm Hg. Two similar series were run with positive potential applied to the center electrode. The general test procedure for a run at a given pressure was as follows:

1) Evacuate test chamber to 15 microns Hg absolute;
2) Pressurize chamber with oxygen to 160 mm of Hg absolute;
3) Add helium to desired test pressure (Note - close pressure line to mercury manometer at 14.7 psia);
4) Apply potential gradient at increasing selected current levels noting voltage.

Because it is extremely difficult to visually determine corona onset, a standardized procedure was established of beginning the readings by increasing the voltage to a point at which the measured current flowing in the system was 0.02 milliamps, the lowest scale division.

12.1 RESULTS

The first and most significant observation in all test runs was the readily observable presence of a corona discharge. In all cases, the discharge was of the classical pattern in that there were numerous spikes and points along the rod for negative applied potential and a more diffuse glowing type of discharge for the positive potential. Tabulated and plotted data from these tests are presented in Figures 34-36 and Table 16. No data for negative potential in pure helium is presented. It was found to be completely impossible to obtain a reproducible result for this set of conditions. Reruns were erratic and continued operation resulted in broader and broader point spreads. Inasmuch as data on pure helium is of secondary importance, this series was

Figure 34. Voltage vs Corona Current Helium.

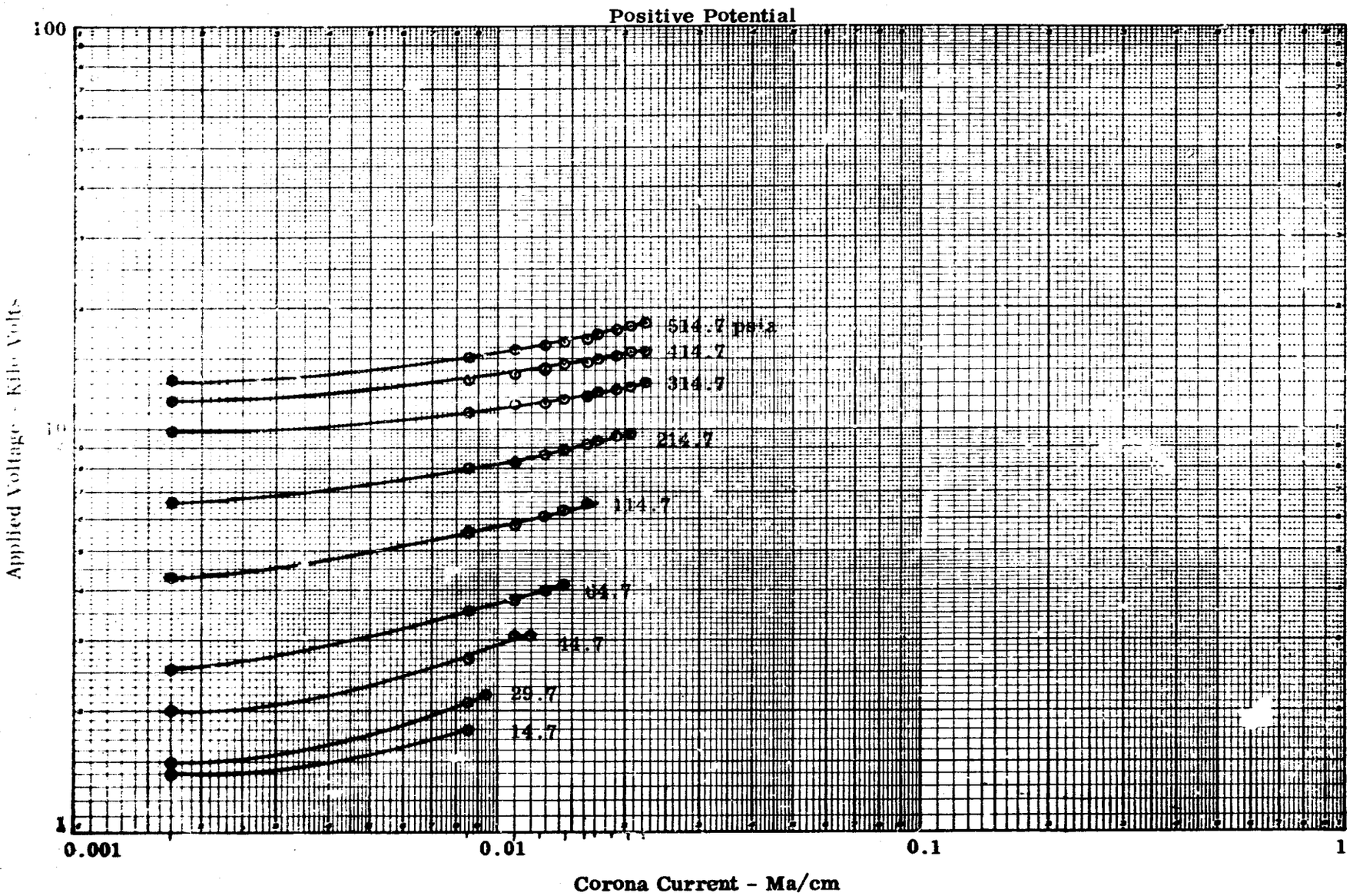

Figure 35. Voltage vs Corona Current. Helium and Oxygen (PO_2 = 160 mm Hg)

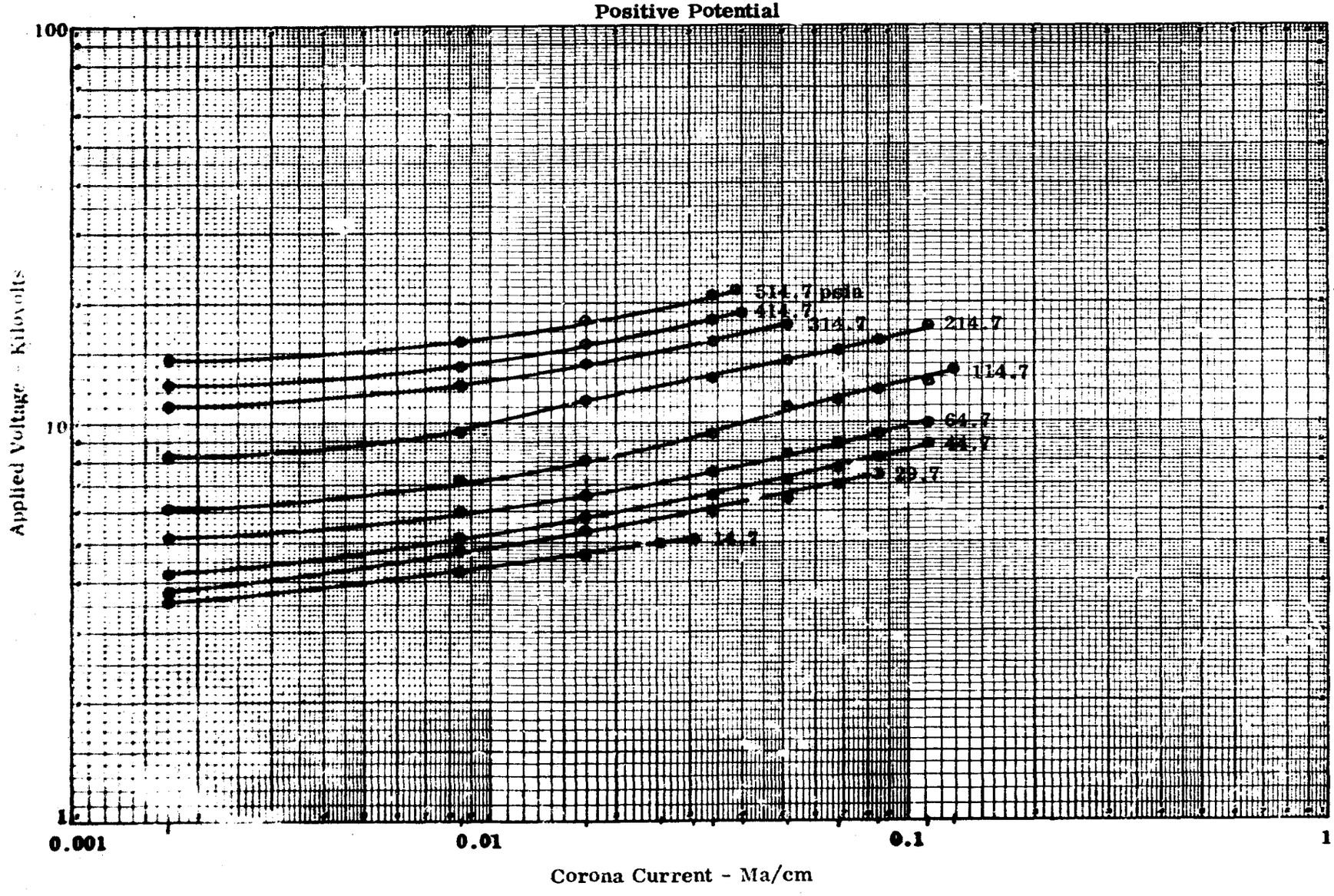

Figure 36 . Voltage vs Corona Current. Helium and Oxygen (PO_2 = 160 mm Hg)

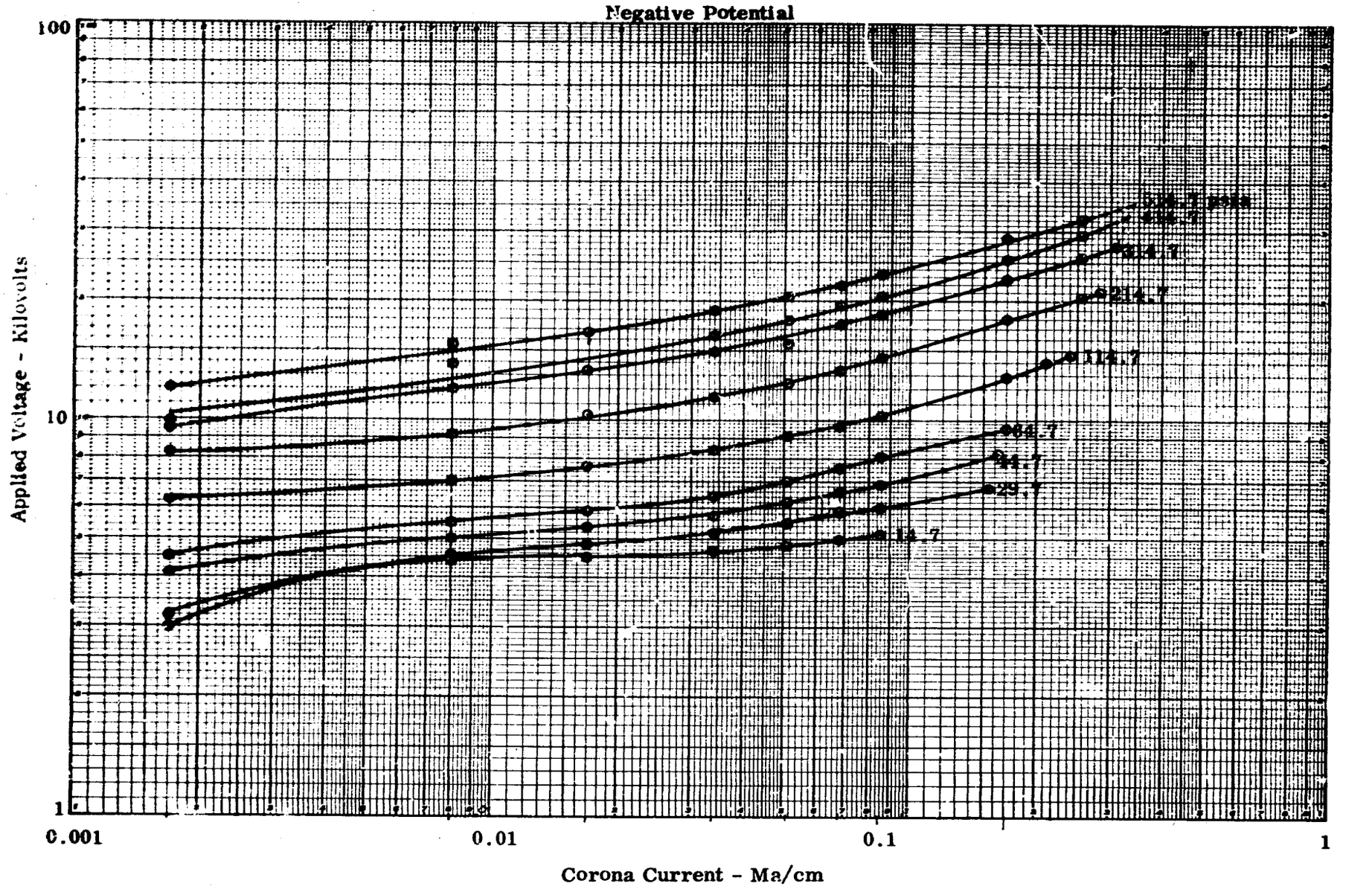

Table 16 Precipator Experiment Results. Applied Voltage vs Current at Various Pressures.

Positive Applied Voltage - Helium

psia / ma/cm	0.001706	0.00855	0.01111	0.01282	0.01453	0.01624	0.01709	0.01880	0.02051	0.02222
				Kilovolts						
14.7	1.4	1.8								
29.7	1.5	2.1	0.00940/2.2							
44.7	2.0	2.7	3.1	0.01197/3.1						
64.7	2.55	3.55	3.8	4.0	4.7					
114.7	4.3	5.6	5.8	6.1	6.35	6.6				
214.7	6.6	8.0	8.3	8.65	8.9	9.2	9.4	9.6	9.8	
314.7	9.95	11.1	11.6	11.9	12.1	12.1	12.4	12.6	12.8	13.1
414.7	11.7	13.3	13.8	14.1	14.5	14.8	15.0	15.2	15.7	15.8
514.7	13.2	15.2	15.8	16.1	16.5	16.9	17.2	17.5	18.0	18.3

Positive Applied Voltage - Helium + O_2 (160 mm Hg)

psia / ma/cm	0.001709	0.008547	0.017094	0.034188	0.051282	0.068376	0.085470	0.1111	0.1282
14.7	3.6	4.3	4.7	0.025641/5.0	0.03077/5.1				
29.7	3.8	4.85	5.4	6.0	6.5	7.0	7.4		
44.7	4.2	5.2	5.8	6.6	7.2	7.7	8.2	8.9	
64.7	5.2	6.0	6.6	7.6	8.4	8.9	9.4	10.0	
114.7	6.1	7.2	8.1	9.4	11.0	11.5	12.1	12.8	13.5
214.7	8.3	9.6	11.4	13.1	14.4	15.2	16.1	17.4	
314.7	11.0	12.5	14.0	16.1	17.7				
414.7	12.5	14.0	15.9	18.2	0.04017/19				
514.7	14.4	16.2	18.1	21.0	0.039316/21.7				

Negative Applied Voltage - Helium + O_2 (160 mm Hg)

psia / ma/cm	0.001709	0.008547	0.017094	0.034188	0.051282	0.068376	0.085470	0.170940		
14.7	3.0	4.4	4.5	4.65	4.8	4.95	5.2			0.08547/5.2
29.7	3.2	4.5	4.8	5.2	5.45	5.8	6.0			0.154/6.7
44.7	4.1	5.0	5.3	5.7	6.2	6.5	6.8			1.1624/8.2
64.7	4.5	5.5	5.9	6.4	7.0	7.5	8.1	9.5		1.7094/9.5
114.7	6.3	7.0	7.65	8.4	9.1	9.65	10.08	13.0	0.213675/14	0.02393/14.4
214.7	8.3	9.2	10.2	11.5	12.4	13.2	14.4	18.0	0.256410/205	0.02820/21
314.7	9.5	12.0	13.2	15.0	15.8	17.3	18.5	22.8	0.256410/25.9	0.03077/27.5
414.7	9.9	13.8	15.8	16.5	18.0	19.4	20.5	25.4	0.256410/29.1	0.02906/31.5
515.7	12.0	15.4	16.8	19.0	20.5	22.0	23.5	29.0	0.256410/32	off scale

discontinued. No difficulty was experienced in the other runs and data on all the points proved to be highly reproducible. In all cases save one, the tests were run until a point discharge occurred. This was not the case for pure helium under negative potential. Under all pressures, the maximum potential that could be applied before exceeding the current capacity of the generating apparatus, 8 ma, was about 4 killovolts.

12.2 CONCLUSIONS

The curves for the three runs on which voltage and current data are available are presented in Figures 34-36 and Table 16. Several inferences can be drawn from an examination of this data.

1) Evidence of a uniform corona discharge was observed under all conditions and at all pressures.

2) Corona onset voltage increases with increasing pressure. (Actually this is a pseudo corona onset that was uniformly determined by the presence of a current flow of 0.02 milliamps.)

3) As pressure is increased the voltage level at which stable coronas can be maintained increases, accompanied by increased current flow.

4) There is a similarity between the positive and negative voltage-current curves for the helium-oxygen mixture, except that higher voltages and greater current flows may be achieved with negative potential. For pure helium, lower voltages, and currents were achieved but the trends are similar for increasing pressure.

The theoretical material preceding the experimental discussion is essentially a summary of currently available theory on this subject and does permit the

aerosol charge calculations necessary to establish the required field gradient for a given aerosol removal system. This experiment has established the possibility of the existence of stable coronas under static conditions, in the environments to be expected in deep submergence vehicles.

SECTION 13.0: PULMONARY DEPOSITION

When aerosols are inhaled into the lung, they are deposited or not deposited, according to many complex but predictable functions. The amount and location of deposition depends on the aerosol properties (size, shape, density); flow dynamics (velocity, gas density), and physiological parameters (breathing rate, residence time, caliber of airway). The sites of deposition for portions of the size distribution spectrum vary, for a given aerosol, with breathing rate, i.e., with the activity or work rate of the breathing organism. Numerous deposition studies have been carried out over the years; the results of many of these studies have been somewhat codified by the Task Group on Lung Dynamics - ICRP.[47]

In the simplest terms, the findings show that the larger particles deposit in the upper airways and the finest in the lower. Deposition is also very high, being almost complete, for particles 10 microns and larger and decreases steadily to about one micron. For smaller sizes, deposition again increases to some unknown but high value approaching 70% or greater. This description of the variability of deposition with particle size is approximate for spherical particles ($\rho = 1$) and varies considerably with other aerosol properties.

It has been demonstrated in the preceding sections that the composition and pressure of the atmosphere to be used for deep submergence systems will cause definite and measurable changes in the motions of the aerosol particles.

Therefore it is logical to consider how pulmonary deposition and the sites of depostion might be affected by this special atmosphere. Models for predicting pulmonary deposition are available in the literature and may be analyzed for the effects of the helium-oxygen atmosphere on deposition.

The first model was developed in 1935 by Findiesen[48] and considers deposition in the lung due to three factors. The factors, already considered and discussed herein, are sedimentation, impaction, and diffusion. Based on increased knowledge of the structure of the lung, Landahl published a revised and improved deposition model in 1950.[49] Landahl revised this model in 1963;[50] further work of Landahl's was published by Hatch in 1964.[51] Beeckmans[52,53] also published a model that takes into account the same basic parameters but uses a slightly different mathematical approach. Of particular interest is the one developed by Beeckmans.[52,53] Beeckmans has thoroughly considered the work of his predecessors, and his structure of the lung is based on Weibel's[54] description, which appears to be the most accurate available.[55]

Although Beeckmans' papers are quite descriptive of his model, there are significant details not available except in his program. Therefore, direct collaboration with Dr. Beeckmans was utilized as the most direct measure of investigation. Before collaboration could begin, however, it was necessary to settle two questions. The first concerned the alteration of breathing mechanics in an individual subjected

to a high-pressure helium-oxygen environment. The second concerned agreement upon generalized equations for the three physical mechanisms that the model considers, viz., sedimentation, diffusion, and impaction. The question of breathing mechanics was answered as a result of a personal conversation[55] with Commander N. R. Anthonisen, U. S. Naval Medical Center. Dr. Anthonisen has participated in studies of simulated dives to 825 ft and reports that the flow rate, cycle time, and tidal volume are about the same in helium-oxygen mixtures as in air at ambient pressures. He expects that if there is a change, it would be in the direction of increased tidal volume and decreased cycle time. His findings justify the use of existing breathing patterns in the model.

The breathing patterns for which the model was run are:

(1) Flow rate = 300 cm^3/sec
Cycle time = 4 sec
Tidal volume = 450 cm^3

(2) Flow rate = 300 cm^3/sec
Cycle time = 8 sec
Tidal volume = 900 cm^3

(3) Flow rate = 300 cm^3/sec
Cycle time = 12 sec
Tidal volume = 1350 cm^3

(4) Flow rate = 1000 cm^3/sec
Cycle time = 4 sec
Tidal volume = 1500 cm^3

Since these patterns are the ones classically used for air, the results may be directly compared with data at ambient conditions.

13.1 MODIFIED AEROSOL DEPOSITION EQUATIONS

Impaction

The impaction equation which is used by both Landahl and Beeckmans is:

$$I = 150\ \rho\ d^2\ V/(R + 150\ \rho\ d^2\ V) \tag{86}$$

where: I = probability of inertial deposition

ρ = particle density

d = particle diameter

R = radius of airway

V = gas velocity

Hatch and Gross[51] indicate that Eq. 86 may be arrived at by beginning with the following expression:

$$I = \frac{P_i}{1 + P_i} \tag{87}$$

where: P_i = impaction parameter

$$= \frac{vV}{gR}$$

where: g = gravitational acceleration

v = sedimentation velocity of particle

$$= \frac{\rho\ g\ d^2}{18\eta}\ \text{(slip correction)}$$

where: η = gas viscosity

Combining:

$$P_i = \frac{\rho d^2 V}{18 \eta R} \text{ (slip correction)} \tag{88}$$

Therefore:

$$I = \frac{\frac{\rho d^2 V}{18\eta R} (s.c.)}{1 + \frac{\rho d^2 V}{18\eta R} (s.c.)}$$

Rewriting:

$$I = \frac{\rho d^2 V (s.c.)}{18 \eta} \Big/ \left(R + \frac{\rho d^2 V (s.c.)}{18\eta} \right) \tag{89}$$

Equation (89) may be used as a general expression for any gas and aerosol system. The value of the slip correction for the helium-oxygen atmosphere at the various pressures would be obtained from the table and graph in Section 5.0. It may also be demonstrated that the relationship originally used by Landahl corresponds to Equation (89). Comparing Equation (89) to Equation (86), the quantity 150 is seemingly equal to $\left(\frac{s.c.}{18\eta}\right)$. The term $(18\eta)^{-1}$ is approximately equal to 300 for air when η is expressed in units of poises. However, Landahl multiplied P_i by sin θ to account for the branching of the airways in the lung. Further, since Landahl uses $\theta = 30^o$ and sin $30^o = 0.5$, the coefficient in his equation is not 300 but 150. Therefore, to generalize Landahl's equation for any gas and branching angle, the factor 150 should be replaced by $\frac{\sin\theta\ (s.c.)}{18\eta}$.

Therefore, when Landahl's equation (Eq. 86) is expressed in general form, it becomes

$$I = \frac{\rho d^2 V \sin \theta \ (s.c.)}{18\eta} \Big/ \left(R + \frac{\rho d^2 V \sin \theta \ (s.c.)}{18\eta} \right) \qquad (90)$$

or, if tabulated, values of v, (Section 5.0) which include the slip correction are to be used the equation may be stated as

$$I = v V \sin \theta \Big/ \left(g R + v V \sin \theta \right) \qquad (91)$$

Sedimentation

The equation used by Beeckmans[53] and his predecessors for deposition due to sedimentation is stated in final form as

$$S = 1 - \exp \left(- g d^2 \rho \tau \cos \psi' / 18\eta \ R \right) \ (s.c.) \qquad (92)$$

where: S = probability of deposition due to sedimentation

τ = mean passage time of the particles

ψ' = angle of inclination of a tube with the horizontal

$\cos \psi'$ is commonly assigned a value of $2/\pi$.[51-53] This equation may be written more simply in terms of the sedimentation velocity and $\cos \psi'$ equals $2/\pi$.

$$S = 1 - \exp \left(- \frac{2 v \tau}{\pi R} \right) \qquad (93)$$

By using Equation (93) one may directly substitute tabulated sedimentation data for the environment under consideration. These tabulations represent an improvement over simply calculated values inasmuch as they already

contain the slip correction factor, as well as corrected sedimentation equations for various ranges of Reynolds number. In fact, the simple Stokes sedimentation equation is used only up to a Reynolds number of 0.05. From 0.05 to 4 we have used Davies' equation,[4] and from 4 to 400 we have used Klyachko's equation[11] (see Section 5.0).

Diffusion

The equation used by Beeckmans[53] and his predecessors for diffusion is

$$D_i = 1 - \exp\left[(-7.31\, k\, T\, \tau / 6\pi\, R^2\, \eta d)\ (s.c.)\right] \qquad (94)$$

where: D_i = probability of deposition due to diffusion

k = Boltzmann's constant

T = absolute temperature

The coefficient of the exponential argument in this equation comes from Townsend's[56] solution of the problem of diffusion to perfectly absorbing walls having a circular cross-section. The dominant first term in his infinite series solution is 7.31. This equation was experimentally verified, and used by Beeckmans without further investigation. Equation (94) can be rewritten more simply in terms of the diffusion coefficient (D) and the slip correction:

$$D_i = 1 - \exp\,(-7.31\, D\tau / 2R^2) \qquad (95)$$

where: D = diffusion coefficient with slip correction

The slip-correction diffusion coefficients for the atmosphere under investigation are tabulated in Section 5.0 and are therefore suitable for direct substitution into this equation and into the model.

13.2 RESULTS

Calculations have been completed for the four previously stated cycle conditions. These conditions are typified by the parameters of flow rate, cycle time, and tidal volume. In discussing each condition, however, we reference only the tidal volume, as that is the number which is different in each of the four cases. For comparative purposes, calculations for air at 14.7 psia and unit density particulates have also been processed. It was found that the computer program would not function in the 0.001 micron size range for the 450 and 900 cm^3 tidal volume runs. To determine the cause of the program's inability to function would have been most difficult and time consuming, and it was felt that the trends were clearly indicated by data obtained for the other two tidal volumes.

The most significant result apparent in this study is that the deposition curve for air almost always lies within the 10 to 500 psia envelope. Lower tract deposition in the helium-oxygen atmosphere decreases with increasing pressure and, at the highest pressures, is significantly less than in air. However, in the respiratory tract this situation reverses at particle diameters below approximately 0.01 micron, and deposition at the high pressures exceeds or equals that in air. While all the curves show the characteristic minimum deposition at approximately 0.1 micron diameter with the expected peaking at 0.01 micron, it was surprising to note that for the data available down to 0.001 micron (1500 and 1350 cm^3 tidal volume) the lower tract deposition decreased remarkably – falling to almost zero at the lower pressures. It is thought that the explanation for this decrease in

efficiency is explainable. It will be noted that the curves for total deposition reach maxima between 0.01 and 0.001 micron even though the lower tract deposition falls off remarkably. Since the increased total and lower tract deposition below 0.1 micron is clearly ascribed to the increased diffusional mobility of particulates with decreasing diameter, the reduction in lower tract deposition below 0.01 micron can be attributed to the fact that the particulates have now become so highly mobile that they are being very efficiently removed in the upper respiratory tract and never reach the lower levels for collection. (See Tables 17 thru 20, and Figures 37 thru 40.)

13.3 CONCLUSIONS

The object of this study was to determine on a theoretical basis if increased personnel risk was to be expected because of altered aerosol deposition patterns in high pressure environments. It is apparent from the calculations presented here that deposition patterns maintain similar shapes and that the quantity deposited decreases with increasing pressure.

Table 17. Particle Retentions in the Total and Lower Respiratory Tract for He-O_2 (PO_2 = 160 mm Hg) at Various Pressures.

Flow Rate = 300 cm^3/sec
Cycle Time = 4 sec
Tidal Volume = 450 cm^3

d=0.001μ psia	ρ = 1 (air) Total	ρ = 1 (air) Lower	ρ = 1 Total	ρ = 1 Lower	ρ = 2 Total	ρ = 2 Lower	ρ = 3 Total	ρ = 3 Lower
10								
14.7								
20								
30								
40								
50								
100								
200								
300								
400								
500								
0.01μ								
10			0.7700	0.2420	0.7700	0.2420	0.7700	0.2420
14.7	0.7340	0.4282	0.7619	0.3079	0.7619	0.3079	0.7619	0.3079
20			0.7530	0.3605	0.7530	0.3605	0.7530	0.3605
30			0.7372	0.4197	0.7372	0.4197	0.7372	0.4197
40			0.7219	0.4532	0.7219	0.4532	0.7219	0.4532
50			0.7076	0.4730	0.7076	0.4730	0.7076	0.4730
100			0.6475	0.4990	0.6475	0.4990	0.6475	0.4990
200			0.5721	0.4780	0.5721	0.4780	0.5721	0.4780
300			0.5273	0.4535	0.5273	0.4535	0.5273	0.4535
400			0.4981	0.4348	0.4981	0.4348	0.4981	0.4348
500			0.4774	0.4206	0.4774	0.4206	0.4775	0.4206
0.1μ								
10			0.3259	0.4010	0.3300	0.3036	0.3341	0.3061
14.7	0.2402	0.2272	0.2934	0.2735	0.2972	0.2760	0.3008	0.2784
20			0.2696	0.2530	0.2729	0.2553	0.2763	0.2575
30			0.2425	0.2295	0.2454	0.2315	0.2483	0.2335
40			0.2266	0.2155	0.2293	0.2174	0.2320	0.2192
50			0.2165	0.2066	0.2190	0.2084	0.2215	0.2101
100			0.1939	0.1864	0.1960	0.1879	0.1980	0.1893
200			0.1814	0.1753	0.1833	0.1765	0.1852	0.1778
300			0.1774	0.1716	0.1793	0.1728	0.1811	0.1741
400			0.1753	0.1697	0.1771	0.1709	0.1789	0.1721
500			0.1740	0.1685	0.1758	0.1697	0.1775	0.1709
1.0μ								
10			0.3046	0.2465	0.3986	0.2996	0.4626	0.3300
14.7	0.2650	0.2305	0.2946	0.2386	0.3867	0.2907	0.4499	0.3210
20			0.2881	0.2334	0.3791	0.2849	0.4426	0.3157
30			0.2821	0.2286	0.3712	0.2789	0.4336	0.3091
40			0.2785	0.2257	0.3671	0.2757	0.4290	0.3057
50			0.2766	0.2242	0.3644	0.2736	0.4264	0.3037
100			0.2722	0.2206	0.3591	0.2695	0.4307	0.2994
200			0.2700	0.2188	0.3563	0.2673	0.4175	0.2970
300			0.2693	0.2183	0.3553	0.2665	0.4166	0.2964
400			0.2687	0.2177	0.3549	0.2662	0.4160	0.2959
500			0.2687	0.2177	0.3545	0.2659	0.4157	0.2957
10μ								
10			0.8463	0.0581	0.8857	0.0063	0.9087	0.0007
14.7	0.8503	0.0545	0.8480	0.0585	0.8854	0.0064	0.9084	0.0008
20			0.8479	0.0587	0.8852	0.0065	0.9082	0.0008
30			0.8477	0.0591	0.8850	0.0065	0.9080	0.0008
40			0.8476	0.0593	0.8849	0.0065	0.9079	0.0008
50			0.8476	0.0593	0.8849	0.0066	0.9078	0.0008
100			0.8474	0.0595	0.8847	0.0066	0.9077	0.0008
200			0.8473	0.0597	0.8846	0.0066	0.9076	0.0008
300			0.8473	0.0597	0.8846	0.0066	0.9076	0.0008
400			0.8473	0.0597	0.8846	0.0067	0.9076	0.0008
500			0.8473	0.0597	0.8846	0.0067	0.9075	0.0008

Table 1 & Particle Retentions in the Total and Lower Respiratory Tract for He-O_2 (PO_2 = 160 mm Hg) at Various Pressures.

Flow Rate = 300 cm^3/sec
Cycle Time = 8 sec
Tidal Volume = 900 cm^3

d=0.001μ psia	ρ = 1 (air) Total	ρ = 1 (air) Lower	ρ = 1 Total	ρ = 1 Lower	ρ = 2 Total	ρ = 2 Lower	ρ = 3 Total	ρ = 3 Lower
10								
14.7								
20								
30								
40								
50								
100								
200								
300								
400								
500								
0.01μ								
10			0.8914	0.3218	0.8914	0.3218	0.8914	0.3217
14.7	0.8789	0.5711	0.8882	0.4093	0.8882	0.4093	0.8882	0.4093
20			0.8851	0.4794	0.8851	0.4794	0.8851	0.4794
30			0.8799	0.5593	0.8799	0.5593	0.8799	0.5593
40			0.8749	0.6069	0.8749	0.6069	0.8749	0.6069
50			0.8699	0.6374	0.8699	0.6374	0.8699	0.6374
100			0.8440	0.6987	0.8439	0.6986	0.8439	0.6986
200			0.7961	0.7057	0.7959	0.7056	0.7959	0.7056
300			0.7565	0.6867	0.7562	0.6864	0.7562	0.6864
400			0.7255	0.6664	0.7250	0.6658	0.7250	0.6658
500			0.7015	0.6488	0.7007	0.6480	0.7007	0.6480
0.1μ								
10			0.4910	0.4696	0.4928	0.4699	0.4982	0.4739
14.7	0.3772	0.3669	0.4455	0.4286	0.4457	0.4277	0.4504	0.4313
20			0.4127	0.3990	0.4117	0.3969	0.4160	0.4002
30			0.3764	0.3658	0.3740	0.3625	0.3776	0.3653
40			0.3554	0.3464	0.3523	0.3425	0.3555	0.3450
50			0.3418	0.3338	0.3382	0.3295	0.3412	0.3318
100			0.3106	0.3047	0.3061	0.2996	0.3086	0.3015
200			0.2925	0.2876	0.2876	0.2821	0.2899	0.2839
300			0.2863	0.2816	0.2813	0.2762	0.2836	0.2779
400			0.2831	0.2786	0.2781	0.2731	0.2802	0.2747
500			0.2811	0.2767	0.2761	0.2711	0.2783	0.2729
1.0μ								
10			0.4413	0.3909	0.5633	0.4752	0.6468	0.5275
14.7	0.4193	0.3720	0.4275	0.3791	0.5464	0.4612	0.6293	0.5138
20			0.4185	0.3713	0.5353	0.4520	0.6191	0.5056
30			0.4100	0.3639	0.5240	0.4425	0.6065	0.4953
40			0.4050	0.3595	0.5181	0.4375	0.6001	0.4901
50			0.4025	0.3573	0.5143	0.4343	0.5962	0.4869
100			0.3964	0.3520	0.5068	0.4279	0.5881	0.4801
200			0.3933	0.3492	0.5029	0.4245	0.5836	0.4764
300			0.3924	0.3484	0.5014	0.4233	0.5823	0.4753
400			0.3915	0.3477	0.5009	0.4228	0.5815	0.4746
500			0.3915	0.3477	0.5003	0.4223	0.5811	0.4743
10μ								
10			0.9353	0.0783	0.9554	0.0086	0.9666	0.0010
14.7	0.9367	0.0734	0.9352	0.0789	0.9552	0.0087	0.9664	0.0010
20			0.9351	0.0792	0.9551	0.0088	0.9663	0.0011
30			0.9349	0.0796	0.9550	0.0089	0.9662	0.0011
40			0.9348	0.0800	0.9550	0.0089	0.9661	0.0011
50			0.9348	0.0800	0.9549	0.0089	0.9661	0.0011
100			0.9348	0.0803	0.9548	0.0090	0.9660	0.0011
200			0.9347	0.0806	0.9548	0.0090	0.9660	0.0011
300			0.9347	0.0806	0.9548	0.0090	0.9660	0.0011
400			0.9347	0.0806	0.9548	0.0091	0.9660	0.0011
500			0.9347	0.0806	0.9548	0.0091	0.9660	0.0011

Table 1 9. **Particle Retentions in the Total and Lower Respiratory Tract for He-O_2 (PO_2 = 160 mm Hg) at Various Pressures.**

Flow Rate = 300 cm^3/sec
Cycle Time = 12 sec
Tidal Volume = 1350 cm^3

d=0.001μ	ρ = 1 (air)		ρ = 1		ρ = 2		ρ = 3	
psia	Total	Lower	Total	Lower	Total	Lower	Total	Lower
10			0.9850	0.0000				
14.7			0.9812	0.0000				
20			0.9776	0.0000				
30			0.9720	0.0000				
40			0.9676	0.0000				
50			0.9640	0.0000				
100			0.9536	0.0000				
200			0.9452	0.0034				
300			0.9412	0.0212				
400			0.9387	0.0528				
500			0.9369	0.0915				
0.01μ								
10			0.9303	0.3490	0.9303	0.3490	0.9303	0.3490
14.7	0.9228	0.6196	0.9281	0.4440	0.9281	0.4440	0.9281	0.4440
20			0.9262	0.5200	0.926.	0.5200	0.9262	0.5200
30			0.9233	0.6068	0.9234	0.6067	0.9234	0.6067
40			0.9208	0.6586	0.9208	0.6586	0.9208	0.6586
50			0.9184	0.6923	0.9184	0.6923	0.9184	0.6923
100			0.9059	0.7656	0.9059	0.7655	0.9059	0.7656
200			0.8797	0.7926	0.8799	0.7928	0.8799	0.7928
300			0.8543	0.7873	0.8555	0.7884	0.8555	0.7884
400			0.8320	0.7754	0.8345	0.7778	0.8345	0.7778
500			0.8133	0.7630	0.8170	0.7668	0.8171	0.7668
0.1μ								
10			0.6038	0.5836	0.6395	0.6181	0.6445	0.6218
14.7	0.4619	0.4518	0.5490	0.5331	0.5938	0.5770	0.5983	0.5805
20			0.5077	0.4948	0.5596	0.5459	0.5638	0.5491
30			0.4604	0.4503	0.5204	0.5097	0.5241	0.5126
40			0.4324	0.4239	0.4970	0.4879	0.5003	0.4906
50			0.4141	0.4065	0.4814	0.4733	0.4846	0.4759
100			0.3719	0.3663	0.4443	0.4382	0.4471	0.4405
200			0.3475	0.3428	0.4216	0.4165	0.4242	0.4181
300			0.3392	0.3348	0.4136	0.4088	0.4162	0.4109
400			0.3348	0.3306	0.4034	0.4047	0.4119	0.4068
500			0.3321	0.3280	0.4067	0.4021	0.4093	0.4042
1.0μ								
10			0.5342	0.4873	0.6958	0.6147	0.7682	0.6575
14.7	0.5068	0.4627	0.5171	0.4720	0.6800	0.6018	0.7531	0.6462
20			0.5058	0.4618	0.6695	0.5931	0.7440	0.6393
30			0.4960	0.4521	0.6587	0.5840	0.7328	0.6305
40			0.4896	0.4463	0.6530	0.5792	0.7270	0.6259
50			0.4854	0.4433	0.6493	0.5761	0.7235	0.6231
100			0.4776	0.4363	0.6420	0.5699	0.7161	0.6171
200			0.4735	0.4325	0.6381	0.5666	0.7119	0.6137
300			0.4724	0.4315	0.6367	0.5654	0.7108	0.6128
400			0.4712	0.4303	0.6362	0.5649	0.7100	0.6121
500			0.4712	0.4304	0.6356	0.5644	0.7096	0.6118
10μ								
10			0.9626	0.0858	0.9759	0.0094	0.9827	0.0011
14.7	0.9636	0.0803	0.9625	0.0864	0.9758	0.0096	0.9826	0.0011
20			0.9624	0.0867	0.9757	0.0097	0.9826	0.0012
30			0.9623	0.0874	0.9756	0.0098	0.9825	0.0012
40			0.9622	0.0877	0.9756	0.0098	0.9824	0.0012
50			0.9622	0.0877	0.9756	0.0098	0.9824	0.0012
100			0.9622	0.0880	0.9755	0.0099	0.9824	0.0012
200			0.9621	0.0884	0.9755	0.0099	0.9824	0.0012
300			0.9621	0.0884	0.9755	0.0099	0.9824	0.0012
400			0.9621	0.0884	0.9755	0.0100	0.9824	0.0012
500			0.9621	0.0884	0.9755	0.0100	0.9823	0.0012

Table 2.0 Particle Retentions in the Total and Lower Respiratory Tract for He-O_2 (PO_2 = 160 mm Hg) at Various Pressures.

Flow Rate = 1000 cm^3/sec
Cycle Time = 4 sec
Tidal Volume = 1500 cm^3

d=0.001μ	ρ = 1 (air)		ρ = 1		ρ = 2		ρ = 3	
psia	Total	Lower	Total	Lower	Total	Lower	Total	Lower
10			0.9726	0.0000				
14.7			0.9680	0.0000				
20			0.9639	0.0000				
30			0.9589	0.0000				
40			0.9556	0.0003				
50			0.9532	0.0014				
100			0.9469	0.0329				
200			0.9419	0.1662				
300			0.9392	0.2874				
400			0.9374	0.3780				
500			0.9360	0.4457				
0.01μ								
10			0.9297	0.6661	0.9297	0.6661	0.9297	0.6660
14.7	0.9136	0.7885	0.9266	0.7159	0.9266	0.7158	0.9266	0.7158
20			0.9229	0.7503	0.9229	0.7502	0.9229	0.7502
30			0.9155	0.7841	0.9155	0.7841	0.9155	0.7841
40			0.9074	0.8004	0.9074	0.8004	0.9074	0.8004
50			0.8989	0.8079	0.8989	0.8079	0.8989	0.8079
100			0.8514	0.7975	0.8514	0.7975	0.8514	0.7975
200			0.7703	0.7380	0.7704	0.7380	0.7704	0.7380
300			0.7184	0.6938	0.7184	0.6938	0.7184	0.6938
400			0.6847	0.6641	0.6847	0.6641	0.6847	0.6641
500			0.6615	0.6434	0.6615	0.6434	0.6615	0.6434
0.1μ								
10			0.5095	0.5021	0.5129	0.5044	0.5163	0.5067
14.7	0.4173	0.4133	0.4779	0.4720	0.4811	0.4741	0.4842	0.4763
20			0.4524	0.4474	0.4555	0.4495	0.4585	0.4516
30			0.4189	0.4149	0.4220	0.4170		
40			0.3959	0.3924	0.3989	0.3944		
50			0.3791	0.3759	0.3822	0.3781		
100			0.3347	0.3320	0.3379	0.3343		
200			0.3056	0.3032	0.3088	0.3055		
300			0.2953	0.2930	0.2984	0.2952		
400			0.2898	0.2875	0.2929	0.2898		
500			0.2863	0.2841	0.2895	0.2864		
1.0μ								
10			0.4759	0.3945	0.6021	0.4609	0.6599	0.4670
14.7	0.4532	0.3715	0.4633	0.3817	0.5912	0.4494	0.6485	0.4549
20			0.4548	0.3729	0.5839	0.4418	0.6419	0.4478
30			0.4464	0.3643	0.5763	0.4339	0.6339	0.4391
40			0.4414	0.3592	0.5724	0.4297	0.6298	0.4346
50			0.4387	0.3564	0.5698	0.4269	0.6274	0.4320
100			0.4325	0.3500	0.5646	0.4214	0.6222	0.4263
200			0.4292	0.3466	0.5618	0.4184	0.6193	0.4232
300			0.4282	0.3456	0.5608	0.4173	0.6185	0.4223
400			0.4273	0.3446	0.5604	0.4169	0.6180	0.4217
500			0.4273	0.3446	0.5600	0.4165	0.6178	0.4214
10μ								
10			0.9617	0.0145	0.9727	0.0005	0.9791	0.0000
14.7	0.9621	0.0142	0.9617	0.0145	0.9726	0.0005	0.9790	0.0000
20			0.9616	0.0146	0.9726	0.0005	0.9790	0.0000
30			0.9616	0.0146	0.9725	0.0005	0.9790	0.0000
40			0.9616	0.0146	0.9725	0.0005	0.9790	0.0000
50			0.9616	0.0146	0.9725	0.0005	0.9789	0.0000
100			0.9616	0.0146	0.9725	0.0005	0.9789	0.0000
200			0.9615	0.0146	0.9725	0.0005	0.9789	0.0000
300			0.9615	0.0146	0.9725	0.0005	0.9789	0.0000
400			0.9615	0.0146	0.9725	0.0005	0.9789	0.0000
500			0.9615	0.0146	0.9725	0.0005	0.9789	0.0000

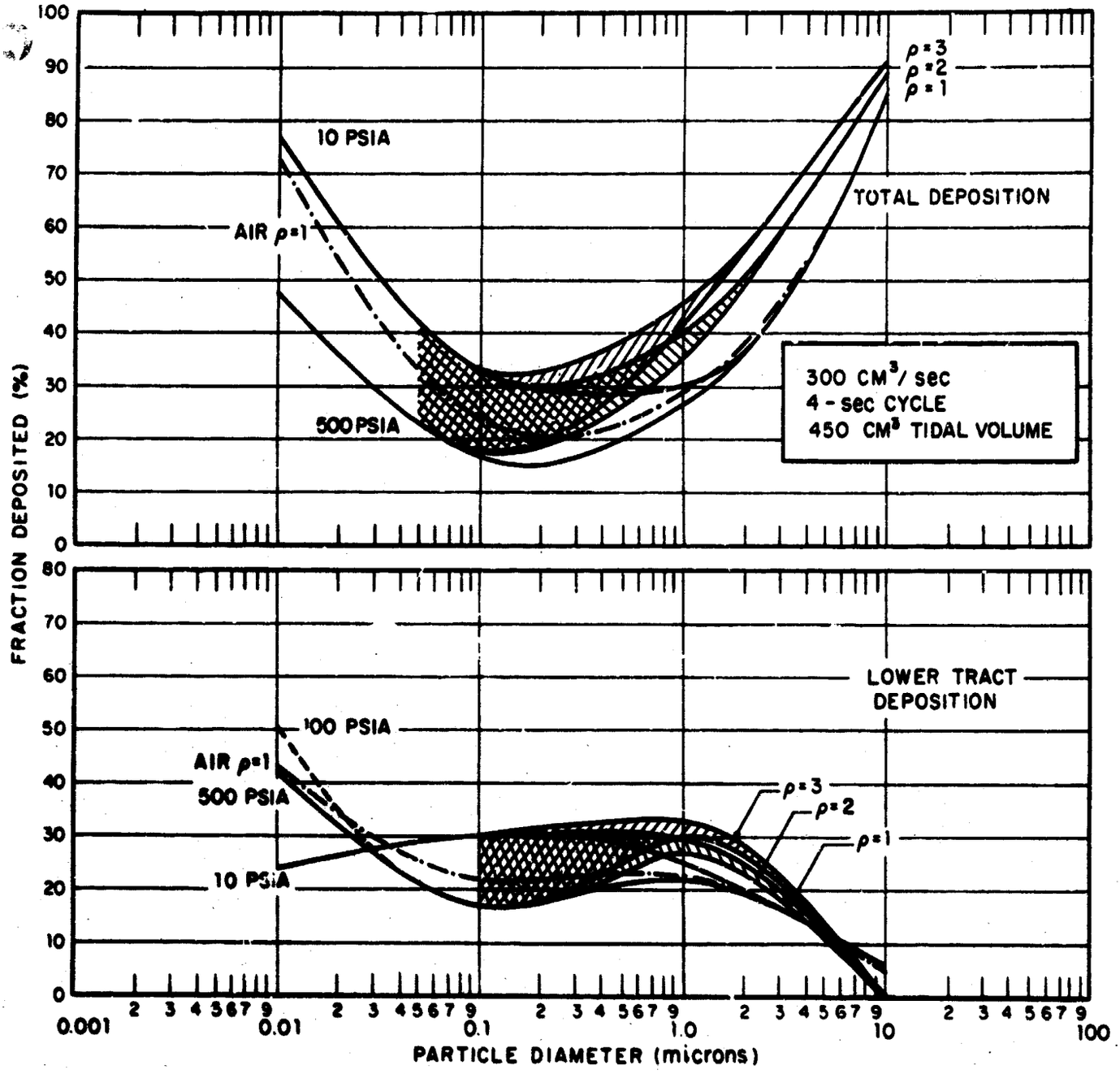

Figure 37. Total and Lower Respiratory Tract Deposition. He-O_2 (PO_2 = 160 mm Hg) at Various Pressures.

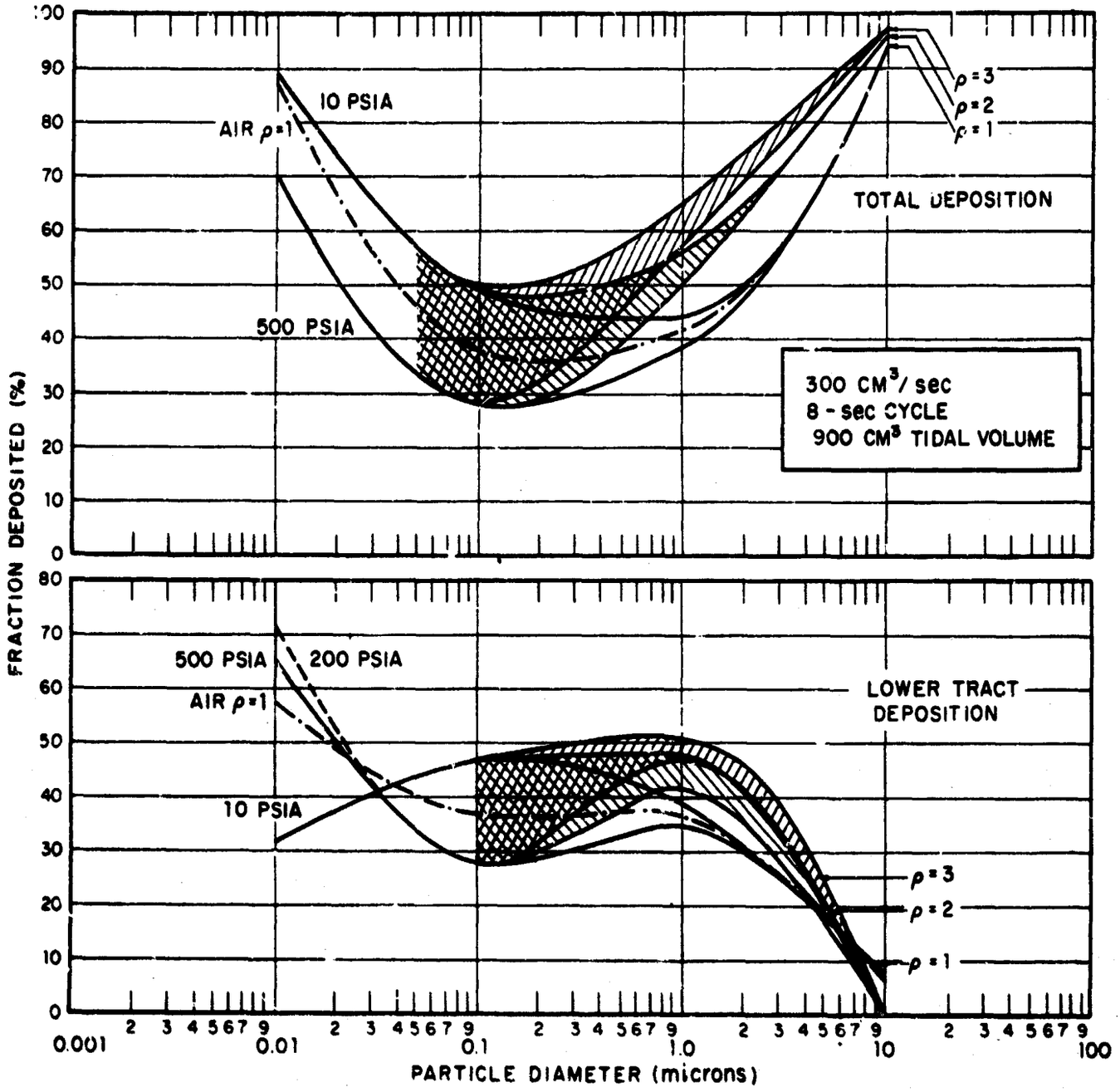

Figure 38. Total and Lower Respiratory Tract Deposition. He-O_2 (PO_2 = 160 mm Hg) at Various Pressures.

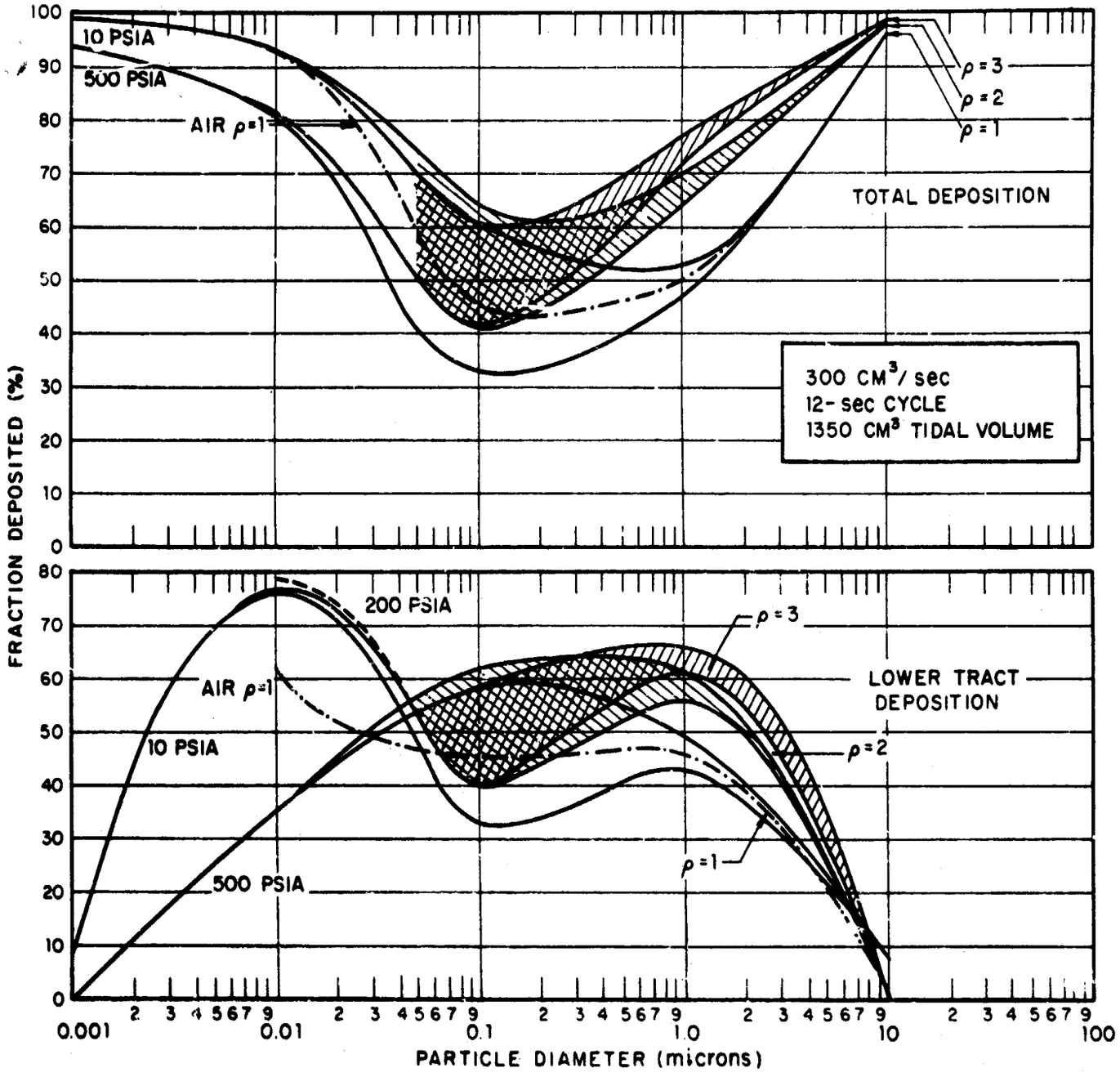

Figure 39. Total and Lower Respiratory Tract Deposition. He-O_2 (PO_2 = 160 mm Hg) at Various Pressures.

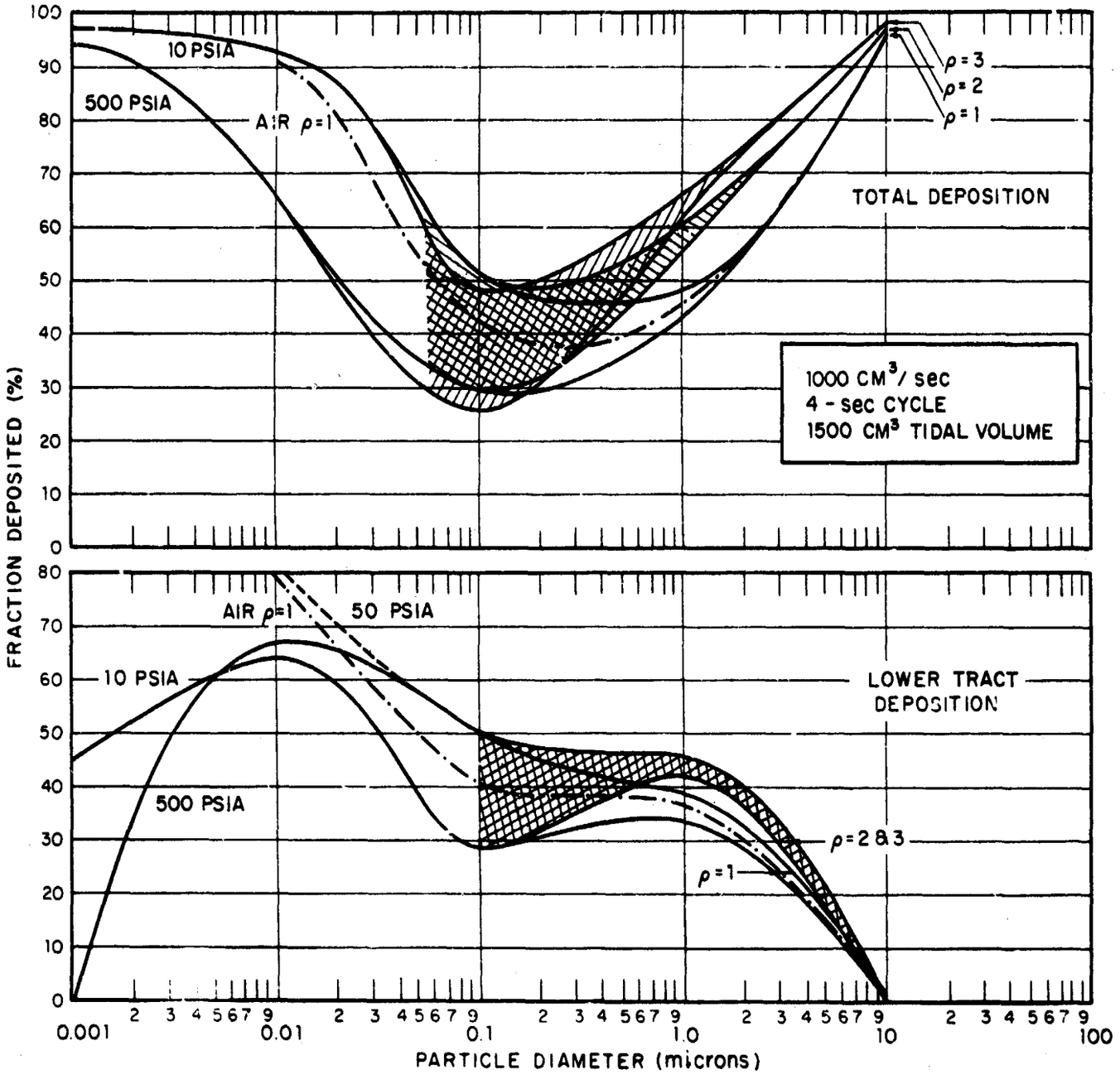

Figure 40. Total and Lower Respiratory Tract Deposition. He-O_2 (PO_2 = 160 mm Hg) at Various Pressures.

14.0 SUMMARY AND CONCLUSIONS

In the introduction to this text three goals were stated as the governing ones for the study which forms the basis for this handbook. Each of the goals has been addressed to some degree and a summation of the work is most clearly stated on a goal basis.

1. Investigate and extrapolate the possibly altered behavior of aerosols in the helium-oxygen environment.

This goal has been dealt with on a theoretical basis. The many factors affecting the behavior of aerosol particles within the extreme environment have been codified into charts and tables. While much work would be required to satisfy a physicist requirements, the departures from the ambient world are not so great as to dissuade the engineer.

2. Determine methods for removing potentially harmful aerosols from the environment.

In this area strong reliance has been made of nuclear submarine experience and only electrostatic precipitation and filtration have been considered. Sufficient physical experimentation on precipitators has been conducted to demonstrate the possibility of the technique but not its applicability. Filtration mechanisms whilst still theoretically functional at the extremes of pressures to be encountered, are reduced in efficiency and subject to stringent appraisal.

3. Determine possible altered toxicological behavior of aerosols.

That the receptor is altered by his environment is demonstrated by the pulmonary deposition models. Alterations of those properties of aerosol particles which render them more or less toxic is yet an open question. However, the initial answers possibly lie with the experiments on the generation of liquid and solid aerosols and the theoretical considerations on evaporation and condensation.

Thus, while satifications have been attained for the engineer and physicist, it remains for the physiologist to achieve the final and necessary answers required for complete personnel protection.

LITERATURE CITED

1. Bond, G.E.: New Developments in High Pressure Living. Arch. Environ. Health 9, 310 (Sept. 1964).

2. Comings, E.W.: High Pressure Technology, McGraw-Hill Book Co., Inc., New York, 1956.

3. Loeb, L.B.: The Kinetic Theory of Gases, Dover Publications, Inc., New York, 1961.

4. Davies, C.N.: Definitive Equations for the Fluid Resistance of Spheres. The Proceedings of the Physical Society, Vol 57, Pt. 4, No. 322 (1 July 1945).

5. Green, H.L. and W.R. Lane: Particulate Clouds: Dusts, Smokes and Mists, E. & F. N. Spon Ltd., England, 1964.

6. Flanagan, V.P.V. and P. Tayler: Tables of Aerosol Physics Functions: Mobility and Falling Speed of Spheres, in Morr, D.J. et al (ed.): Atmospheric Environment, Vol. 1, Pergamon Press, London, England, 1967.

7. Metnieks, A.L. and L.W. Pollak: Tables and Graphs for use in Aerosol Physics. Part 1: Mobility v. Radius and Vice Versa. Geophys. Bull., No. 19. School of Cosmic Physics, Dublin Inst. for Adv. Studies, Dublin, Ireland, 1961.

8. Fuchs, N.A. and I.B. Stechkina: Resistance of a Gaseous Medium to the Motion of a Spherical Particle of a Size Comparable to the Mean Free Path of the Gas Molecules. Trans.of the Faraday Society, 58, 475, Pt. 7 (July 1962)

9. Millikan, R.A.: Coefficient of Slip in Gases and the Law of Reflection of Molecules from the Surfaces of Solids and Liquids. Phys. Rev. 21, 217-238, (March, 1923).

10. Megaw, W.J. and A.C. Wells: A High Resolution Charge and Mobility Spectrometer for Radioactive Submicrometre Aerosols. J. of Scientific Instruments (J. of Physics E), Series 2, Vol. 2 (1969).

11. Fuchs, N.A.: The Mechanics of Aerosols. The MacMillian Company, New York, 1964.

12. Whytlaw-Gray, R. and H.S. Patterson: Smoke: A Study of Aerial Disperse Systems. Edward Arnold & Co., London, England, 1932.

13. Davies, C.N. (ed.): Aerosol Science. Academic Press, New York, 1966.

14. Gussman, R.A.: Agglomeration. Masters Thesis, Univ. of Cincinnati, 1960.

15. Cawood and R. Whytlaw-Gray: Disperse Systems in Gases; Dust, Smoke and Fog. (a discussion), Gurney & Jackson, London, England, (Apr. 1936).

16. Billings, C. E.: Personal Communication, July 1968.

17. Booth, A. H.: A Method of Calculating Fission Gas Diffusion from UO_2 Fuel and its Application to the X-2-f Loop Test, Atomic Energy Comm. of Canada, Rept. No. CRDC 721, Chalk River, Canada (1957).

18. Courant, R. and D. Hilbert: Methods of Mathematical Physics, Vol. 1, p. 76. Interscience Publishers, Inc., New York, N. Y., 1953.

19. Ince, E. L.: Ordinary Differential Equations. Dover Publications, Inc., New York, N. Y., 1956.

20. Abramowitz, M. (ed.): Handbook of Mathematical Functions, Chap. 7. Dover Publications, Inc., New York, N. Y., 1965.

21. Sinclair, D: Stability of Aerosols in Behavior of Aerosol Particles in Handbook on Aerosols, pp. 64-76. U. S. Atomic Energy Commission, Washington, D. C., 1950.

22. Fuchs, N.A.: Evaporation and Droplet Growth in Gaseous Media. Pergamon Press, New York, 1959.

23. Orr, C., Jr.: Particulate Technology. The MacMillian Company, New York, 1966.

24. Amelin, A.G.: Theory of Fog Condensation. Wiener Bindery Ltd., Israel, 1967.

25. Bradley, R.S.: The Rate of Nucleation at High Pressures. J. of Colloid Science 15, 525, 1960.

26. Gussman, R.A., C.E. Billings and L. Silverman: Factors in Condensation Nuclei Counters for Measurement of Aerosol Agglomeration. Presented at the Seventh USAEC Air Cleaning Conf., Brookhaven National Lab., Upton, L.I., New York, Oct. 10-12, 1961. Office of Technical Services, Dept. of Commerce, Washington, D.C., (Mar 1962).

27. Polydorova, M.: The Preparation and Properties of a Tungsten Oxide Aerosol. Staub, V. 25, #12, p. 16-18, English Translation, (Dec 1965).

28. Binek, Bedrich: Sampling Finely Dispersed Aerosols for Electron-Microscopic Particle Analysis. Staub, V. 25, #7, p. 13-19, English Translation, (July 1965).

29. Maiwald, E.: A Tungsten Oxide Test Aerosol. Staub, V. 25, #12, p. 13-15, English Translation. (Dec. 1965).

30. Goldsmith, P., F.G. May and R.D. Wiffen: Chromium Trioxide Aerosol from Heated 80:20 Nickel-Chromium Wire. Nature 210, p. 475-477 (Apr. 30, 1966).

31. Corn, Morton: Statistical Reliability of Particle Size Distributions Determined by Microscopic Techniques. AIHA J., V. 26, #1, p. 8-16 (Jan-Feb. 1965)

32. Drinker, P. and T. Hatch: Industrial Dust, McGraw-Hill Book Co., Inc., New York, 1954.

33. Doyle, A.W., R. Dennis, D.B. Lull, R.A. Gussman, G.A. Pacholke, C.O. Hommel (1966): New Techniques for Dissemination of Chemical Agents - Annual Summary Report. Performed under Contract No. DA-18-108-AMC-249(A) for Edgewood Arsenal, Maryland. Rept. No. 66-14-G, GCA Corporation, Bedford, Mass. (Sept.)

34. Lord Rayleigh: Theory of Sound. Vol. I and Vol II, 346-49. Dover Publ., N.Y. 1945.

35. Perron, R.R., J.R. Swanton, and E.S. Shanely (1963): A Practical Ultrasonic Oil Burner. API Res. Conf. on Distillate Fuel Combust., Proc., API Pub. 1702

36. Peskin, R. and R. Raco (1963): Ultrasonic Atomization of Liquids. J. Acoust. Soc. Ame 35, No. 9, 1378-81.

37. C.F. Casella & Co., Ltd.: Instruction Leaflet 3018/RI for the Cascade Impactor.

38. Richardson, E.G. (ed.): Aerodynamic Capture of Particles. Pergamon Press, New York, 1960.

39. Gussman, R.A., C.E. Billings and L. Silverman: Open Hearth Stack Gas Cleaning Studies (May 1961 to Oct. 1961). Semi-Annual Rpt. SA-16, Harvard University (Feb. 1962).

40. Silverman, L., E.W. Conners, Jr., D.M. Anderson: Electrostatic Mechanisms in Aerosol Filtration by Mechanically Charged Fabric Media and Related Studies. Rpt. No. NYO-4610, U.S. Atomic Energy Commission, Oak Ridge, Tenn. (Sept. 1956).

41. Kirsh, A.A. and N.A. Fuks (1968): Investigations of Fibrous Aerosol Filters. Diffusional Deposition of Aerosols in Fibrous Filters. Colloid J. (USSR), 30

42. Billings, C.E. and L. Silverman: Aerosol Sampling for Electron Microscopy. APCA J., Vol. 12, No. 12, pp. 586-590 (Dec. 1962).

43. Gussman, R.A., R. Dennis and L. Silverman: Notes on the Design and Leak-testing of Sampling Filter Holders. AIHA J., Vol. 23, No. 6, pp. 480-481 (Nov-Dec. 1962).

44. First, M.W. et al (1970): Semiannual Progress Report - Harvard Air Cleaning Laboratory, Sept. 1, 1969 - Feb 28, 1970. NYO-841-22, Harvard School of Public Health, Boston, Mass. (Apr 1970).

45. White, H.J.: Industrial Electrostatic Precipitation. Addison-Wesley Publishing Co., Inc., Reading, Mass., 1963.

46. Liu, B.Y.H. and H. Yeh: Effect of Pressure and Electric Field on the Charging of Aerosol Particles. Univ. of Minnesota, Minneapolis, Minn., Particle Laboratory Publication No. 119, October 1967.

47. International Radiological Protection Commission: Deposition and Retention Models for Internal Dosimetry of the Human Respiratory Tract. Health Physics, Vol. 12, No. 1, 173-207, Pergamon Press, 1966.

48. Findeisen, W.: The Deposition of Small Airborne Particles in the Human Lung During Respiration. Arch. Ges. Physiol. 236:367 (1955).

49. Landahl, H.D.: On The Removal of Air-Borne Droplets by the Human Respiratory Tract: 1. The Lung. Bull. of Mathematical Biophysics, Vol. 12, p. 43, 1950.

50. Landahl, H.D.: Particle Removal by the Respiratory System Note on the Removal of Airborne Particulates by the Human Respiratory Tract with Particular Reference to the Role of Diffusion. Bull. of Mathematical Biophysics, Vol. 25, 1963.

51. Hatch, T.F. and P. Gross: Pulmonary Deposition and Retention of Inhaled Aerosols. Academic Press, New York, 1964.

52 Beeckmans, J.M.: The Deposition of Aerosols in the Respiratory Tract. 1. Mathematical Analysis & Comparison with Experimental Data. Canadian J. of Physiology & Pharmacology, Vol. 43, p. 157 (1965).

53. Beeckmans, J.M.: Correction Factor for Size-Selective Sampling Results, Based on a New Computed Alveolar Deposition Curve. Ann. Occup. Hyg., Vol. 8, p. 221-231, Pergamon Press (1965).

54. Weibel, E.R.: Morphometry of the Human Lung. Academic Press, New York, 1963.

55. Anthonisen, N.R., Cdr., U.S. Naval Medical Corp., Mar. 1969.

56. Townsend, J.S.: The Diffusion of Ions into Gases. Trans. Roy. Soc., 193A, p. 125-158 (1900).

APPENDIX I: Normal Properties of Aerosols

During the calculation of the aerosol properties presented in Section 5.0 it became apparent that existing tabulations at ambient conditions were unsatisfactory. The most difficult problems center about the obscurity of the information, the fact that no one set of tables is complete for all functions of interest, inadequate ranges covered, and variation in physical constants used. Accordingly, a new set of calculations were effected for air at ambient conditions and are included herewith together with all necessary source material.

TABLES FOR USE IN AEROSOL PHYSICS Unit Density Spheres

Particle Diameter (microns)	Slip Correction Factor	Sedimentation Velocity (cm/sec)	Corrected Sedimentation Velocity (cm/sec)	Reynolds Number Terminal Velocity	Diffusion Coefficient (cm^2/sec)	Corrected Diffusion Coefficient (cm^2/sec)	Mobility (sec/g)	Corrected Mobility (sec/g)	Relaxation Time (sec)	Corrected Relaxation Time (sec)
μM	(S. C.)	v	v (S. C.)	Re	D	D (S. C.)	B	B (S. C.)	τ	τ (S. C.)
0.001	2.1697+02	3.0110-09	6.5330-07	2.0046-15	2.3545-04	5.1004-02	5.8620+09	1.2719+12	3.0694-12	6.6595-10
0.002	1.0877+02	1.2044-08	1.3100-06	1.6037-14	1.1772-04	1.2804-02	2.9310+09	3.1880+11	1.2277-11	1.3354-09
0.003	7.2788+01	2.7099-08	1.9701-06	5.4124-14	7.8482-05	5.7057-03	1.9540+09	1.4206+11	2.7624-11	2.0083-09
0.004	5.4668+01	4.8177-08	2.6337-06	1.2829-13	5.8861-05	3.2179-03	1.4655+09	8.0117+10	4.9110-11	2.6848-09
0.005	4.3858+01	7.5276-08	3.3009-06	2.5057-13	4.7089-05	2.0649-03	1.1724+09	5.1410+10	7.6734-11	3.3648-09
0.006	3.6638+01	1.0840-07	3.9715-06	4.3299-13	3.9241-05	1.4377-03	9.7701+08	3.5796+10	1.1050-10	4.0484-09
0.007	3.1488+01	1.4754-07	4.6457-06	6.8758-13	3.3635-05	1.0591-03	8.3744+08	2.6369+10	1.5040-10	4.7357-09
0.008	2.7625+01	1.9271-07	5.3235-06	1.0264-12	2.9431-05	8.1302-04	7.3276+08	2.0242+10	1.9644-10	5.4266-09
0.009	2.4621+01	2.4398-07	6.0050-06	1.4613-12	2.6161-05	6.4411-04	6.5134+08	1.6037+10	2.4862-10	6.1213-09
0.01	2.2218+01	3.0110-07	6.6901-06	2.0046-12	2.3545-05	5.2312-04	5.8620+08	1.3025+10	3.0694-10	6.8197-09
0.02	1.1415+01	1.2044-06	1.3749-05	1.6037-11	1.1772-05	1.3438-04	2.9310+08	3.3458+09	1.2277-09	1.4015-08
0.03	7.8247+00	2.7099-06	2.1284-05	5.4124-11	7.8482-06	6.1489-05	1.9540+08	1.5290+09	2.7624-09	2.1615-08
0.04	6.0366+00	4.8177-06	2.9002-05	1.2829-10	5.8861-06	3.5532-05	1.4655+08	8.8466+08	4.9110-09	2.9645-08
0.05	4.9698+00	7.5276-06	3.7485-05	2.5057-10	4.7089-06	2.3399-05	1.1724+08	5.8257+08	7.6734-09	3.8129-08
0.06	4.2613+00	1.0840-05	4.6192-05	4.3299-10	3.9241-06	1.6722-05	9.7701+07	4.1634+08	1.1050-08	4.7087-08
0.07	3.7591+00	1.4754-05	5.5462-05	6.8758-10	3.3635-06	1.2644-05	8.3744+07	3.1480+08	1.5040-08	5.6536-08
0.08	3.3649+00	1.9271-05	6.5238-05	1.0264-09	2.9431-06	9.9621-06	7.3276+07	2.4803+08	1.9644-08	6.6493-08
0.09	3.0508+00	2.4398-05	7.5511-05	1.4613-09	2.6161-06	8.0994-06	6.5134+07	2.0166+08	2.4862-08	7.6973-08
0.1	2.8667+00	3.0110-05	8.6316-05	2.0046-09	2.3545-06	6.7494-06	5.8620+07	1.6804+08	3.0694-08	8.7988-08
0.2	1.8693+00	1.2044-04	2.2514-04	1.6037-08	1.1772-06	2.2006-06	2.9310+07	5.4789+07	1.2277-07	2.2950-07
0.3	1.5611+00	2.7099-04	4.2386-04	5.4124-08	7.8482-07	1.2252-06	1.9540+07	3.0505+07	2.7624-07	4.3125-07
0.4	1.4149+00	4.8177-04	6.8166-04	1.2829-07	5.8861-07	8.3283-07	1.4655+07	2.0736+07	4.9110-07	6.9486-07
0.5	1.3299+00	7.5276-04	1.0011-03	2.5057-07	4.7089-07	6.2623-07	1.1724+07	1.5592+07	7.6734-07	1.0205-06
0.6	1.2742+00	1.0840-03	1.3612-03	4.3299-07	3.9241-07	4.9999-07	9.7701+06	1.2449+07	1.1050-06	1.4079-06
0.7	1.2347+00	1.4754-03	1.8217-03	6.8758-07	3.3635-07	4.1538-07	8.3744+06	1.0340+07	1.5040-06	1.8578-06
0.8	1.2053+00	1.9271-03	2.3227-03	1.0264-06	2.9431-07	3.5472-07	7.3276+06	8.8318+06	1.9644-06	2.3677-06
0.9	1.1824+00	2.4398-03	2.8639-03	1.4613-06	2.6161-07	3.0933-07	6.5134+06	7.7017+06	2.4862-06	2.9398-06
1	1.1642+00	3.0110-03	3.4454-03	2.0046-06	2.3545-07	2.7410-07	5.8620+06	6.8245+06	3.0694-06	3.5733-06
2	1.0821+00	1.2044-02	1.3833-02	1.6037-05	1.1772-07	1.2739-07	2.9310+06	3.1716+06	1.2277-05	1.3285-05
3	1.0547+00	2.7099-02	2.8582-02	5.4124-05	7.8482-08	8.2777-08	1.9540+06	2.0609+06	2.7624-05	2.9136-05
4	1.0410+00	4.8177-02	5.0154-02	1.2829-04	5.8861-08	6.1277-08	1.4655+06	1.5257+06	4.9110-05	5.1125-05
5	1.0328+00	7.5276-02	7.7748-02	2.5057-04	4.7089-08	4.8635-08	1.1724+06	1.2109+06	7.6734-05	7.9254-05
6	1.0274+00	1.0840-01	1.1136-01	4.3299-04	3.9241-08	4.0315-08	9.7701+05	1.0037+06	1.1050-04	1.1352-04
7	1.0235+00	1.4754-01	1.5108-01	6.8758-04	3.3635-08	3.4424-08	8.3744+05	8.5707+05	1.5040-04	1.5393-04
8	1.0205+00	1.9271-01	1.9647-01	1.0264-03	2.9431-08	3.0035-08	7.3276+05	7.4779+05	1.9644-04	2.0047-04
9	1.0182+00	2.4398-01	2.4834-01	1.4613-03	2.6161-08	2.6638-08	6.5134+05	6.6322+05	2.4862-04	2.5315-04
10	1.0164+00	3.0110-01	3.0665-01	2.0046-03	2.3545-08	2.3931-08	5.8620+05	5.9583+05	3.0694-04	3.1198-04
20	1.0092+00	1.2010+00	1.2117+00	1.6082-02	1.1772-08	1.1869-08	2.9310+05	2.9551+05	1.2277-03	1.2378-03
30	1.0055+00	2.6984+00	2.7051+00	5.3734-02	7.6482-09	7.8911-09	1.9540+05	1.9647+05	2.7624-03	2.7775-03
40	1.0041+00	4.7367+00	4.7561+00	1.2614-01	5.8861-09	5.9103-09	1.4655+05	1.4715+05	4.9110-03	4.9311-03
50	1.0033+00	7.2867+00	7.3186+00	2.4255-01	4.7089-09	4.7244-09	1.1724+05	1.1763+05	7.6734-03	7.6986-03
60	1.0027+00	1.0263+01	1.0291+01	4.0994-01	3.9241-09	3.9348-09	9.7701+04	9.7968+04	1.1050-02	1.1080-02
70	1.0023+00	1.3572+01	1.3604+01	6.3250-01	3.3635-09	3.3714-09	8.3744+04	8.3940+04	1.5040-02	1.5075-02
80	1.0021+00	1.7127+01	1.7162+01	9.1217-01	2.9431-09	2.9491-09	7.3276+04	7.3426+04	1.9644-02	1.9684-02
90	1.0018+00	2.0878+01	2.0908+01	1.2585+00	2.6161-09	2.6208-09	6.5134+04	6.5253+04	2.4862-02	2.4902-02
100	1.0016+00	2.4883+01	2.4844+01	1.6512+00	2.3545-09	2.3583-09	5.8620+04	5.8717+04	3.0694-02	3.0746-02

Note: Exponents are presented in computer format. Thus, $1.0291+01 = 1.0291 \times 10^{1} = 10.291$ and $1.6002-02 = 1.6002 \times 10^{-2} = 0.016002$.

BASIS OF THE TABLE

Physical constants used in preparation to table:

$\lambda = 6.53 \times 10^{-6}$ cm = mean free path of gas molecules in air
$\eta = 1.810 \times 10^{-4}$ poise = viscosity of air
$k = 1.3708 \times 10^{-16}$ erg/°C = Boltzmann's constant
$T = 293$°K = absolute temperature (20°C)
$\rho = 1$ g/cm^3 = particle density
$\rho' = 1.205 \times 10^{-3}$ g/cm^3 = density of air
$g = 981$ cm/sec^2 = acceleration due to gravity

Slip Correction Factor[1]

$$S.C. = 1 + \frac{2A\lambda}{d}$$

$$A = 1.257 + 0.400 \exp(-1.10\, d/2\lambda)$$

Mobility[2]

$$B = (3\pi\eta d)^{-1}$$

Diffusion Coefficient[2]

$$D = kBT$$

Relaxation Time[3]

$$\tau = d^2\rho/18\eta$$

Reynolds Number (Terminal Velocity)[2]

$$Re = C_D\, Re^2/24 = \rho\rho' g\, d^3/18\eta^2$$ Note: C_D = drag coefficient

Sedimentation Velocity[2]

1. For values of Re up to 0.05: $v = (\rho-\rho')g\, d^2/18\eta$
2. For values of Re from 0.05 to 4: $v = \left[C_D\, Re^2/24 - 2.3363\cdot10^{-4}\left(C_D\, Re^2\right)^2 + 2.0154\cdot10^{-6}\left(C_D\, Re^2\right)^3 - 6.9105\cdot10^{-9}\left(C_D\, Re^2\right)^4\right] \eta/\rho' d$

[1] Davies, C.N.: Definitive Equations for the Fluid Resistance of Spheres. The Proceedings of the Physical Society, Vol 57, Pt 4, No. 322 (1 July 1945).
[2] Green, H.L. and Lane, W.R.: Particulate Clouds: Dusts, Smokes and Mists. E.&.F.N. Spon Ltd., London, 1964 (2nd edition).
[3] Davies, C.N. (ed.): Aerosol Science. Academic Press, London, 1966.

APPENDIX II: Symbols

A = a numerical factor having a value of approximately unity

A_o = first Cunningham correction coefficient = 1.257

B = second Cunningham correction coefficient = 0.400, mobility of the aerosol particles

C = third Cunningham correction coefficient = 1.10, in filtration, a numerical factor of 0.5 to 0.75

C_D = drag coefficient

D = diffusion coefficient

D_i = probability of deposition due to diffusion

E = collecting field strength, efficiency of intact filter, voltage

E_D = diffusional filtration efficiency

E_G = gravitational filtration efficiency

E_I = inertial filtration efficiency

E_j = filtration efficiency due to all mechanisms (j = ERIGM Qq)

E_M = molecular filtration efficiency

E_o = charging field strength

E_{Qq} = electrostatic filtration efficiency (Also: E_{oq}, only fiber is charged; E_{Qo}, only aerosol is charged)

E_R = direct interception filtration efficiency

$E_{T(D)}$ = total collection efficiency of the filter (by diffusion)

$E\beta_j = E_j$ and includes consideration of the interference effect

F = drag on particle, driving frequency

F_b^* = dimensionless force acting on a unit fiber length

I = current, probability of inertial deposition

I_d = collision integral

K = agglomeration coefficient

$K_{1,2,3}$ = thermal conductivity

M = collection efficiency, molecular weight

Mg = count median diameter

Mg_1 and Mg_2 = observed and corrected particulate diameters

$\overset{h}{Mg}$ = count median diameter of high mode

$\overset{\ell}{Mg}$ = count median diameter of low mode

$\overset{h}{Mg}'$ = mass median diameter of high mode

$\overset{\ell}{Mg}'$ = mass median diameter of low mode

N_D = gravational filtration parameter

N_I = inertial filtration parameter

N_M = molecular filtration parameter

N_o = ion concentration

N_{Qq} = electrostatic filtration parameter

N_R = direct interception filtration parameter

P = pressure in atmospheres

P_c = critical pressure

P_e = Peclet number

P_i = impaction parameter

P_{pc} = psuedo critical pressure

Q = liquid flow rate

R = radius, gas constant

R_1 = radius of discharge electrode

R_2 = radius of collecting electrode

R_e = Reynolds number

S = ratio of particulate sphere of influence to particle radius, saturation, probability of deposition due to sedimentation

Stk. = Stokes number

T = absolute temperature

T_c = critical temperature

T_d = droplet temperature

T_{pc} = pusedo critical temperature

U_o = velocity of particle (re: mobility, B)

V = gas velocity, filter face velocity

V' = applied potential

V_L = molecular volume

Y = mole fraction

Z = electric mobility of ions

Z_2 = electric mobility of O_2 ions

Z_3 = electric mobility of He ions

Z_r = reduced electric mobility of ions

$\bar{c}$ = R.M.S. velocity

d = particle diameter (in filtration as d_p); droplet diameter

d_f = fiber diameter

e = electronic charge

f = fraction

g = gravitational acceleration

h = height

i = current per unit length of electrode

k = Boltzmann's constant, an integer 1, 2, 3, . . ., etc.

m = ion mass, droplet mass

n = number concentration of particles, number of electronic charges, e

n_o = initial number concentration of particles

n_s = saturation charge

p = a factor (re: electrification), droplet vapor pressure

p_t = liquid vapor pressure

q = charge acquired in time, t

r = radial distance from electrode centerline

r_{12} = collision diameter

s = fraction of molecules reflected diffusely

t = time

u = drift velocity of particles

v = sedimentation velocity

α = evaporation (condensation) coefficient

β = f(s) (re: slip correction), volume fraction of fibers

γ = 0.499 as extracted from the current expression for λ. surface tension

Δ = vapor shell thichness

Δp = pressure drop across filter

δ = 1 for specular reflections of the molecule from a particle but generally $\delta = (1 + \pi s/8)$ (re: slip correction), saturation

ϵ = dielectric constant

ϵ_o = dielectric constant of a vacuum. 8.85434×10^6 amp-sec/volt-cm

η = viscosity of the fluid medium

θ = integer

λ = mean free path of gas molecules

μ = micron

$\nu = (RT/2\pi M)$

ρ = particle density

ρ_L = liquid density

ρ' = gas density

σ_g = geometric standard deviation

τ = relaxation time, mean passage time of particles

$\chi = \frac{2\lambda}{d}$, the Knudsen number

ψ' = angle of inclination of a tube with the horizontal

α = packing density

APPENDIX III: Evaporation Condensation - Calculation of Necessary Parameters

III. I INTRODUCTION

Because of a lack of the detailed experimental data required for calculation of droplet evaporation rates, the various methods used in calculating the transport and other properties are presented in extension. Note that all the calculations are based upon properties that are themselves deduced from quasi-empirical equations given in the literature and stated to be correct within limits ranging from about ± 4 to $\pm 20\%$.

III. 2 MOLECULAR DIFFUSION

In considering the condensation, evaporation, and nucleation of any substance in a given atmosphere, a necessary parameter is the diffusivity of that substance in the atmosphere. Such a determination has been made for water vapor in the helium-oxygen environment at pressures ranging from 10 to 500 psia. Because data for this situation is not available, the calculations were performed using empirical equations. Since these equations are useful for calculating the diffusivities of substances other than water and because of an error in the most readily available reference source*, the relationships are presented in detail.

*Note: The method of calculating diffusivities of mixtures is presented in the 4th Edition of the Chemical Engineers' Handbook (Ref. III-2). However, while it is well discussed, it contains a major numerical error. Therefore, it is recommended that the original source by Wilke and Lee (Ref. III-1) be utilized.

The diffusion coefficient of one component through a stagnant multi-component mixture may be calculated from equation (III-1)

$$D_{1(23)} = \frac{1 - Y_1}{(Y_2/D_{12}) + (Y_3/D_{13})} \qquad \text{(III-1)}$$

where Y = mole fraction of each component

D = diffusion coefficient - cm^2/sec

$D_{1(23)}$ = H_2O vapor diffusing through He-O_2

D_{12} = diffusivity of H_2O and O_2

D_{13} = diffusivity of H_2O and He

Thus: 1 refers to H_2O

2 refers to O_2

3 refers to He

The mole fractions of each component was determined from a knowledge of the fact that the oxygen partial pressure is maintained constant at 160 mm mercury and the partial pressure of water vapor at saturation (vapor pressure) should be constant at a value of 23.37 mm of mercury. The diffusivity of water vapor through oxygen and water vapor through helium was calculated according to the equation of Wilke and Lee.(III-1)

$$D_{12} = \frac{B\,T^{3/2}\left[(1/M_1) + (1/M_2)\right]^{1/2}}{P\,(r_{12})^2\,I_d}\,, \qquad \text{(III-2)}$$

where

M_1 & M_2 = molecular weights of the respective components,

$$B = 10.7 - 2.46\left[(1/M_1) + (1/M_2)\right]^{1/2} \times 10^{-4},$$

T = absolute temperature - ^{o}K

$$r_{12} = \frac{r_1 + r_2}{2} = \text{collision diameter - } \mathring{A} \text{ from table of values,}^{(III-2)}$$

I_d = collision integral - from table after calculating force constants also from table,[III-2] and

P = absolute pressure - atm.

The results of this series of calculations are shown in Table 7 and Figure A-1. The diffusion coefficient varies from a value of 0.736 at 10 psia to 0.026 to 500 psia. The value for water vapor in air at ambient pressure is about 0.220 cm^2/sec.

III. 3 THERMAL CONDUCTIVITY

Thermal conductivity of the gas mixture in which a droplet is evaporating is an important component of the evaporation (condensation) equation that varies with atmospheric composition and pressure. The thermal conductivity (K^{o}_{123}) may be determined from the following equations:[III-2]

$$K^{o}_{123} = \frac{Y_1 K^{o}_1 M_1 + Y_2 K^{o}_2 M_2 + Y_3 K^{o}_3 M_3}{Y_1 M_1 + Y_2 M_2 + Y_3 M_3} \quad , \qquad \text{(III-3)}$$

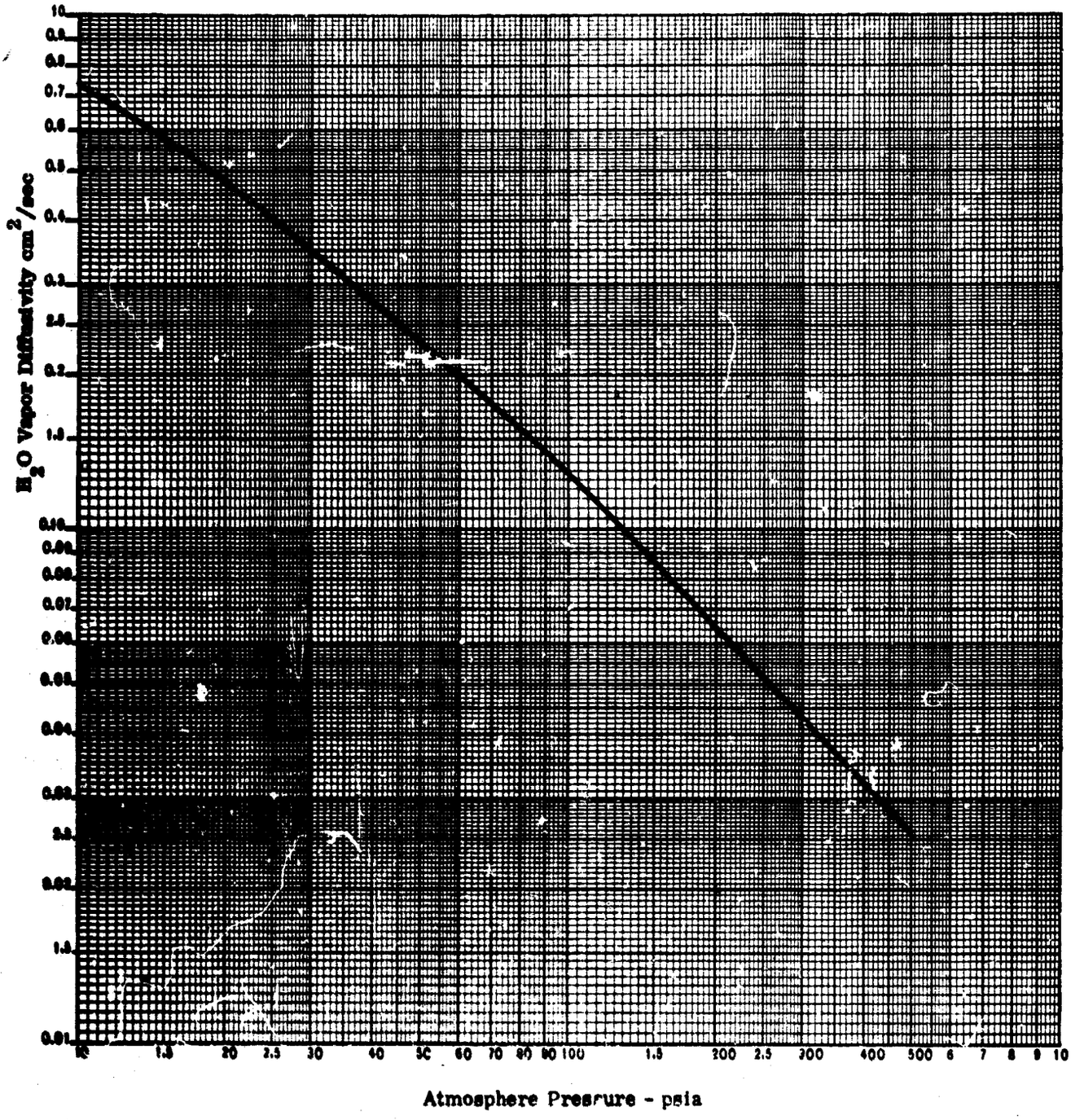

Figure A-1 Water Vapor Diffusivity in the Oxygen-Helium Atmosphere vs Pressure.
(PO_2 = 160 mm Hg; PH_2O = 23.37 mm Hg; T = 20°C)

where

K^{o}_{123} = thermal conductivity of the mixture at ambient pressure - cal/sec-cm-^{o}K,

K^{o}_{1} = thermal conductivity of H_2O vapor at ambient pressure,

K^{o}_{2} = thermal conductivity of O_2 vapor at ambient pressure, and

K^{o}_{3} = thermal conductivity of He vapor at ambient pressure.

From the above equation, the thermal conductivity may be determined (usually ambient) at the pressure for which tabulated values are quoted. Several solutions of the equation are necessary since, in our case, the mole fractions of the gas are varied with increasing pressure. To determine the thermal conductivity at the pressure of interest (K_{123}) it is first necessary to determine the psuedo critical pressure and temperature of the mixture. This is accomplished according to the mole fraction of each component by the following equations:(III-2)

$$T/T_{pc} = \frac{T}{Y_1 (T_c)_1 + Y_2 (T_c)_2 + Y_3 (T_c)_3} \quad , \qquad \text{(III-4)}$$

where

T = temperature of the gas mixture - ^{o}K and

T_c = critical temperature of each component (1, 2, 3) ;

$$P/P_{pc} = \frac{P}{Y_1 (P_c)_1 + Y_2 (P_c)_2 + Y_3 (P_c)_3} \quad , \qquad \text{(III-5)}$$

where

P = absolute pressure of the gas mixture - atm and

P_c = critical pressure of each component (1, 2, 3).

After determination of the critical properties of the mixture, the thermo-conductivity at the stated pressure (K_{123}) may be found through the use of Figure A-2 and the following equation.

$$K_{123} = K^{o}_{123} \, (K_{123}/K^{o}_{123}) \qquad \text{(III-6)}$$

In the case of the helium-oxygen atmosphere and water vapor up to 500 psia, the psuedo-critical properties of the gas are asympototic to unity in Figure A-2; therefore the values at ambient pressure are suitable for use as combined by the mixture equation. The variation in the tabulated (Table 7) values with increasing pressure is due not to the effects of pressure, but to the fact that the mole fraction of each component varies as the pressure is increased.

III. 4 VAPOR PRESSURE

The vapor pressure of liquids tends to increase slightly with increasing pressure. According to Bradley, this increase may be determined by the Poynting equation:(III-3)

$$\frac{p'_t}{p_t} = \exp\left(\frac{P' V_L}{R T}\right) \quad , \qquad \text{(III-7)}$$

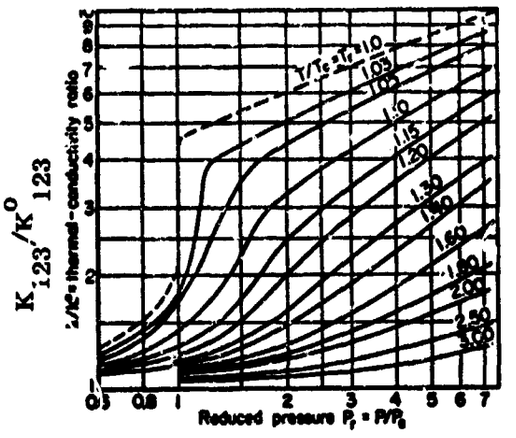

$$P_r = P/P_{pc}$$

Figure A-2. Curve for Determining the Thermal Conductivity of a Gas at Pressures Greater Than Ambient. (After Perry, R.H. et al (eds.): Chemical Engineers Handbook (4th ed), McGraw-Hill Book Co., New York, 1963).

where

p_t = vapor pressure of the bulk liquid - dynes/cm^2,

p_t' = vapor pressure of the bulk liquid at the pressure of interest (P) dynes/cm^2,

P' = pressure of the environment - dynes/cm^2,

T = temperature of the environment - ^oK,

R = gas constant - 8.317×10^7 ergs/^oK-mole, and

V_L = molecular volume - cm^3/g-mole

For water vapor in the helium-oxygen environment at 500 psia, this increase amounts to only 2.5% and has therefore been neglected for the entire series of calculations.

III.5 DROPLET VAPOR PRESSURE

The evaporation or condensation rate of the droplet depends on the vapor pressure of the surrounding vapor (p_t) and the vapor pressure of the droplet (p). Because of the droplet's curved surface, the molecules are less tightly held then they would be in a plain surface that results in a higher vapor pressure over the droplet than for the liquid itself.[III-4] The droplet vapor pressure may be calculated from the classical Gibbs-Thompson relationship:

$$\ln\left(\frac{p}{p_t}\right) = \frac{4\gamma M_l}{R\,\rho_L\,T_d\,d} \quad , \qquad \text{(III-8)}$$

where

p = droplet vapor pressure - dynes/cm^2,

ρ_L = liquid density g/cm^3,

d = droplet diameter - cm,

γ = surface tension of the liquid - dynes/cm, and

T_d = droplet temperature - ^oK.

Note: Strictly speaking, the temperature used in this equation is the actual temperature of the evaporating droplet rather than the ambient temperature. This, then, results in an equation with two unknowns: the droplet temperature (T_d) and the vapor pressure of the droplet (p).

The droplet temperature may be calculated from the following relationship:

$$T_d = \frac{L M_1 D_{1(23)}}{K_{123} R T} \left[\frac{\delta \; p_t - p}{2 D_{1(23)} / d\nu \; \alpha + d/d + 2} \right] , \qquad \text{(III-9)}$$

where

L = latent heat of vaporization of the liquid - cal/g

Δ = vapor shell thickness $\approx \lambda$ the molecular mean free path,

$\nu = (RT/2\pi \; M_1)^{1/2}$ - cm/sec,

α = evaporation (or condensation) coefficient = 0.04 for pure H_2O (III-6) and

δ = degree of saturation assumed = 1 (i.e. 100% RH).

This now results in two equations and two unknowns, the solution of which is given in Table 6.

APPENDIX III: Literature Cited

III-1 Wilke, C.R. and C.Y. Lee: Estimation of Diffusion Coefficients for Gases and Vapors. Industrial & Engineering Chemistry, Vol. 47, No. 6, p. 1253 (1955).

III-2 Perry, R.H., C.H. Chilton, S.D. Kirkpatrick (eds.): Chemical Engineers' Handbook (4th ed). McGraw-Hill Book Co., New York, 1963.

III-3 Bradley, R.S.: The Rate of Nucleation at High Pressures. J. of Colloid Science 15, p. 525, (1960).

III-4 Green, H.L. and W.R. Lane: Particulate Clouds: Dusts, Smokes and Mists. E. & F. N. Spon Ltd., London, 1964.

III-5 Orr, C., Jr.: Particulate Technology. The MacMillian Company, New York, 1966.

III-6 The Physical Chemistry of Aerosols. A General Discussion of the Faraday Society. University Press Ltd., Aberdeen, Scotland, 1961.

APPENDIX IV: Protocol for Simulated High Pressure Diving Experiment

IV. 1 PURPOSE

The purpose of this appendix is to lay down the details and identify problem areas related to the atmospheric sampling of the environment within an inhabited high pressure vessel to determine the aerosol content. Based upon general experience in atmospheric sampling and the theoretical and experimental generated on the project, three related, feasible experiments have been designed as detailed below. The experiments are designed to answer the following questions:

(a) What quantity of aerosols can be expected to arise from mere habitation of the chamber (and/or whatever other experiments are being carried out during the investigation)?

(b) What is the mass concentration of aerosol during various activity periods?

(c) What quantity of the collected aerosol vaporizes and is lost during depressurization of the sample?

(d) What is the chemical analysis of the portion of the aerosol which vaporizes?

(e) What is the chemical analysis of the portion of the aerosol which remains?

(f) What is the day-to-day variability of the above?

(g) What is the number concentration of aerosols in the chamber in the micron range?

(h) What portion of the above collected sample will be lost during depressurization?

(i) As above - size distributions with photographic records before and after depressurization.

(j) What is the submicron size distribution and numbers concentration as determined by electron microscopy (i.e. only after depressurization)?

(k) What is the day-to-day variability of the above?

The experiments described below require dive participation by a trained aerosol physicist, if the experiment involves a simulated chamber dive. If this is not the case, then certain phases of each experiment may be eliminated as detailed below and a Navy diver can be trained to do the remaining portions of thw work which must be carried out within the chamber

IV. 2 MASS CONCENTRATION DETERMINATION

The determination of mass concentration within the atmosphere will be carried out with a modified version of the so-called high volume sampling technique used in air pollution. The procedure is as follows:

(a) Weigh a 4" disc of all glass, fired, high efficiency filter media in the laboratory.

(b) Re-weigh the same disc in the environment.

(c) Draw 15 to 20 cfm of the atmosphere thru the filter for a stipulated period of time.

(d) Re-weigh the filter within the environment.

(e) Seal the filter into a pressure vessel.

(f) Upon return to the laboratory expand the gas contained in the pressure vessel to atmospheric pressure and sample via gas chromatography.

(g) Re-weigh the filter in the laboratory at ambient conditions.

(h) Perform micro-chemical analysis of filter.

The items which will be determined from the above procedure are:

(a) Airborne mass concentration within the chamber.

(b) Percentage of airborne mass concentration which could not exist at ambient conditions.

(c) Chemical composition of above.

(d) Chemical composition of remaining fractions.

The foregoing samples will be obtained on the following schedule:

(a) One sample operating continuously during compression.

(b) While "on the bottom" one sample for each "activity" period, i.e. one sample during sleeping and during such other activity periods as designated for the particular dive.

(c) One sample per day during ascent.

IV. 3 SUBMICRON PARTICULATE SAMPLING

The sampling of the submicron particulate fraction of the atmosphere may be accomplished with a thermal precipitator probably of the Casella-type which uses a water aspiration technique to achieve the necessary flow. Because of the composition of the atmosphere, it is necessary to weld a thermocouple to the hot wire of the precipitator and measure its actual temperature in air so that a corresponding temperature can be achieved in the atmosphere in which it is to actually be used. Simply, it is be a matter of measuring the temperature in the ambient environment and providing increased d. c. electrical power to achieve that temperature in $He-O_2$. Deposition occurs on the usual glass slide which may be uncoated but can have temporarily afixed to it a carbon coated microscope grid. In this manner evaluation may be selectively by either scanning electron microscopy of normal electron microscopy. No evaluation should be attempted within the confines of the atmosphere since the electron microscope operates under vacuum. This technique will only yield information concerning the fraction (if any) of the particulate which does not evaporate upon depressurization. The electron photomicrographs produced for this sampling may be evaluated for numbers concentration and size distribution.

The sampling schedule should be such that representative samples are obtained during periods of no activity, normal activity, and unusual activity.

It is considered possible to train a Navy diver to gather these samples.

IV.4 SAMPLING FOR MICRON SIZE PARTICULATES

Micron size particulates may be sampled from the atmosphere using a modified Casella cascade impactor. Experience indicates that this is a highly reliable device giving accurate results when the slides are analyzed by light field microscopy. Further, the analysis is simplified by having the particulates divided into four stages.

(a) Prepare slides within chamber.

(b) Run impactor concurrently with the thermal precipitator on the schedule described above.

(c) Analyze slides within the chamber by light field microscopy for numbers concentration and size distribution.

(d) Obtain photomicrographs of representative fields of each slide for every sample.

(e) At the completion of tests, but prior to ascent, select a representative slide and make sequential photomicrographs of it, without changing field, during ascent.

(f) Under ambient conditions, in the laboratory, repeat sizing and counting (unless no evaporation has been demonstrated).

The information yielded from this technique will be:

(a) Numbers concentration.

(b) Representative size distributions

(c) Fraction of numbers concentration which can not exist under ambient conditions.

(d) Difference in distribution related to above.

(e) Graphical depiction of those particles which evaporate as it happens.

APPENDIX V: Annotated Bibliography

The goal of this literature search was to determine the extent of existing knowledge of aerosols in high pressure environments. While nothing specific was uncovered the sources that were examined and bear some relation to the overall project are detailed below.

ARNEST, Richard T.: Atmosphere Control in a Closed Space Environment (Submarine). U.S. Naval Medical Research Lab Rpt. #367, Bureau of Medicine & Surgery, Navy Dept., Vol. 20, No. 21, 14 Dec 1961.

Abstract: The material presented in this report is a summation of class lectures on submarine medicine. The various aspects of atmospheric control within the submarine is discussed in great detail from a medical point of view. Particularly useful is a listing of more than 25 atmospheric contaminants, their sources and maximum allowable concentrations. Additional information includes symptoms, long term effects, measurement techniques, and methods of control and removal.

BECK, E.J.: Environment Control in Pressurized Underwater Habitats. U.S. Naval Civil Engineering Lab., Port Hueneme, Calif., Tech Rpt. R496, Nov. 1966. AD #642 835

Abstract: A study was made to identify those environmental factors which would have to be controlled in order that man could live and work beneath the sea. The state-of-the-art of undersea habitation is described, limitations and areas of possible major improvements are listed, and possible approaches to improvement are outlined. The developmental routes suggested are aimed at reducing cost and complexity, establishing more normal environments, and above all, reducing the hazards of working in the ocean.

Environmental factors considered are atmosphere, sanitation, food storage and preparation, heating, and the effects of special atmospheres on voice communica-

tion. The peculiar requirements for providing a tolerable atmosphere at any but the shallowest depths have, by known approaches, produced major changes in all other areas. (Author's abstract)

BOND, George F.: New Developments in High Pressure Living. Archives of Environ. Health, Vol. 9, p. 310, Sept. 1964.

Abstract: Six years of experimentation were carried out to develop the proper synthetic breathing mixtures of helium nitrogen and oxygen to permit continuous submergency at 200 ft depth. The percentage of oxygen was usually such as to be equivalent to the atmospheric partial pressure of O_2 i.e. about 160 millimeters Hg. Small amounts of nitrogen were also used. There are indications that these artificial atmospheres are superior to the ones man commonly breathes. However, at the writing of this paper the problems of body temperature control and voice communication have not been solved.

BOYLAN, L.: Soviet-Bloc Submersible Development. MTS Journal, Vol. 3, No. 2, pp. 21-44 (March 1969).

This is the first of three articles discussing the history, state of the art, and future development of Soviet-bloc submersible research. This article relates the 45-year history of deep submersible development starting with the founding of the Soviet salvage organization, EPRON, and the construction of the Danilenko diving chamber. Included in this paper are physical descriptions and the missions of all the Soviet-bloc submersibles built since 1923. There are photographs and/or sketches of each device. The author comments that the past history of Soviet-bloc submersible development is not very impressive but he adds that the forthcoming articles which include discussions of the habitat and sealab programs improves the Eastern European involvement.

BROWN, Ivan W. and Barbara G. Cox (editors): Compression and Decompression Problems. Nat'l. Aca. of Science, Nat'l Research Council, Washington, D.C. (Rpt. 1404). Proceedings of the Third Internat'l. Conf. on Hyperbaric Medicine, Duke Univ., Durham, No. Carolina, Nov. 17-20, 1965.

Abstract: Generalized discussion and guidelines regarding decompression sickness, air embolism, oxygen toxicity, nitrogen narcosis air problems, vertigo migraine, etc.

CARHART, Homer W.. The Maintenance of a Habitable Atmosphere. U.S. Naval Research Lab., Washington, D.C. (presented at the Underwater Tech. Conf., New London, Conn., May 5-7, 1965.

Abstract: An updated review of the various aerosol and gaseous contaminant control devices used in nuclear submarines is presented. Additionally a brief section is presented outlining the problems in high pressure environments using helium and possibly hydrogen as the diluent gas. However, the problems outlined deal with the absorption and removal of carbon monoxide, dioxide, etc. Aerosols are not specifically treated. There is an implication that virtually the total nuclear submarine aerosol problem is related to cigarette smoking and since this is impossible in the high pressure atmosphere the problem will not be important.

CARPENTER, E.P.: NOTS Participation in Sealab II Project. U.S. Naval Ordnance Test Station, Rpt. #NOTS TP 4130, China Lake, Calif., Sept. 1966.

Detail discussion is presented for mechanical logistical problems in siting and removing the Sealab II project. The various systems are discussed but useful detail on atmospheric control is not specifically presented.

COUSTEAU, Cap. Jacques-Yves: Working for Weeks on the Sea Floor. Nat'l. Geographic, April 1966.

Abstract: Detailed and highly illustrated description on Conshelf III experiment. Approximately 3 weeks were spent on the ocean floor at a depth of 328 ft and a pressure of 11 atmospheres. This was a saturation dive with the breathing mixture being helium and oxygen. The divers lived within the environment and regularly left it using diving gear and breathing the special mixture to perform simulated work projects.

COX, T.L.: Safety in the Cachalot Saturation Diving System Operations. J. Hydronautics, Vol. 2, No. 4, pp. 187-191 (Oct. 1968).

The Cachalot Saturation Diving system has proved itself much safer than normal deep sea diving; however, the saturated diver must be kept under pressure. A sudden return to one atmosphere of pressure would be fatal. This paper treats, (1) the handling of the saturated diver living in a pressurized chamber at the surface, (2) transferring from there to the underwater work site, and (3) working in the hostile underwater environment. Six divers at a time live in a 26-ft-long, 7-ft-diam chamber. Methods for control of oxygen and inert gas partial pressures, heat, humidity, and contaminants are discussed. Two divers leave the main chamber and enter a diving bell which takes them underwater to the work site. This bell must be handled so as not to endanger the lives of the divers. We must, however, achieve maximum underwater work hours. Problems of handling the bell in rough weather and protecting the vital supply, communication, and monitoring lines are discussed. Divers exit from the bell through a hatch in the bottom, but remain connected to it by 100-ft umbilical lines. In case of any emergency, the bell provides a nearby haven for safety. (author's abstract)

EBERSOLE, Lt. Comm. John H.: New Dimensions of Submarine Medicine. Submarine Medicine, Vol 262, No. 12, p. 599, 24 Mar. 1960.

Detailed discussions of the various problems involved in maintaining the atmosphere during long periods of submergence. The methods of scrubbing carbon dioxide as well as the additional toxicological problems encountered with the monoethanolamine solution are discussed. Average flow rates are given for the up-take of oxygen per man and per hour. While insufficient oxygen can be stored in high pressure flasks the details of the current system are stated to be classified at the time of this paper's presentation. Carbon monoxide is eliminated by the catalytic "burning" technique. This method oxidizes the carbon monoxide to carbon dioxide which is then handled by the CO_2 scrubbing system. This system also serves to oxidize other atmospheric contaminants particularly the volatile hydrocarbons. However, there is also the problem that some hydrocarbons are not completely oxidized and toxic and irritating intermediates are formed. Freon is extensively used in submarines and while of itself is a relatively non-toxic substance it is readily decomposed to hydrocloric acid etc. in the presence of open flames. Several sources of hydrocarbons are indicated such as paints, waxes, cleaning fluids, etc. The most effective control technique is a rigorous substitution program. The chief source of aerosol concentrations are tobacco smoke and electrostatic precipitators are suggested for

abatement purposes. Ozone has been found to be generated by various electric devices but the rates and concentrations are sufficiently low so that increased ventilation can be utilized as an abatement technique. The balance of the paper deals with reports of the first long dives of Skate and Seawolf.

EBERSOLE, Lt. Comm. John H.: Submarine Medicine on U.S.S. Nautilus and U.S.S. Seawolf. Proc. of the Royal Society of Medicine, Vol. 51, p. 63

Abstract: The initial evaluation of the medical problems on the nuclear submarines Nautilus and Seawolf are presented. The paper deals mainly with radiation exposures and the safety of the environment. Other comments refer to the ventilation system and CO and CO_2 removal facilities.

HAMREN, F.E., Jr.: Makai Range Habitat Readied. UST, p. 46, (Feb. 1969).

The Habitat II is described as the first transportable undersea habitat capable of supporting four men for 20 days at depths down to 580 feet. It is being built by Pittsburgh-Des Moines Steel Co. for undersea research by Makai Range Inc. It can be fully outfitted, pressurized and depressurized at dockside and towed to its offshore site. There is a full description of the facilities aboard Habitat II which include a 30 inch emergency hatch on each of the two cylindrical sections which, together with a central entry sphere, comprise the system. A sketch shows the locations of the facilities available.

KINNE, O. and S. Ruff: Manned Underwater Laboratory in the North Sea. NASA Rpt. No. TT-F-11,785, National Aeronautics and Space Administration, Washington, D.C. (June 1969).

The design of the projected underwater laboratory (UWL) at Helgoland is briefly described. Provisions for the maintenance and medical surveillance of the laboratory personnel are indicated. The future research program, which consists of a medical, a psychological and a marine biology research program, is outlined. (authors' abstract)

KINSEY, Jack L.: Some Toxicological Hazards in Submarines. Federal Proc. 19, No. 3, Part II: Problems in Toxicology, p. 36, 1962.

Abstract: The paper describes seven systems used in nuclear submarines to control pollutants generated therein. Briefly described are the specific control methods for carbon dioxide and carbon monoxide. Aerosol concentrations within the craft are found to stabilize at about 400 micrograms per cubic meter consisting of approximately 80% organic substances. One of the chief sources of aerosol production is found to be cigarette smoking. Air ions also tend to reach stable concentrations averaging about 450 positive and 240 negative ions. The fact that higher concentrations are not found is attributed to their binding with the high aerosol concentrations. The excess of positive ions is attributed to their slightly lower mobility. Monitoring is carried out with the Mk 3 analyzer designed by NRL. It consists of five analytical channels for oxygen, carbon monoxide, carbon dioxide, hydrogen and Freon.

KOTTLER, C.: Underwater Systems within the Scientific, Technological, and Economic Framework. J. Hydronautics, Vol. 3, No. 1, pp. 2-11, (Jan 1969).

This paper presents the economic and technological framework within which advanced underwater systems will fit. Many companies and governmental agencies are continuing research into a large number of areas directly or indirectly connected with oceanographic activities. Environmental analysis is yielding better long range predictions as well as some control. Mathematical models with computer assistance provide methods for mission and system analysis. In addition, new subsystems (e.g., nuclear power, scuba, dynamic positioning, etc.), and new or improved materials are extending vehicle system capabilities by orders of magnitude, thereby permitting missions only dreamed of before.
Much needed oceanographic and weather data for analysis of the dynamics of oceanographic processes is possible using a system of instrumented buoys. Military and commercial operations would find environmental analysis extremely valuable.

KRUEGER, Albert P. and Richard F. Smith: The Effects of Air Ions on the Living Mammalian Trachea. J. of General Physiology, Vol. 42, No. 1, p. 69-82, Sept. 20, 1958.

The paper discusses the effects of air ions on the rate of ciliary action. Generally positive ions tend to decrease the beat, the negative ions tend to increase it.

KRUEGER, Alpert P. and Richard F. Smith: The Physiological Significance of Positive and Negative Ionization of the Atmosphere. Man's Dependence on the Earthly Atmosphere, Karl Schaeffer, (ed.), The Macmillian Co., New York. Proc. of the First Internat'l. Symposium on Submarine & Space Medicine, U.S. Submarine Base, New London, Conn., Sept. 8-12, 1958.

Abstract: The histroy of atmospheric electricity is briefly cataloged together with methods of generating and measuring ions in air. Detailed are natural and artificial sources of ions and the observed physiologic effects of positive and negative ions on both extripated tissues and intact animals. As a generality negative ions seem to have beneficial effects and promote feelings of wellbeing while the positive ions have the opposite effect.

LEARY, Frank: Vehicles for Deep Submergence. Space/Aeronautics, Vol. 49, No. 4, p. 52, Apr. 1968.

A generalized description of all the current and recently past submergence projects is presented. Emphasis is placed upon the mission capabilities of the vessels with very little mention being made of life-support systems. No differentiation is pointed out between saturation dive vessels and normal pressure types.

Man's Extension into the Sea: Marine Technology Society - transactions of the Joint Symposium, 11-12 Jan 1966, Washington, D.C.

This is a report of a symposium whose purpose was to disseminate knowledge gained from the Sealab II experiments. A great deal of engineering detail is presented on the Sealab II experiments and items discussed cover: design and construction, logistics, crew selection and training, proplusive efficiency of divers in the sea, ocean engineering, underwater photography problems, human physiology, underwater weather station, measurement of human performance, value of saturation diving, salvage operations, flexible structures and unusual engineering problems are all discussed.

MAVOR, James W., et al: Alvin, 6000 Ft. Submergence Research Vehicle. The Soc. of Naval Architects and Marine Engineers, No. 3, p. 1-32, (1966).

Alvin, a deep-submergence oceanographic research submarine was commissioned on June 5, 1964, reached her designed operating depth of 6000 feet during trials in July, 1965, and maintained a deep-diving schedule in February and March 1966. The vehicle, displacing 30,000 lb on an overall length of 22 ft, carries a payload of 1400 lb and a complement of one pilot and one or two observers. Five plexiglas windows and a mechanical arm permit observation, collection, and manipulative tasks. The design of Alvin is described in some detail and the lessons learned from operations over a two-year period are presented and discussed. The logistic support used with Alvin operation is described, including a seagoing catamaran built for the task. (Author's Abstract)

McCONNAUGHEY, W.E.: Atmosphere Control of Confined Spaces from Man's Dependence on the Earthly Atmosphere, Karl Schaefer (ed.), The Macmillian Co., New York. (Presented at the Proc of the First International Symposium on Submarine & Space Medicine, U.S. Submarine Base, New London, Conn., Sept. 8-12, 1958.

The technical considerations for choosing between a non-regenerative lithium hydroxide CO_2 absorption system and a regenerative MEA scrubber system are

presented for nuclear submarines and submergence times in excess of ten days, the heavier, bulker, MEA system is utilized. Descriptions are also presented for the CO burner and electrostatic precipitator used for the removal of aerosols.

McCONNAUGHEY, W.E.: Atmosphere Control on Submarines. BuShips Journal, p. 11, May 1960.

See paper by same author "Atmosphere Control of Confined Spaces".

DEPT. of the NAVY, Office of Naval Research & Bureau of Medicine & Surgery, Washington, D.C.: A Bibliographical Sourcebook of Compressed Air, Diving and Submarine Medicine. Vol I - Hoff, E.C., Feb. 1948. Vol II - Hoff, E.C. and L.J. Greenbaum, Nov. 1954. Vol III - Greenbaum, L.J. and E.C. Hoff, Dec. 1966.

These three volumes cover all aspects of the problems of compressed air diving, medical, physiological, etc. The volumes have been developed over a period of years and in each case emphasis is shifted and changed to fully explain new and important developments. In addition to this specific bibliographic material and annotation there are long summaries on each subtopic.

U.S. NAVAL Research Lab., Washington, D.C.: The Present Status of Chemical Research in Atmosphere Purification and Control on Nuclear-Powered Submarines.
Miller, R.R. and Piatt, V.R., NRL Rpt. No. 5465, 21 Apr 1960
Piatt, V.R., et al, NRL Rpt. No. 5630, 14 July 1961
Piatt, V.R., et al, NRL Rpt. No. 5814, 29 Aug. 1962
Carhart, H.W. and Piatt, V.R., NRL Rpt. No. 6053, 31 Dec. 1963
Lockhart, L.B., Jr. and V.R. Piatt, NRL Rpt. No. 6251, 23 Mar 1965
Alexander, A., et al, NRL Rpt. No. 6491, 11 Jan 1967

This series of reports represents continuing discussions of the detailed progress and research results of various projects intended to continuously improve the habitability of submarine atmospheres and discern long range problems. The

subjects covered deal with aerosols, gases, and vapors, their sources, instruments and techniques for detection and control methods. Control is generally effected by collection devices or substitution techniques. Significant details are presented for all phases of the research and it is possible to continuously follow the statement of a problem, development of a technique and ultimate solution, in the reports of several successive years.

NONHEBEL, G. (ed.): Purification of the Atmosphere in Nuclear-Powered Submarines from Gas Purification Processes, George Newnes Ltd., London, Pt. C, p. 799, 1964.

This chapter is contained in a general book on gas purification and briefly outlines the gaseous and aerosol problems in nuclear submarines. Tables are given for compounds which have been identified in submarine atmospheres, the concentrations normally found, and acceptable concentrations. Flow charts are also given for the purification chain and detailed descriptions are presented for the various gas purification systems.

PAULI, D.C. and G.P. Clapper (eds.): An Experimental 45-Day Undersea Saturation Dive at 205 Feet. Office of Naval Research, Dept. of the Navy, Washington, D.C. ONR Rpt. No. ACR-124, March 8, 1967

This document of over 400 pages represents a complete description of the Sealab II experiment. All phases and aspects of the dive have been covered in considerable detail. With specific relation to atmosphere control there is no mention of aerosols whatsoever. Carbon dioxide was controlled with lithium-hydroxide canisters. Hydrocarbons and odors were controlled by the use of large filters of activated charcoal.

QUINN, A.: Project Tektite I - Four-man Underwater Laboratory. UST, pp. 48-49, (Feb. 1969).

This article discusses the coming operation Tektite I sponsored by the Navy, NASA, Department of the Interior and General Electric. It will take place at a depth of 50 ft. at Great Lameshur Bay, Virgin Islands National Park, St. John Island. Four men will conduct extensive marine science studies on the ocean floor and evaluate man's psychological and physiological reactions to a long term mission, (60 days), under saturated diving conditions.

RAMSKILL, Eugene A.: Providing Better Air for Bottled Up Men. SAE Journal, Paper 352D, June 1961

The complete atmospheric control system for nuclear submarines is detailed in outline form. Components include an electrostatic precipitator, catalytic combustor, particulate filter, cooling coil, activated charcoal and CO_2 remover. Inputs are the submarine atmosphere itself and an oxygen generator. An atmosphere analyzer (undescribed) has the ability to sample the system at several points in the cycle. A table is also presented on the various constituents of nuclear submarine atmospheres and representative concentrations found therein.

SAKHALOV, I.N.: Undersea Research Vehicles. Dept. of the Navy, Office of the Chief of Naval Operations, Office of Naval Intelligence, Translation Section, ONI Translation No. 2092, August 1965, AD No. 633 826.

A brief discussion is given on two proposed undersea research vehicles. Details are given as to their range, mobility and facilities. However no details are available on atmospheric systems. Stated usage for these vehicles is for research for the fishing industry.

SAUNDERS, Raymond A.: A New Hazard in Closed Environmental Atmospheres. Arch. Environ. Health, Vol. 14, p. 380, Mar 1967.

A government contractor recently evaluated a completely integrated life support system in an experiment which involved maintaining five men for 30 days in a hermetically sealed environmental chamber. Undesirable contaminants developed in the chamber and persisted in spite of the contaminant control system. The atmosphere acquired an odor which became increasingly disagreeable. The crew developed anorexia, became nauseated, suffered severe vomiting, and developed headaches and odd facial sensations. These symptoms together with other difficulties prompted test termination after four days. Preliminary efforts to pin-point the cause of the sickness were unsuccessful.

Later analysis of the chamber atmosphere at the Naval Research Laboratory identified 23 volatile compounds. Among these were monochloroacetylene and dichloroacetylene. The latter compound is known to produce symptoms identical to those experienced by the chamber crew. Dichloroacetylene has since been found at low concentration in a submarine atmosphere also.

A few chlorinated hydrocarbons customarily have been tolerated in most closed environmental atmospheres because of their general usefulness and relatively low toxicity. Such was the case in both these instances. The toxicant was produced through the action of an improperly operating element of the environmental control system on one of these compounds. (Author's Abstract)

SAUNDERS, R.A. and R.H. Gammon: The Sealab II Trace-Contaminant Profile. Naval Research Laboratory, Rpt. No. 6636, Washington, D. C., Dec. 4, 1967.

Adsorption of contaminants on activated charcoal was one of the methods used to sample the atmosphere of Sealab II. The contaminant material was later recovered by slowly heating the charcoal in an evacuated system and retaining the desorbate in liquid-nitrogen-cooled traps. The desorbate mixture was resolved with a vapor-phase chromatograph. The eluted components were passed directly into a rapid-scanning mass spectrometer for positive identification. Components were also collected from the effluent of the chromatograph and identified by means of their infrared spectra. Over 30 different compounds were identified in the charcoal desorbate. Added to those already known, the total number of atmospheric contaminants which have been identified in Sealab II now amounts to 40. These include refrigerants, saturated and unsaturated aliphatic hydrocarbons, cyclic aliphatic hydrocarbons, chlorinated hydrocarbons, and aromatic hydrocarbons. The characteristic feature of the Sealab II contaminant profile, like that of Sealab I, was a predominance of hydrocarbon contaminants. Some of the more prominent contaminants in the Sealab II atmosphere were cyclic aliphatic hydrocarbons which are not generally encountered as dominant trace contaminants in closed environmental atmospheres. (Author's Abstract)

SCHAEFER, Karl E.: Basic Physiological Problems in Submarine Medicine from Man's Dependence on the Earthly Atmosphere, Karl Schaefer (ed.) The Macmillian Co., New York. Presented at the Proc. of the First International Symposium on Submarine & Space Medicine, U.S. Submarine Base, New London, Conn., Sept. 8-12, 1958.

The very basic requirements of man the "open system" living in a submarine "closed system" are presented. Discussed in detail are questions of adaptation to various gas and contaminant concentrations and the relationship between natural and artificial time cycles.

SCHAEFER, Karl E.: Airborne Condensation Droplets, Ions May be Major Health Factors in Habitability of Closed Spaces. Heating, Piping & Air Conditioning, p. 101-105, May 1959; p. 123-125, June 1959 and p. 139-140, July 1959

Three components of the submarine atmosphere which previously have escaped major attention are discussed. These included (1) trace substances, (2) condensation droplets (nuclei) and (3) positive or negative ions. The biological effects of ions are discussed with a general indication that negative ions are beneficial and positive ones are not. During submergence there are found to be marked increases in both positive and negative and ions and condensation nuclei. The increase of ions in fleet type submarines is thought to be due to radioactive dials. In modern nuclear-powered submarines there is a constant source of radiation which contributes to the ion formation. The increase in condensation nuclei and condensation droplets are possibly due to temperature extremes found within the vessel which give rise to supersaturated conditions and the condensation of moisture on the ions. It was also found that higher temperatures generally decrease the number of ions and that humidity and ion content have an inverse relationship. It was also noted that the number of positive ions increased more than the negative ones. The general conclusion is that the production of the ions in a submarine is from radiation sources.

SCHAEFER, Karl E.: Experiences with Submarine Atmospheres. J. of Aviation Medicine, Vol. 30, p. 350-359, May 1959.

The problems of submarine medicine experienced during long submergence periods are reviewed. Thermal exchange in the normal apartment and submarine are compared. The role of trace substances and ionization patterns of the atmosphere in confined spaces are discussed. Emphasis is placed on chronic carbon dioxide toxicity which has been in the past a cardinal problem

of submarine medicine. Differences in the combined effects of increased CO_2 and low oxygen under accute and chronic conditions are analyzed. (Author's Abstract)

SCHAEFER, Karl E. and James H. Dougherty: Interaction of Aerosols and Air Ions. Bureau of Medicine & Surgery, Rpt. No. 380, Dept. of the Navy, Vol. XXI, No. 11, 29 Mar 1962

An experiment is described wherein variations in ion concentrations of small, medium and large ions were investigated with relation to numbers of condensation nuclei. The nuclei were generated from DOP. Results indicate that the air ions do become attached to aerosol particles and their measurable numbers are decreased. This finding is pointed out as being of importance in physiologic studies of the effect of air ions when the aerosol concentration is unknown.

SCHAEFER, Karl E.: Environmental Physiology of Submarines and Spacecraft. Archives of Environmental Health, Vol. 9, p. 320-331, Sept. 1964.

Description of experiments to check the 1-1/2% TLV used in submarines for carbon dioxide concentrations. The conclusion of the evaluation was that the TLV of 0.5% CO_2 recommended by the ACGIH is supported. The TLV for carbon monoxide in submarines is reduced from 100 ppm to 25 ppm. Additional values are given for 90 days continuous exposure on various other toxic trace substances most of which are below the currently accepted values for 8 hour exposures.

The bulk of the aerosol concentration in submarines is mainly attributed to cigarette smoking. Concentrations of aerosol on a submarine were reduced by 1/3 when smoking was temporarily prohibited during a specific trip. Maximum concentrations of positive and negative ions were found to be approximately 1,000 per cc. Increases in the aerosol concentration caused a decrease in the number of small ions and an increase in the large to medium size ions. Further increases in aerosol concentration lead to a general decrease of small and large ions. Condensation nuclei concentrations

in the submarine atmosphere increased ten to twenty-fold during periods of submergence. Aerosols are further found to be significant in concentrating trace substances present in the atmosphere.

SCHULTE, John N.: The Medical Aspects of Closed Cabin Atmosphere Control. Military Medicine, p. 40, Jan 1961.

The paper describes some initial studies on the cruise of nuclear submarines. Briefly mentioned are the toxic substances and levels observed, episodes during equipment failure and the results of physiological and hematological studies before, during, and after the trips.

SENGEYEV, S.: Sadko, Guest of Leningrad. Moscow, Szvestiya, Russia, 15 Nov. 1967.

This article is a narrative account by the author of the dive of the Russian "submarine house" Sadko-2 to a depth of 25 meters in the Black Sea with two men aboard for 10 days. There is a brief description of the living accommodations aboard. The experiments performed by the men are described as "broad" but there is only reference to investigation of the layer of discontinuity and an underwater current study.

SMITH, W.D., F.J. Woods and M.E Umstead: Submarine Atmosphere Studies Aboard the U.S.S. SCAMP. U.S. Naval Research Lab, Washington, D.C. Oct. 4, 1965. (AD No. 474 373)

An improved model of the original NRL Total Hydrocarbon Analyzer was successfully tested aboard the USS SCAMP. It was demonstrated that the ship's air banks can be used as a source of air for the operation of the Total Hydrocarbon Analyzer, a procedure which will facilitate use of the instrument aborad ship. Detailed analyses were made of the concentrations of methane, Freon-12, and "total hydrocarbons," with particular attention given to the methods of sampling and of sample introduction. A slowly rising level of methane and Freon-12 during submergence was observed, but little variation in contamination level from compartment to compartment was noted. (Author's Abstract)

STARK, James E.: Concepts of Atmosphere Control in Submarines. Archives of Environmental Health, Vol. 9, p. 315, Sept 1964.

The discussion recognizes the need to control carbon monoxide and carbon dioxide as major items but deals in general with the trace substances. Four basic approaches are listed to atmosphere control. The first is screening of materials proposed for entry into the submarine. The second is consideration of the constructional material used in the submarine, such as paints, adhesives and lagging, etc. The third consideration for control is the processes of detection and analysis and the fourth and final consideration is removal systems for conversion or destruction of toxic materials.

The need for further study of an establishment of TLV's for the unusual conditions of submarines is emphasized.

VERZAR, Fritz: Physiological and Toxicological Significance of Atmospheric Condensation Nuclei from Man's Dependence on the Earthly Atmosphere, Karl Schaefer (ed.), The Macmillian Co., New York. Presented at the First International Symposium on Submarine and Space Medicine, U.S. Submarine Base, New London, Conn., Sept. 8-12, 1958.

The number of atmospheric condensation nuclei affects the condition of air in confined spaces. Droplets condensing on nuclei can precipitate toxic substances from the air and raise the concentration to toxic levels. This can occur in the ambient air or in the respiratory tract during normal respiration. Temperature and humidity measurements show that this precipitation takes place mainly on mucous membranes between the nose and the larynx.

Condensation nuclei of atmospheric or human origin (smoking) can be filtered out. Sunrays can produce nuclei in air by photochemical action on trace substances and should, therefore, be prevented from entering the confined space. (Author's Abstract)

WINGET, Clifford, L., et al: A Technical Guide to the Deep Submergence Research Vehicle (DSRV) Alvin for use in Planning Scientific Missions. Woods Hole Oceanographic Institution, Woods Hole, Mass., Dec 1967.

This report is a detailed brochure for scientists who are contemplating the use of Alvin for research purposes. Complete information is presented regarding all the systems available, their capabilities, and details given even down to the types of clothing which should be worn. A form is also presented on which the scientific mission may be outlined for consideration.